AD-A080 369 AIR FORCE INST OF TECH WRIGHT-PATTERSON AFB OH SCHOO--ETC F/G 9/5
A STATISTICAL MODEL FOR MULTIPATH REFLECTION EFFECTS OF ANTENNA--ETC(U)
DEC 79 J L FRACK
UNCLASSIFIED AFIT/GE/EE/79-14 NL

AFIT/GE/EE/79-14

(6) A STATISTICAL MODEL FOR MULTIPATH REFLECTION EFFECTS OF ANTENNAS MOUNTED ON AIRCRAFT.

(9) Master's THESIS

(14) AFIT/GE/EE/79-14

(10) Jeffrey L. Frack
2Lt. USAF

Approved for public release; distribution unlimited

(11) Dec 79 (12) 101

012225

AFIT/GE/EE/79-14

A STATISTICAL MODEL FOR MULTIPATH REFLECTION EFFECTS OF ANTENNAS MOUNTED ON AIRCRAFT

THESIS

Presented to the Faculty of the School of Engineering
of the Air Force Institute of Technology
Air Training Command
in Partial Fulfillment of the
Requirements for the Degree of
Master of Science

by

Jeffrey L. Frack, B.S.
2Lt. USAF
Graduate Electrical Engineering

December 1979

Preface

At the time I started looking for a thesis topic I decided that the type of problem I wanted to solve would be one that involved the two areas I had been studying: communications and electromagnetics/antennas. I felt that Capt. Stanley Robinson would be the person who would have the best insight into a problem that included both of these areas. After some consultation we settled on this problem suggested by Maj. Jurgen Gobien at Rome Air Development Center. Together, Capt. Robinson and I formulated an approach to the problem but came to a dead end after an extensive literature search. Finally, we hit on an approach that worked and got the ball rolling. The results we came up with are for a simple case and there is so much more that needs to be done. This is true with any research, though. Probably the most important result of this thesis is that I have had the chance to take things from the classroom and apply them to a real world problem. I have really had a start at being able to think problems through for myself and make some engineering decisions. That is the real worth of this work to me. All the mistakes I have made along the way have been a real aid to my learning. If only I could start this study where it is being stopped.

I would like to thank Capt. Robinson for all the hours he has spent putting up with inexperience and getting me to really think deep about the thought processes involved in doing research of this type. I would also like to thank Lt. Col. Carpinella

and Capt. Golden for their help with my drafts and clearing up my conceptual difficulties. A special thanks goes to Capt. Donald Ottinger at Rome Air Development Center for his help in attaining and interpreting the data plots. Also much thanks goes to Mr. David Potts and the people in the Hybrid Simulation Division at the ASD Computer Center for their help in digitizing the data so it could be run through the computer.

I want to give extra special thanks and recognition to the three most important people in my life: my wife, Linda; my daughter, Jennifer; and my son, Michael. These three have been a real joy to me in my times of frustration and depression. I want to thank Linda for all her support and Jennifer and Michael for all those much needed and pleasant distractions. Lastly, and most importantly, I want to thank God for the patience and perserverence he has given me.

Jeffrey L. Frack

Contents

List of Figures

Abstract

A statistical model of the effects of multipath reflections for antenna arrays mounted on aircraft is developed to predict antenna system performance as a function of communication signal arrival angle. Each array element is assumed to have a quiescent pattern function that is a Gaussian random process with known statistics. Using these assumed statistics of the array elements the statistics of the array pattern function are determined. These array statistics are used to determine the performance of the system. Three performance measures are used: the probability that, at each arrival angle, the pattern function is above some threshold; probability level curves to show what threshold function the array pattern will be above a specified percentage of the time; and the probability the array function will be above some threshold on an interval of arrival angle. These performance measures are calculated numerically for a particular array configuration and plotted versus arrival angle. As the statistical variance of the elements increases the system performance, on the average, decreases. Therefore, for large fluctuations in the conditions that affect multipath over the length of an aircraft's mission, the system performance will be poorer than a mission with smaller fluctuations. An illustration of the technique is done using measured data to determine the statistics of the array and these results are then compared against the results for the assumed case.

I Introduction

A. Background

Whenever a new communication system is designed, the question is always asked: how will it perform? Part of this system performance determination involves the antenna that is used as part of the system. Any antenna system will be altered in its operating characteristics by reflections from the object to which it is mounted and other objects in the vicinity. This is particularly true of antennas mounted on aircraft. Engines, wings, and armament all provide points of reflection and thus, distortion for the antenna. The way in which these multipath reflections affect the operating characteristics varies with the aircraft configuration (armament and antenna placement, etc.) and the orientation of the aircraft with respect to the arrival angle of the communication signal . In order to determine system performance antenna engineers make many measurements; however, each set of measurements is only valid for one arrival angle, operating frequency, set of weather conditions, and aircraft geometrical configuration. During the course of a mission an aircraft can assume an infinite number of orientations; plus the aircraft can pass through different weather and the aircraft geometry can change due to the release of ordinance and the build-up of ice. This would seem to indicate the need for many, many measurements for each combination of angle, weather conditions, frequency, and geometry. Even if such measurements were practical, the great volume of data would give little insight into overall

system performance. It would seem much simpler to develop a statistical model and statistically motivated performance measures to predict performance over a range of arrival angles and conditions such as weather and aircraft geometry.

B. Problem Statement

The problem, then, is to develop a statistical model for the multipath reflections of antennas mounted on aircraft. This model is to be used for predicting communications performance.

C. Approach

Since aircraft movements, weather conditions, and the times at which ordinance are released are random effects, the multipath reflection effects will be modeled as being random also. For basic simplicity a one-dimensional linear array with N nonisotropic elements is used to model the multipath effects. The elements that comprise the array are assumed to have different quiescent patterns which are assumed to be complex Gaussian random processes. This assumption is made mainly for mathematical convenience, however the assumption can be justified. If the number of reflection points is large enough, by the central limit theorem for random processes, the pattern would become nearly Gaussian. With these assumptions about the individual elements the statistics for the entire array can be found.

Once the model is set up, certain performance measures can be developed. One measure of performance is the probability that, at each arrival angle, the array gain will be above some threhold level. Another measure of performance is confidence levels; i.e.

what curve will the array gain be above a specified percentage of the time? The third performance measure involves looking at the pattern on some interval of arrival angle and determining an estimate on the probability that the pattern will be above some level on that interval.

Since data is available in the form of polar plots from three antenna elements located at different points on the aircraft, the performance measures can be evaluated using sample statistics to illustrate the approach.

D. Outline

In chapter II the model is developed for the array and its associated statistics are determined based on assumptions about the individual elements. The pattern functions for the individual elements and then the array pattern function are broken into their respective real and imaginary parts to find the probability density function of the magnitude of the array pattern function. This will be needed later for some of the performance measure calculations.

Chapter III introduces the performance measures. Motivation for why these performance measures are being used is presented. There are three performance measures that are developed. The first is the probability that the magnitude of the array pattern function is above some threshold at each arrival angle. The second performance measure developed involves the level curves to show what threshold function the array gain is above some specified fraction of the time. Finally, a probability for the array gain being above some threshold on an angular

interval is developed.

In chapter IV a configuration is assumed and the performance measures are plotted for arrival angles from 0 to 360 degrees in one plane. This is done using assumed statistics and then statistics determined from measured data. Conclusions are drawn concerning the change in performance due to changes in the variance of the array function and the differences between the assumed statistics and the measured data are discussed. Recommendations for extensions of this study are then made.

II The Model

This chapter develops a model for multipath using a linear array. Using assumed statistics for the array elements, the statistics for the entire array are determined. The statistics for the array are then used to find the probability density of the magnitude of the array pattern function.

A. Array and Assumed Statistics

For simplicity, the multipath effects will be modelled using an antenna array with N arbitrarily (but not randomly) spaced, nonisotropic elements. If each element has a quiescent electric field pattern, $G_i(\theta)$, the total scalar electric field pattern function is given by

$$f(\theta)= \sum_{i=1}^{N} e^{j\psi_i} G_i(\theta) w_i \qquad (1)$$

where

$k=2\pi/\lambda$

λ is the operating wavelength

$$\psi_i = kx_i \cos\theta \qquad (2)$$

x_i is the spacing of the ith element from the array origin

θ is measured from the array axis

w_i is a complex beam steering weight which is assumed constant. See Figure 1 for the details of the array. To include the effects of multipath, which are unknown apriori, the $G_i(\theta)$ are assumed to be complex Gaussian random processes with known statistics

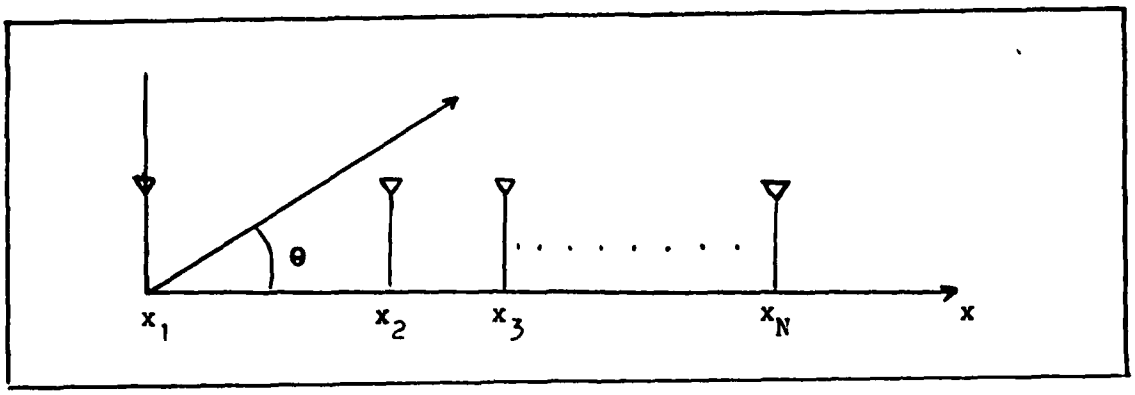

Figure 1. N Element Array.

$$E[G_i(\theta)] = \overline{G_i(\theta)} \tag{3}$$

$$E[G_i(\theta)G_i^*(\theta')] = R_i(\theta,\theta') \tag{4}$$

$$E[G_i(\theta)G_j^*(\theta')] = R_{ij}(\theta,\theta') \tag{5}$$

$$E[G_i(\theta)G_i(\theta')] = R_{oi}(\theta,\theta') \tag{6}$$

$$E[G_i(\theta)G_j(\theta')] = R_{oij}(\theta,\theta') \tag{7}$$

These statistics are assumed here to be known, but they can be determined from actual data measurements. With these statistics the autocovariance and the crosscovariance of $G_i(\theta)$ can be found to be

$$C_{Gi}(\theta,\theta') = R_i(\theta,\theta') - \overline{G_i(\theta)}\,\overline{G_i^*(\theta')} \tag{8}$$

$$C_{Gij}(\theta,\theta') = R_{ij}(\theta,\theta') - \overline{G_i(\theta)}\,\overline{G_j^*(\theta')} \tag{9}$$

B. Statistics of $f(\theta)$

The first things that need to be determined, based on these assumptions, are the statistics of the pattern function, $f(\theta)$. The mean of $f(\theta)$ (the ensemble average pattern function) is given by

$$E\left[f(\theta)\right] = \sum_{i=1}^{N} w_i \, e^{j\psi_i} \, \overline{G_i(\theta)} \tag{10}$$

The autocorrelation of $f(\theta)$ becomes

$$E\left[f(\theta)f^*(\theta')\right] = \sum_{i=j}^{N} R_i(\theta,\theta') \left|w_i\right|^2 + \sum_{i\neq j}^{N}\sum R_{ij}(\theta,\theta') \, w_i w_j^* \, e^{j(\psi_i - \psi_j')} \tag{11}$$

From eqns. 10 and 11 the covariance of $f(\theta)$ can be found to be

$$C_f(\theta,\theta') = E\left[f(\theta)f^*(\theta')\right] - E\left[f(\theta)\right] E\left[f^*(\theta')\right] \tag{12}$$

$$= \sum_{i=j}^{N}\left[R_i(\theta,\theta') - \overline{G_i(\theta)} \; \overline{G_i^*(\theta')}\right] \left|w_i\right|^2 + \sum_{i\neq j}^{N}\sum\left[R_{ij}(\theta,\theta') - \overline{G_i(\theta)} \; \overline{G_j^*(\theta')}\right] e^{j(\psi_i - \psi_j')} w_i w_j^* \tag{13}$$

This can also be expressed as

$$C_f(\theta,\theta') = \sum_{i=j}^{N} C_{Gi}(\theta,\theta') \left|w_i\right|^2 + \sum_{i\neq j}^{N}\sum C_{Gij}(\theta,\theta') \, e^{j(\psi_i - \psi_j')} w_i w_j^* \tag{14}$$

The second moment of $f(\theta)$ is found from

$$E\left[f(\theta)f(\theta')\right] = \sum_{i=j}^{N} R_{oi}(\theta,\theta') e^{j(\psi_i - \psi_j')} (w_i)^2 + \sum_{i\neq j}^{N}\sum R_{oij}(\theta,\theta') e^{j(\psi_i - \psi_j')} w_i w_j \tag{15}$$

The covariance type function associated with this second moment is found by subtracting the product of the means. Thus,

$$C_o(\theta,\theta') = E\left[f(\theta)f(\theta')\right] - E\left[f(\theta)\right] E\left[f(\theta')\right]$$

$$= \sum_{i=j}^{N} \left[R_{oi}(\theta,\theta') - \overline{G_i(\theta)}\ \overline{G_i(\theta')} \right] e^{j(\psi_i - \psi'_j)} (w_i)^2$$
$$+ \sum_{i \neq j}^{N} \sum \left[R_{oij}(\theta,\theta') - G_i(\theta)\ G_j(\theta') \right] e^{j(\psi_i - \psi'_j)} w_i w_j \qquad (16)$$

These statistics of $f(\theta)$ are not necessarily useful in their own right. They are, however, useful as tools to get toward the performance measures of chapter III.

One of the performance measures involves the notion of correlation distance. Correlation distance for the array is the angular distance apart two samples of the pattern must be to be uncorrelated. This is really a measure of the rate at which the pattern changes with angle. Small correlation distance means that the pattern undergoes relatively large changes with a small change in angle. Thus the uncorrelated sample points are closer together.

All of the performance measures evaluated by this thesis involve the magnitude of $f(\theta)$, given by

$$|f(\theta)| = \sqrt{(Ref(\theta))^2 + (Imf(\theta))^2} \qquad (17)$$

where

$Ref(\theta)$= the real part of $f(\theta)$

$Imf(\theta)$= the imaginary part of $f(\theta)$

$f(\theta) = Ref(\theta) + jImf(\theta)$ (18)

The magnitude of $f(\theta)$ is used because most antenna measurements are power measurements and do not include phase information. What really turns out to be most useful is the probability density of $|f(\theta)|$. This is determined next.

C. Probability Density of $|f(\Theta)|$

In order to determine the density of $|f(\Theta)|$, the statistics of the real and imaginary parts of $f(\Theta)$ need to be found. Once the joint statistics of $Ref(\Theta)$ and $Imf(\Theta)$ are determined it is just a transformation to find those of $|f(\Theta)|$. To determine the means of $Ref(\Theta)$ and $Imf(\Theta)$ it is necessary to look at $G_i(\Theta)$ and break it into real and imaginary parts. $G_i(\Theta)$ can be expressed as

$$G_i(\Theta) = ReG_i(\Theta) + jImG_i(\Theta) \tag{19}$$

The mean of $G_i(\Theta)$ becomes

$$\overline{G_i(\Theta)} = Re\overline{G_i(\Theta)} + j\overline{ImG_i(\Theta)} \tag{20}$$

where $ReG_i(\Theta)$ and $ImG_i(\Theta)$ are joint Gaussian random processes. Combining eqns.(1)(17)and(18)the real and imaginary parts of the mean of $f(\Theta)$ can be expressed as

$$\overline{Ref(\Theta)} = \sum_{i=1}^{N} (Re(w_i)\cos\psi_i - Im(w_i)\sin\psi_i)\overline{ReG_i(\Theta)} - (Re(w_i)\sin\psi_i + Im(w_i)\cos\psi_i)\overline{ImG_i(\Theta)} \tag{21}$$

$$\overline{Imf(\Theta)} = \sum_{i=1}^{N} (Re(w_i)\sin\psi_i - Im(w_i)\cos\psi_i)\overline{ReG_i(\Theta)} + (Re(w_i)\cos\psi_i - Im(w_i)\sin\psi_i)\overline{ImG_i(\Theta)} \tag{22}$$

The covariances of $Ref(\Theta)$ and $Imf(\Theta)$ are found by breaking the covariance of $f(\Theta)$, $C_f(\Theta,\Theta')$, and the second moment, $C_o(\Theta,\Theta')$, according to real and imaginary parts. $C_f(\Theta,\Theta')$ is defined as

$$C_f(\Theta,\Theta') = E[f(\Theta)f^*(\Theta')] - E[f(\Theta)]\,E[f^*(\Theta')]$$

$$= \overline{Ref(\theta)Ref(\theta')} - \overline{Ref(\theta)}\ \overline{Ref(\theta')} + \overline{Imf(\theta)Imf(\theta')}$$
$$- \overline{Imf(\theta)}\ \overline{Imf(\theta')} - j\overline{Ref(\theta)Imf(\theta')} + j\overline{Ref(\theta)}\ \overline{Imf(\theta')}$$
$$+ j\overline{Ref(\theta')Imf(\theta)} - j\overline{Ref(\theta')}\ \overline{Imf(\theta)} \qquad (23)$$

Likewise, $C_o(\theta,\theta')$ becomes

$$C_o(\theta,\theta') = \overline{Ref(\theta)Ref(\theta')} - \overline{Ref(\theta)}\ \overline{Ref(\theta')} - \overline{Imf(\theta)Imf(\theta')}$$
$$+ \overline{Imf(\theta)}\ \overline{Imf(\theta')} + j\overline{Ref(\theta)Imf(\theta')} - j\overline{Ref(\theta)}\ \overline{Imf(\theta')}$$
$$+ j\overline{Ref(\theta')Imf(\theta)} - j\overline{Ref(\theta')}\ \overline{Imf(\theta)} \qquad (24)$$

The covariance terms of $Ref(\theta)$ and $Imf(\theta)$ can be found from these two equations (23 and 24) to be

$$\overline{Ref(\theta)Ref(\theta')} - \overline{Ref(\theta)}\ \overline{Ref(\theta')} = \tfrac{1}{2}Re[C_f(\theta,\theta') + C_o(\theta,\theta')] \qquad (25)$$
$$\overline{Imf(\theta)Imf(\theta')} - \overline{Imf(\theta)}\ \overline{Imf(\theta')} = \tfrac{1}{2}Re[C_f(\theta,\theta') - C_o(\theta,\theta')] \qquad (26)$$
$$\overline{Ref(\theta')Imf(\theta)} - \overline{Ref(\theta')}\ \overline{Imf(\theta)} = \tfrac{1}{2}Im[C_f(\theta,\theta') + C_o(\theta,\theta')] \qquad (27)$$
$$\overline{Ref(\theta)Imf(\theta')} - \overline{Ref(\theta)}\ \overline{Imf(\theta')} = -\tfrac{1}{2}Im[C_f(\theta,\theta') - C_o(\theta,\theta')] \qquad (28)$$

The performance measures of chapter III involve only $|f(\theta)|$ at a given angle, θ, at any one time, so the concern here is only first order and thus, $\theta=\theta'$. The covariance terms now reduce to having a variance interpretation. Variance is a measure of how much the pattern changes at a given angle, θ, when changes are made in the conditions that affect multipath (aircraft geometry,orientation of the aircraft, weather, icing, etc.). The variance of the real part of $f(\theta)$ becomes

$$\sigma_R^2(\theta) = \overline{Ref(\theta)Ref(\theta)} - \overline{Ref(\theta)}\ \overline{Ref(\theta)} \qquad (29)$$

The variance of Imf(θ) is given by

$$\sigma_I^2(\theta) = \overline{Imf(\theta)Imf(\theta)} - \overline{Imf(\theta)}\ \overline{Imf(\theta)} \qquad (30)$$

To check for correlation between Ref(θ) and Imf(θ), a correlation coefficient, r, is defined as

$$r = \frac{E\left[(Ref(\theta) - \overline{Ref(\theta)})(Imf(\theta) - \overline{Imf(\theta)})\right]}{\sigma_R(\theta)\ \sigma_I(\theta)}$$

$$= \frac{Im\left[C_f(\theta,\theta) + C_0(\theta,\theta)\right]}{2\,\sigma_R(\theta)\ \sigma_I(\theta)} \qquad (31)$$

At any given angle, θ, the random processes are random variables. Since Ref(θ) and Imf(θ) are made up of sums of the real and imaginary parts of $G_i(\theta)$, which are joint Gaussian random variables, then they are joint Gaussian random variables whose joint density is given by (Ref 6: 182)

$$f(u,v) = \frac{(1-r^2)^{-\frac{1}{2}}(2\pi)^{-1}}{\sigma_R(\theta)\ \sigma_I(\theta)} \exp\left[\frac{-1}{2(1-r^2)}\left\{\frac{(u-\bar{u})^2}{\sigma_R^2(\theta)} - \frac{2r(u-\bar{u})(v-\bar{v})}{\sigma_R(\theta)\ \sigma_I(\theta)} + \frac{(v-\bar{v})^2}{\sigma_I^2(\theta)}\right\}\right] \qquad (32)$$

In general, one could use this joint density in the transformation of eq.(17)to find the density of $|f(\theta)|$. This is very complex and beyond the scope of this thesis. A relatively simple solution does exist, however, when Ref(θ) and Imf(θ) are uncorrelated with common variance. This implies that r=0 and $\sigma_R^2(\theta)=\sigma_I^2(\theta)$. One way of meeting these conditions is by making two assumptions. The first is that the real and imaginary parts of $G_i(\theta)$ are uncorrelated with equal covariances and thus,at each θ , have egual variances. This is reasonable since there is nothing in the physical setting of the problem that would favor one quadrature

over the other. The second assumption is that the individual element functions, $G_i(\theta)$, are uncorrelated from each other. Because each of the element patterns depends upon an identical aircraft geometry and there is mutual coupling between the antennas, this assumption is not altogether realistic. Actually, then, what is assumed here is that the crosscorrelation between the elements is negligible compared to the autocorrelation of each element. With these assumptions various reductions occur in the statistics. The crosscorrelation of the elements (eq. 5) becomes the product of the means and the crosscovariance (eq. 9) becomes zero. The autocovariance (eq. 8) becomes twice the covariance of the real part of $G_i(\theta)$ since the real and imaginary parts are uncorrelated with equal covariances. The covariance of $f(\theta)$ then reduces to

$$C_f(\theta,\theta') = 2\sum_{i=1}^{N}\left\{ E\left[\mathrm{Re}G_i(\theta)\mathrm{Re}G_i(\theta')\right] - \mathrm{Re}\overline{G_i(\theta)}\ \mathrm{Re}\overline{G_i(\theta')}\right\}|w_i|^2 \quad (33)$$

For similar reasons $R_{oij}(\theta,\theta')$ and $R_{oi}(\theta,\theta')$ are both zero which causes $C_o(\theta,\theta')$ to become

$$C_o(\theta,\theta') = 0 \quad (34)$$

From eq.(33)it is evident that $C_f(\theta,\theta')$ is a real function. This combined with eq(34)causes the correlation coefficient, r, to become

$$r = \frac{\mathrm{Im}\left[C_f(\theta,\theta)\right]}{\sigma_R(\theta)\,\sigma_I(\theta)} = 0 \quad (35)$$

The variances of the real and imaginary parts of $f(\theta)$ are then equal to $\frac{1}{2}\mathrm{Re}\left[C_f(\theta,\theta)\right]$. This can be shown by combining eqns.

(25),(26),(29),(30),(32). The variances can then be expressed as

$$\sigma^2(\theta) = \sigma_R^2(\theta) = \sigma_I^2(\theta) = \sum_{i=1}^{N} \sigma_{Gi}^2(\theta)\left[(\mathrm{Re}(w_i))^2 + (\mathrm{Im}(w_i))^2\right] \qquad (36)$$

where

$$\sigma_{Gi}^2(\theta) = \overline{\mathrm{ReG}_i(\theta)\mathrm{ReG}_i(\theta)} - \overline{\mathrm{ReG}_i(\theta)}\ \overline{\mathrm{ReG}_i(\theta)} \qquad (37)$$

This $\sigma_{Gi}^2(\theta)$ is the variance of both the real and imaginary parts of $G_i(\theta)$. It is found from $C_{Gi}(\theta,\theta')$ by setting $\theta=\theta'$ at a given angle, θ. With $\mathrm{Ref}(\theta)$ and $\mathrm{Imf}(\theta)$ being uncorrelated joint Gaussian random variables with common variance, their joint density is given by

$$f_{\mathrm{Ref,Imf}}(u,v) = \frac{(2\pi)^{-1}}{\sigma_{\Sigma}^2(\theta)} \exp\left[-\tfrac{1}{2}\frac{(u-\bar{u})^2 + (v-\bar{v})^2}{\sigma^2(\theta)}\right] \qquad (38)$$

From the joint density of $\mathrm{Ref}(\theta)$ and $\mathrm{Imf}(\theta)$ the density of $|f(\theta)|$ can be determined (Ref 6 : 195-196). If $|f(\theta)|$ is given by eq(17) and $\mathrm{Ref}(\theta)$ and $\mathrm{Imf}(\theta)$ are uncorrelated joint Gaussian random variables with different means and common variance, then the probability density of $|f(\theta)|$ is given by

$$f_z(z) = \frac{z}{\sigma^2(\theta)} \exp\left[\frac{-z^2+\overline{\mathrm{Ref}(\theta)}^2+\overline{\mathrm{Imf}(\theta)}^2}{2\,\sigma^2(\theta)}\right] I_o\left[\frac{z\sqrt{\overline{\mathrm{Ref}(\theta)}^2+\overline{\mathrm{Imf}(\theta)}^2}}{\sigma^2(\theta)}\right] \qquad (39)$$

for all $z \geq 0$, where $z = |f(\theta)|$ and I_o is the modified Bessel function of order zero.

In summary, this chapter has presented a model for multipath reflection effects. Statistics for the array were determined using the assumed known statistics of the individual elements of the array. All the geometry, weather, frequency, etc. effects are

taken into account in the statistics of $G_i(\Theta)$. The statistics of $f(\Theta)$ were then found from the known statistics and these were used to determine statistics for $Ref(\Theta)$ and $Imf(\Theta)$. The general case for the joint density of $Ref(\Theta)$ and $Imf(\Theta)$ was too complex to perform the transformation to determine the density of the magnitude of $f(\Theta)$. To simplify the transformation the $G_i(\Theta)$ were assumed uncorrelated from each other with uncorrelated real and imaginary parts that had equal covariances. This led eq. 39, the density of the magnitude of $f(\Theta)$. This density function is what is needed to determine the performance measures of chapter III.

III Performance Measures

Now that the model has been established, what need to be determined are measures of system performance that use the model. There are three performance measures developed in this chapter along with some motivation for why one would want to use these performance measures.

A. Probability that $|f(\theta)|$ is Greater Than a Threshold

In a typical communications scenario, usually there is a minimum signal to noise ratio below which reliable communication is impossible. This signal to noise ratio corresponds to a particular relative antenna gain. The question might be asked, how reliable are communications in a certain direction given that a certain relative gain needs to be obtained. Since the way in which multipath affects the relative gain can be viewed as being random, a measure of reliability would be the probability that $|f(\theta)|$ is above some threshold value, R, in a given direction. This probability is found by integrating the density of $|f(\theta)|$,

$$Pr\{|f(\theta)| > R\} = \int_R^\infty f_{|f(\theta)|}(z)\, dz \qquad (40)$$

The density of the magnitude of $f(\theta)$ was calculated in chapter II and is given by eq.(39). This equation was based on the assumptions that the underlying $G_i(\theta)$ are uncorrelated and their real and imaginary parts are uncorrelated with equal covariances. Thus, the probability that $|f(\theta)|$ is greater than some threshold, R, is given by

$$\Pr\{|f(\theta)|>R\} = 1 - \int_{R}^{\infty} \frac{z}{\sigma^2(\theta)} \exp\left[\frac{-z^2 + \overline{\mathrm{Re}f(\theta)}^2 + \overline{\mathrm{Im}f(\theta)}^2}{2 \cdot \sigma^2(\theta)}\right] \cdot I_o\left[\frac{z \sqrt{\overline{\mathrm{Re}f(\theta)}^2 + \overline{\mathrm{Im}f(\theta)}^2}}{\sigma^2(\theta)}\right] dz \qquad (41)$$

The density of the magnitude of $f(\theta)$ is not integrable in closed form and must be integrated numerically. These results are plotted in chapter IV for one particular aircraft configuration.

B. Level Curves

Along the same idea as the first performance measure where a certain confidence is placed on communications reliability given some threshold, the second measure examines the converse. The question to be answered is what curve, $R(\theta)$, will the magnitude of $f(\theta)$ be above a specified percentage of the time? In other words, what is the maximum relative gain the system will operate above p percent of the time? Given a direction angle, θ, the probability statement becomes

$$\Pr\{|f(\theta)|>R(\theta)\} = p \qquad (42)$$

The threshold function, $R(\theta)$, can be determined by solving the the integral equation

$$\int_{R}^{\infty} f_z(z)\, dz = p \qquad (43)$$

Again this integration needs to be done numerically. With the assumption of a certain array configuration $R(\theta)$ is computed and plotted in chapter IV.

C. Probability $|f(\theta)|$ is Above a Threshold On an Angular Interval

The first two performance measures were obtained using a probability statement at each value of θ. Since, for an antenna, one is concerned with the performance over some angular interval, the distribution at each angle is insufficient to predict overall performance. If $|f(\theta)|$ at a given θ is greater than $R(\theta)$, then with probability 1 $|f(\theta+\Delta\theta)|$ will be greater than $R(\theta)$ also if $\Delta\theta$ is small enough. This is because of a strong correlation between $f(\theta)$ and $f(\theta+\Delta\theta)$ for $\Delta\theta$ small enough. If $\Delta\theta$ is large enough $f(\theta)$ and $f(\theta+\Delta\theta)$ become uncorrelated. Thus an estimate can be made of the probability that $|f(\theta)|$ is greater than R on an entire interval.

Let $\underline{\theta}$ be the set of θ_n where $(\theta_1,\theta_2,\ldots,\theta_N)$ are far enough apart for $f(\theta_1)$, $f(\theta_2)$, ..., $f(\theta_N)$ to be uncorrelated. Since the $f(\theta_n)$ are jointly normal and uncorrelated, they are also independent. In view of this independence, the probability that $|f(\theta)|$ will exceed R over the entire interval is given by the product of the probabilities at the independent sample points. Thus,

$$\Pr\{|f(\theta)|>R \quad \theta\in\underline{\theta}\}=\prod_{n=1}^{N}\Pr\{|f(\theta_n)|\geq R\} \tag{44}$$

where N is the number of independent sample points in the interval. This type of performance measure is useful in the following scenario. Suppose an aircraft pilot needs to communicate with his wing man who could located anywhere on an interval of 30 degrees centered at 90 degrees from the first pilot's direction of flight. The question is asked, how reliable are the communications

between the pilot and his wingman? Equivalently, what is the probability that the relative gain will be above the minimum needed for reliable communication? This probability measure can be obtained using the probability at independent sample points. In order to determine how far apart samples must be to be independent, the correlation distance for the array has to be found. Appendix A involves calculating the covariance of the array pattern function. This is then used to find the correlation distance. For example, if the correlation distance for the array were 15 degrees the probability would be given by

$$\Pr\{|f(\theta)| > R \quad 75^{\circ} \leq \theta \leq 105^{\circ}\} = \Pr\{|f(75)| > R\} \cdot \Pr\{|f(90)| > R\} \cdot \Pr\{|f(105)| > R\} \tag{45}$$

These probabilities can be obtained from the probabilities determined by the probability that $|f(\theta)|$ is greater than R at any θ (the first performance measure). An actual sample calculation is performed in chapter IV and measured data is done in Appendix A.

These performance measures have been developed to predict communication system performance using the model from chapter II. Now what remains is to calculate the performance measures and plot the results to see how the system performs with changes in variance and mean. This leads into chapter IV.

IV Numerical Results and Conclusions

The model and the resulting performance measures have been developed in general for an N element linear array with arbitrary element spacings. In order to get some specific results for illustration purposes a particular configuration for the array must be assumed.

A. Configuration for the Array

The configuration to be examined in this chapter is that of a three element array with one wavelength spacing between the elements. Three elements are assumed because measured data is available for three elements located at different places on the aircraft. Current application uses one wavelength spacing. Details concerning the measured data are found in Appendix A. Even though the array configuration may be , in practice, more complex, the basic proceedure is the same as for this simple case. The array pattern will be the quiescent or unadapted pattern with the w_i set equal to one. There is, therefore, no beamsteering. Since from a power plot there is no way to find phase information, there is no way to tell how much of the pattern is due to the real part and how much is due to the imaginary part of $G_i(\theta)$. For simplicity, then, the mean of $G_i(\theta)$ will be assumed to be purely real. It should be emphasized that the results that follow are only valid for this particular array configuration. The technique is perfectly general, but the calculations become more involved for more elements and

different spacings. ith these assumptions in mind the parameters for the density of $|f(\theta)|$ become

$$w_i = 1 \quad \text{for all } i \tag{46}$$

$$E[G_i(\theta)] = \overline{\mathrm{Re}G_i(\theta)} \tag{47}$$

$$E[\mathrm{Im}G_i(\theta)] = 0 \tag{48}$$

$$\mathrm{Re}f(\theta) = \sum_{i=1}^{5} \cos\psi_i \mathrm{Re}G_i(\theta) - \sin\psi_i \mathrm{Im}G_i(\theta) \tag{49}$$

$$\mathrm{Im}f(\theta) = \sum_{i=1}^{5} \sin\psi_i \mathrm{Re}G_i(\theta) - \cos\psi_i \mathrm{Im}G_i(\theta) \tag{50}$$

$$\sigma_R^2(\theta) = \sigma_I^2(\theta) = \sigma^2(\theta) = \sum_{i=1}^{5} \sigma_{Gi}^2(\theta) \tag{51}$$

$$\psi_1 = 0 \tag{52}$$

$$\psi_2 = 2 \cos\theta \tag{53}$$

$$\psi_3 = 2 \cos\theta \tag{54}$$

These parameters were developed in chapter II.

The best relative gain that can obtained from each antenna element is 0 db or a relative gain of one. Since multipath causes a degradation in antenna gain, the best that can be obtained is a relative gain of one which corresponds to having no multipath. The mean of each element will be assumed to be $3\ \sigma_{Gi}(\theta)$ down from a gain of one($\sigma_{Gi}(\theta)$ is standard deviation) so that with probability nearly equal to one, the pattern for each element will not exceed a relative gain of one. This is to make the model fit the physical constraints. For the simplicity of the numerical calculations each random pattern function,

$G_i(\Theta)$, will be assumed to have constant and equal means and variances. This is not true with the real data, however this assumption is made to get a first order look at the changes in performance due to changes in variance.

B. $\underline{Pr\{|f(\Theta)|>R\}}$

The first performance measure to be evaluated is the probability that $|f(\Theta)|$ is greater than a threshold, R, at each angle, Θ. The expression to be evaluated (eq.(41)) is not integrable in closed form so it is done numerically. The results of this are plotted for R=1 in Figure 2 for four different values of assumed variance. Curves for R=1,2,3 are found in Appendix B for the same four values of variance. As the variance increases the probability that $|f(\Theta)|$ exceeds 3 is nearly zero. Since large variance indicates wider variations about a smaller mean, the probability that $|f(\Theta)|$ is greater than three standard deviations away from the mean is very small. This indicates that the assumption about the mean will yield pattern functions that are less than the maximum gain. The actual data never exceeds 0 db. The trend in the plots of Figure 2 is that as variance increases the probabilities of being able to communicate tend to decrease. This would indicate that a mission that involved far sweeping changes in aircraft orientation, conditions of the atmosphere, aircraft geometrical configuration(due to icing and release of ordinance) which will change the number of reflections, and polarization (all yielding higher variance) yields probabilities of being able to reliably communicate that are

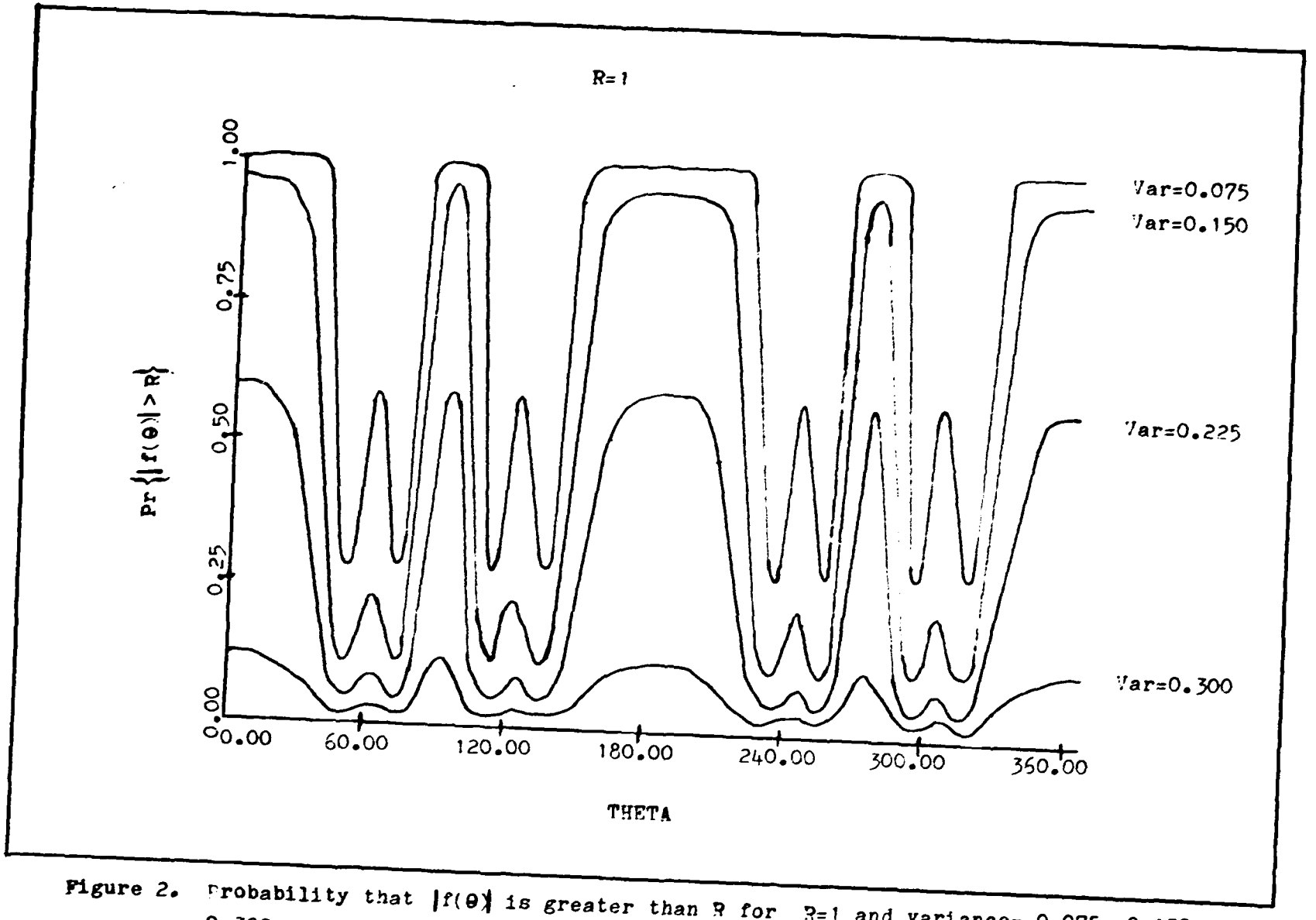

Figure 2. Probability that $|f(\theta)|$ is greater than R for R=1 and variance= 0.075, 0.150, 0.225 0.300.

much lower than a mission which has more stable conditions.

C. Level Curves

The second performance measure developed in chapter III were the level curves. The solution to the integral equation of eq.(43) is found at each angle, Θ, and then plotted versus Θ in Figures 3-5. These plots are for four different variances and at confidence levels of 70%, 80%, 90%. Figure 6 is a plot of the free space pattern in the same plane; i.e. a three element array with no multipath. This is for comparison to see actually how much degradation there is due to multipath. As the variance increases the threshold function, $R(\Theta)$, decreases. Increase in variance indicates greater fluctuations, thus, in order to stay above the curve with the same confidence, the value of the function has to be less. Also it should be pointed out that as the percentage increases the threshold function decreases for the same basic reason.

As the effect of the multipath becomes less, the variance also becomes less until when there is no multipath the variance becomes zero, at which point the pattern should be that of the free space plot(Figure 6). It should be pointed out that the 0.075 variance curves in Figures 3-5 begin to show nulls at the same locations and beamwidths on the same order as the free space pattern. Smaller variances could not be used numerically because the probability density approaches an impulse as the variance approaches zero and the exponential term of eq. (39) goes out of bounds for computer evaluation.

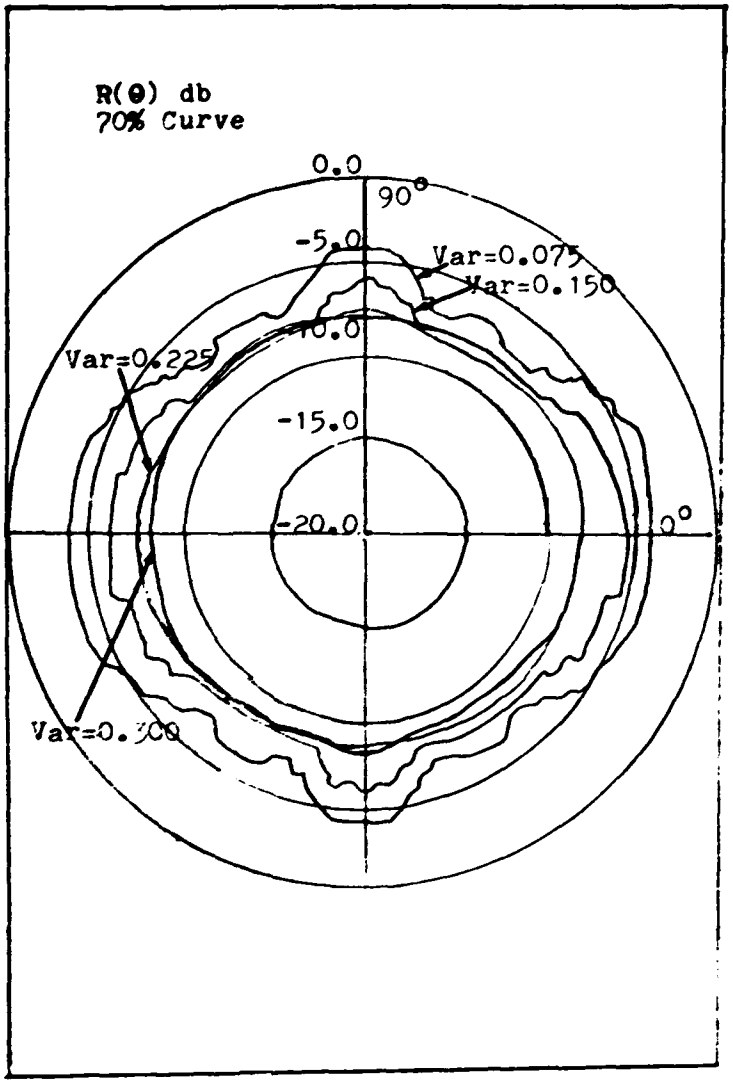

Figure 3. Level Curve for 70% confidence.

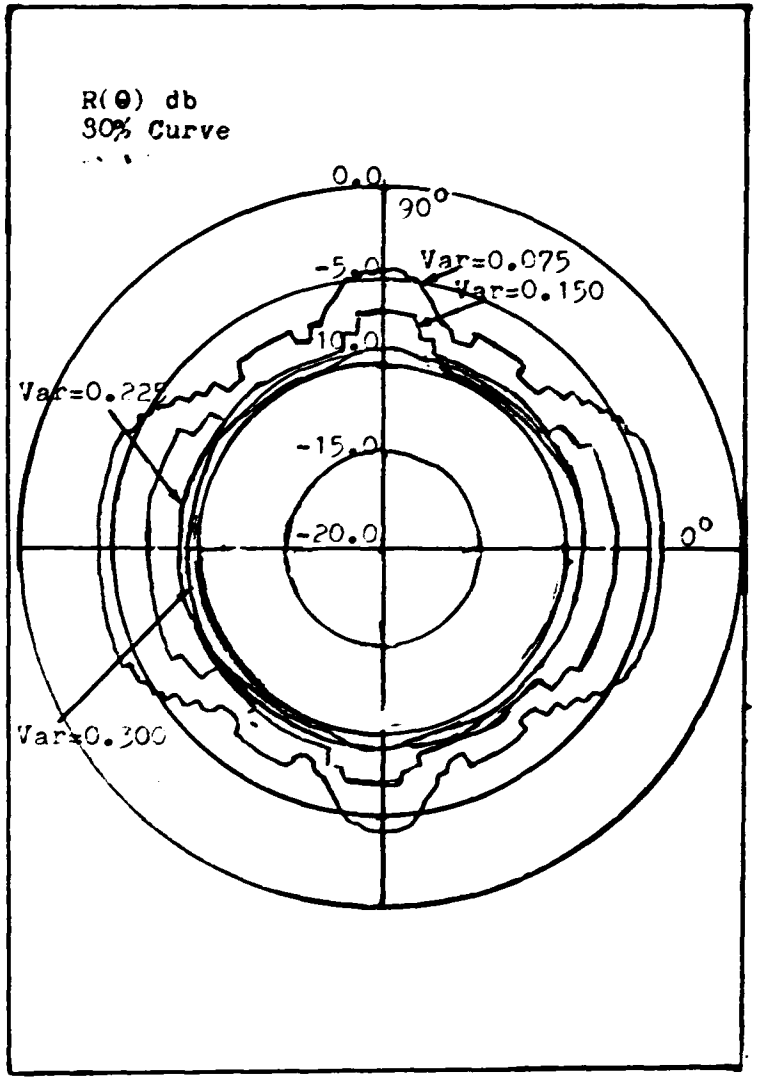

Figure 4. Level Curve for 80% confidence.

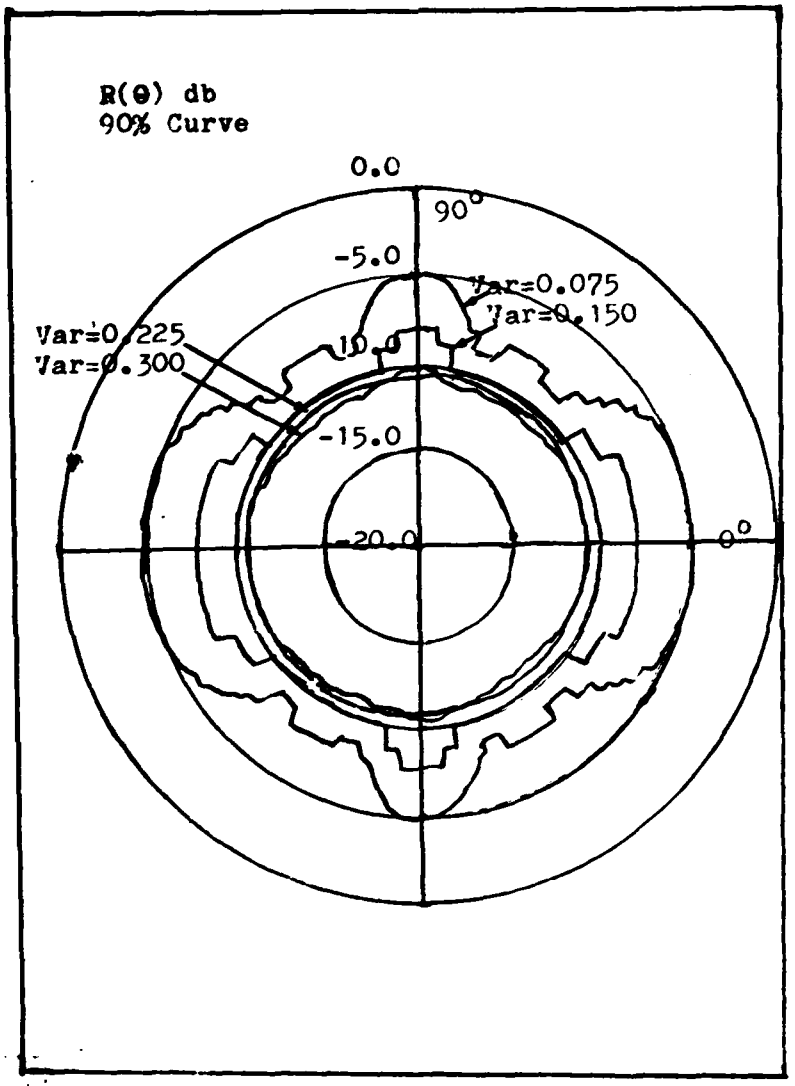

Figure 5. Level Curve for90% confidence.

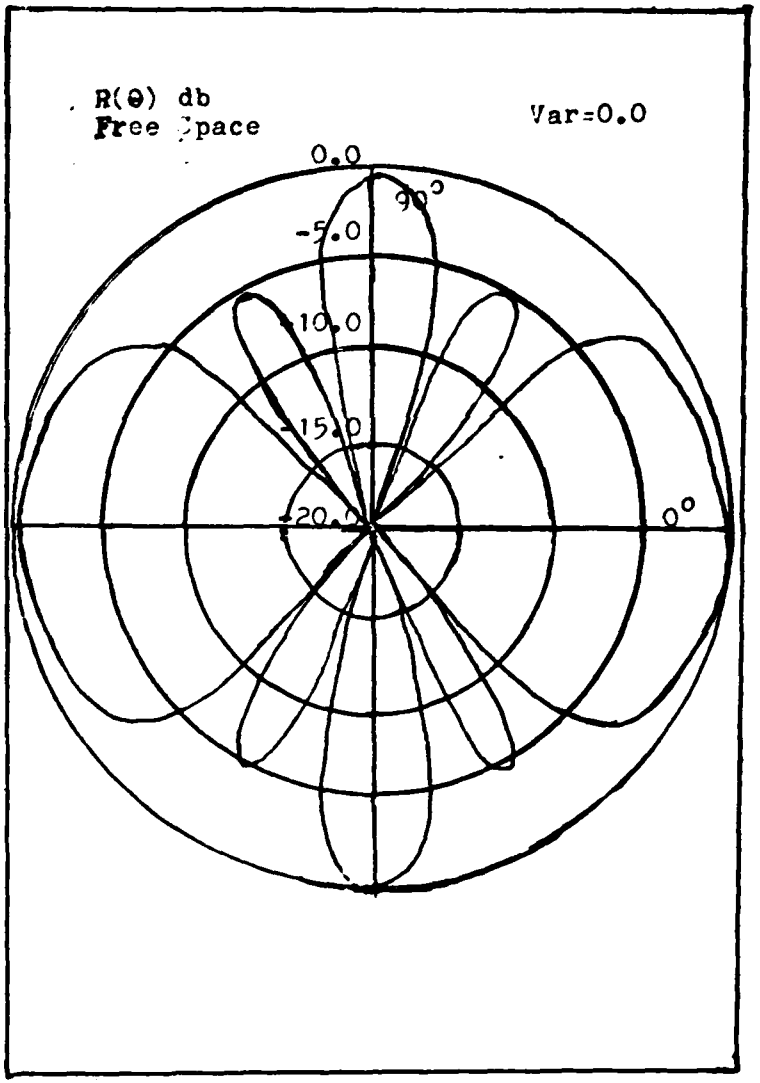

Figure 6. Free Space plot for 3 element array;one wavelength spacing.

D. $\Pr\{|f(\Theta)|>R\}$ on an Interval of Arrival Angle

In chapter III a general example was done to indicate performance on an angular interval. Now the same example will be done using the plotted performance measures. From eq.(45) the the probability that the magnitude of $f(\Theta)$ is greater than some R on the interval from 75 degrees to 105 degrees, assuming a correlation distance for the array of 15 degrees, was

$$\Pr\{|f(\Theta)|>R;75\le\Theta\le105\} = \Pr\{|f(75)|>R\}\Pr\{|f(90)|>R\} \cdot\Pr\{|f(105)|>R\} \quad (45)$$

Assuming a variance for the array of 0.225 and R=1 (corresponding to a gain of -4.77db) the probabilities can be found by sampling the curve for variance=0.225 in Figure 2 at 75, 90, and 105 degrees. Thus,

$$\begin{aligned}\Pr\{|f(\Theta)|>1\ ;\ 75\le\Theta\le105\} &= \Pr\{|f(75)|>1\}\Pr\{|f(90)|>1\} \cdot\Pr\{|f(105)|>1\} \\ &=(0.09)(0.6)(0.09) \\ &=0.00486 \quad (55)\end{aligned}$$

The probability of reliable communications on the entire 30 degree interval is low for this large of variance. That is, of course, assuming that R=1 is the gain threshold below which the minimum signal to noise ratio is not attained.

E. Measured Data

The previous results have depended on the assumption of the elements having indentical and constant means and variance

The true tests of performance should surely include the statistics of the measured data. The data analysis is outlined in Appendix A. Using the statistics calculated in Appendix A the same performance calculations were done. The results are plotted in Figures 7-10. The data plots have the same general shape as the theoretical curves but there are some differences. Figure 7 is a plot of the probability that $|f(\Theta)|$ is greater than R, for each Θ, using a sample mean and variance at each Θ. The differences between this and the theoretical curves come about from a number of things. The theoretical analysis assures stationarity for the mean and variance. These two quantities are not constant over all Θ and thus not strictly stationary. This accounts for much of the fluctuations. The data runs for the level curves (Figures 8-10) are remarkably similar to the 0.075 variance plots of Figures 3-5. This may not be a true picture of actual closeness because of the compression capability of the logarithm function used in calculating db gain. The differences that do occur are again because of the lack of stationarity of the data.

F. Utility of the Model

The question will be raised, how can this model be used? It was pointed out at the start that the model was general for an N element linear array with arbitrary (but nonrandom) spacings. An antenna engineer with a lot of antenna data (on the order of 100-200 plots) now has a method through which to calculate system performance. All that needs to be done is analyze the

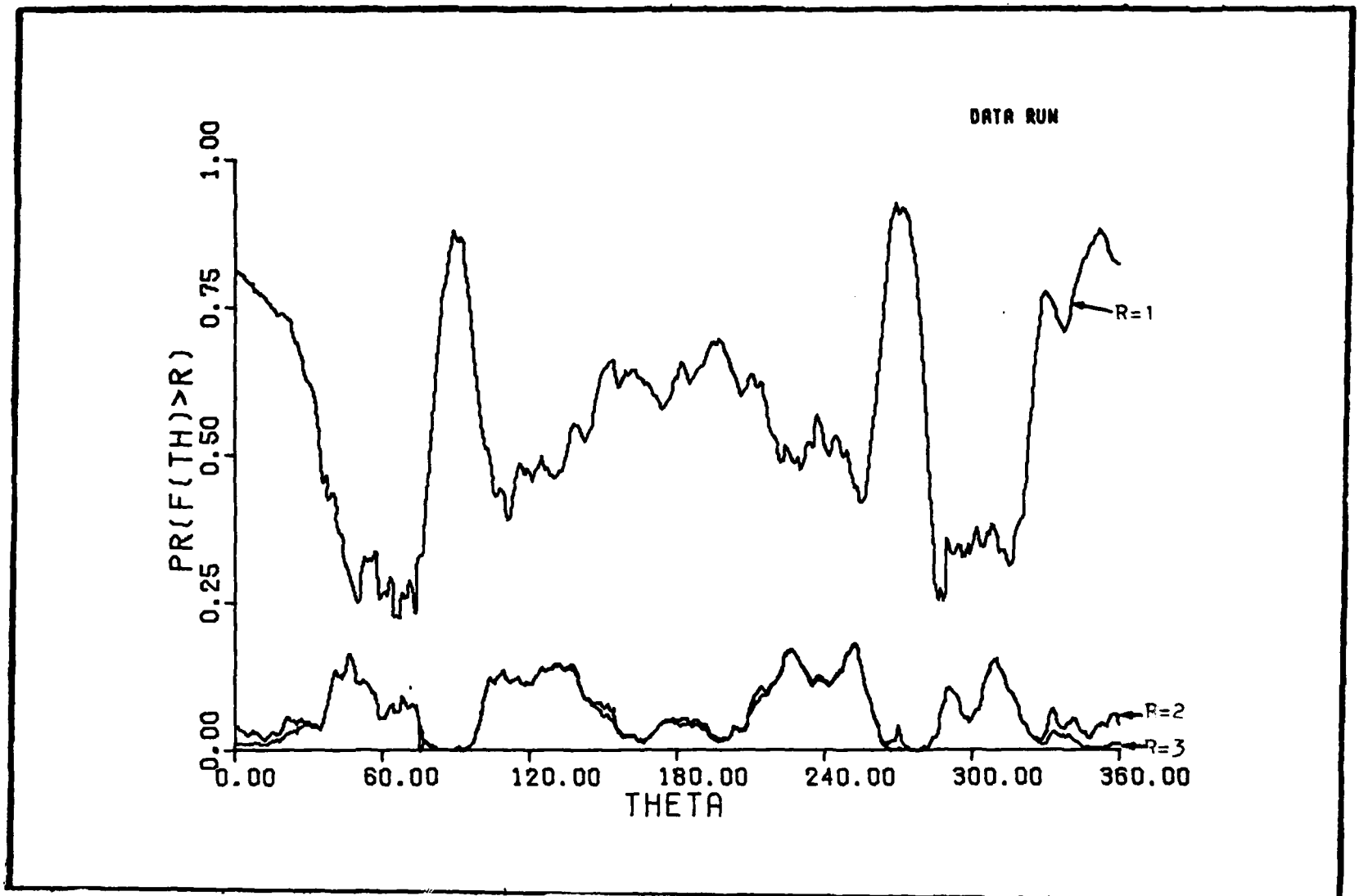

Figure 7. Probability that f(θ) is greater than R=1,2,3 using sample statistics calculated from measured data.

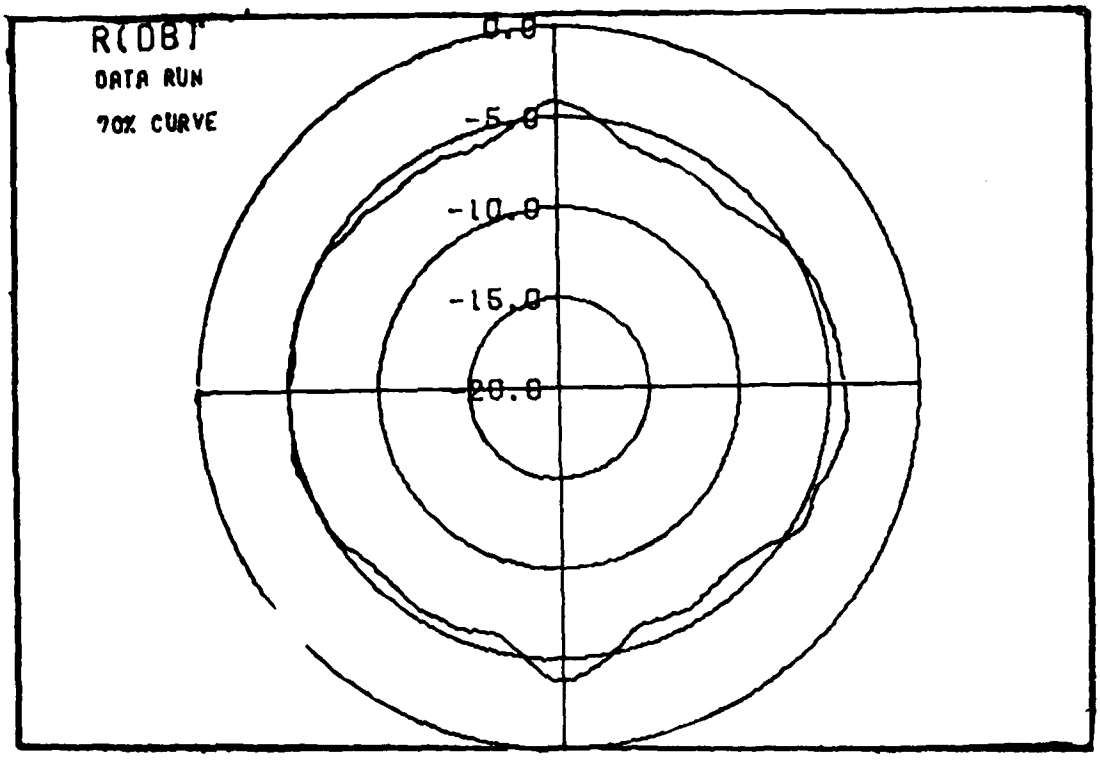

Figure 8. Level Curve for 70% confidence using statistics from measured data.

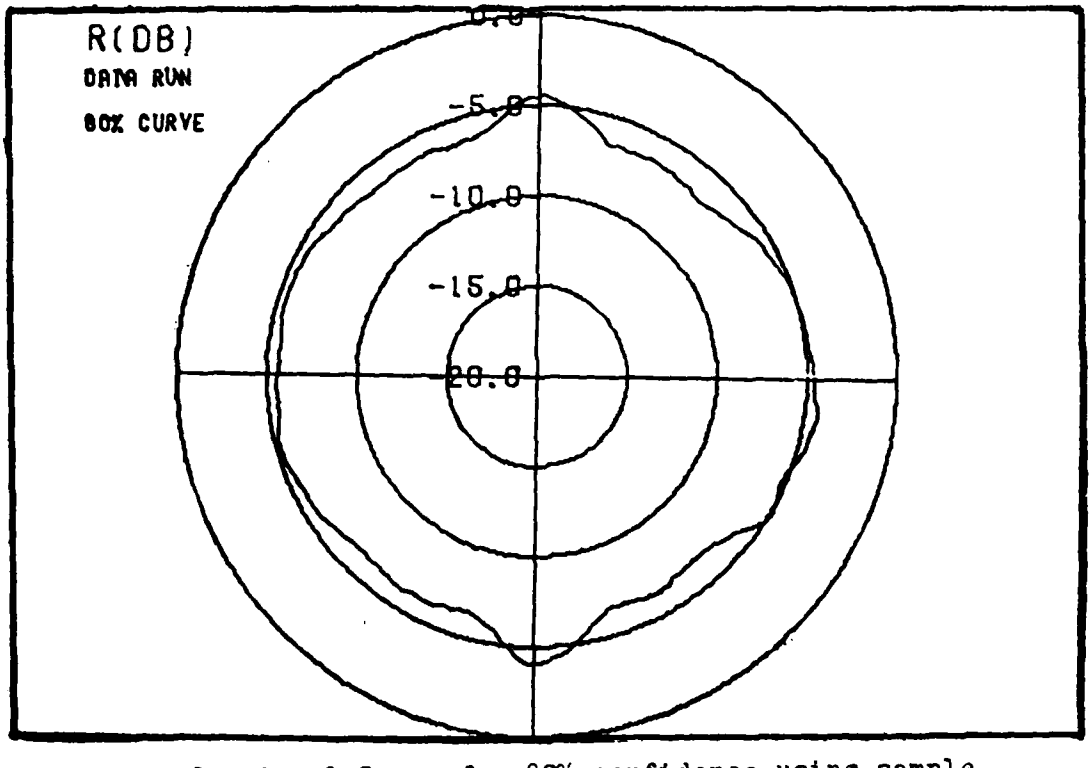

Figure 9. Level Curve for 80% confidence using sample statistics from measured data.

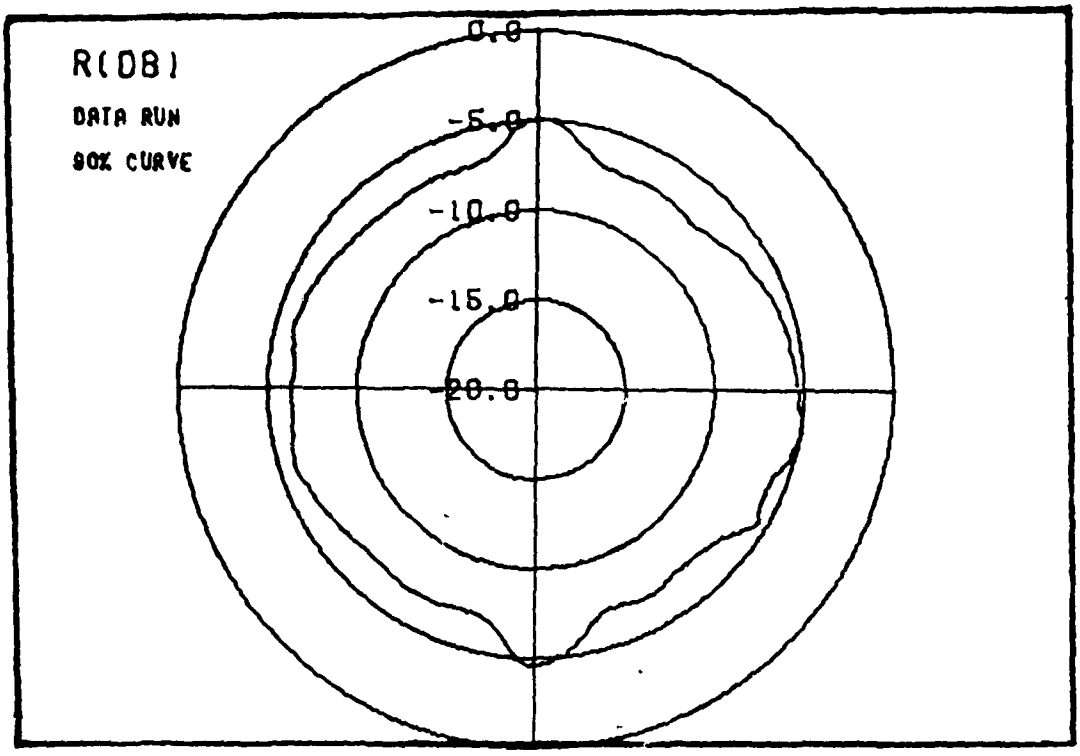

Figure 10. Level Curve for 90% confidence using sample statistics from measured data.

data as in Appendix A to determine sample statistics in order to get mean, variance and correlation distance. After deciding upon a cofiguration and assigning sample statistics to each element, he can then systematically do the same type of calculations to determine how much gain degradation multipath will give to the system. The probability of $f(\Theta)$ being greater than R at each Θ will probably not be of much use in its own right, but when used to find the probability on an angular interval it becomes very useful. If the correlation distance is greater than or equal to the length of the interval then the probability can be obtained by one sample point. Thus the probability at one point describes the probability over the whole interval.

Typically, an antenna engineer might have tried to predict system performance by taking an average of relative gain. That does not take into account the randomness associated with the multipath effect. By using statistics to determine the performance, the engineer can make a prediction that will acknowledge the randomness encountered over the length of a mission.

As an example of the usefulness of this technique the following problem is examined. Suppose a system is designed so that the minimum signal to noise ratio required for reliable communication is achieved at a maximum of 1/3 the free space maximum relative gain. There are several angles on the free space pattern that correspond to 1/3 the maximum or -4.77 db. At those angles what is the probability the antenna gives that gain or more in the presence of multipath? For example, from Figure 6 -4.77 db corresponds to 40 degrees. From Figure 2 this corresponds to a probability of nearly 1 for variance of 0.075 and decreases to about 0.05 for a variance of 0.30. Thus, for small variance there will be reliable communications at an arrival angle of 40 degrees in the presence of multipath. That reliability decreases appreciably for higher variances.

This study has only involved the antenna portion of the communication system. To really check performance of the entire system one needs to consider the modem and the rest of the system. Since signal to noise ratio is a measure of communications performance, some way has to be found to use the antenna performance to predict performance in terms of signal to noise ratio. This study has looked at performance in terms of signal to noise ratio

given a relative gain or $|f(\theta)|$. To get the overall signal to noise ratio all one has to do is average over the statistics of $|f(\theta)|$ and thus arrive at a measure of performance for the overall system.

G. Recommendations

This study has been simplistic in that the array considered was a one dimensional array. A logical extension would be to extend this model to include two and three dimensional arrays and also examine the effects of multipath in three dimensions instead of just one plane. Also assumed in this development was the uncorrelatedness of the elements and no beamsteering was used; either. The next step is to examine the case where the elements are correlated and adapt the pattern in response to some jamming threat. New performance measures for the adapted array should be developed. When the adapted weights are substituted back into the equations for performance developed in this thesis, the statistics become quite difficult to evaluate.

Bibliography

1. Agrawal, V.D. and Y.T. Lo. "Distribution of Sidelobe Level in Random Arrays," Proceedings of the IEEE: 1764-1765, October, 1969.

2. Freund, J.E. Mathematical Statistics (Second Edition). Englewood Cliffs, New Jersey: Prentice-Hall, Inc., 1971.

3. Gardner, W.A. and L.E. Franks. "Characterization of Cyclostationary Random Processes," IEEE Transactions on Information Theory, IT-21: 4-14, January 1975.

4. Kraus, J.D. Antennas. New York: McGraw-Hill Book Company, 1950.

5. Lo, Y.T. "A Mathematical Theory of Antenna Arrays with Randomly Spaced Elements," IEEE Transactions on Antennas and Propagation, AP-12: 257-268, May 1964.

6. Papoulis, A. Probability, Random Variables, and Stochastic Processes. New York: McGraw-Hill Book Company, 1965.

7. Papoulis, A. Signal Analysis. New York: McGraw-Hill, Inc., 1977.

8. Peebles, P.Z. Communication System Principles. Reading, Massachusetts, 1976.

9. Ricardi, L.J. A Summary of Methods for Producing Nulls in an Antenna Radiation Pattern. ESD-TR-76-254. Technical Note 1976-38, Lincoln Laboratories, Massachusetts Institute of Technology, Lexington, Massachusetts: 2 September 1976.

10. Steinberg, B.D. Principles of Aperture and Array System Design. New York: Wiley and Sons, 1976.

11. Van Trees, H.L. Detection, Estimation, and Modulation Theory. New York: John Wiley and Sons, 1968.

12. Ziemer, R.E. and W.H. Tranter. Principles of Communications. Boston: Houghton-Mifflin, 1976.

13. ----- IBM System/360 Scientific Subroutine Package (Third Edition). (360-CM-03X) Version II Programmers Manual: White Plains, New York, 1967.

Appendix A: Data Analysis

A. Measurements

Measured data is available for three individual, but identical antennas located at different places on an A-10 aircraft. The data was obtained through Capt. Donald Ottinger at RADC/DCID at Rome Air Development Center, Griffiss AFB, New York. Figure 11 shows a side view of the A-10 with the antenna locations marked. Measurements were taken for the antennas one at a time. These measurements were made at a fixed location in space while the aircraft was rotated through 360 degrees of azimuth angle. The elevation angle was then changed and the aircraft was rotated again. Figure 12 illustrates the physical setup for the measurements. Azimuth plots were taken for elevation angles of -15, 0, 15, and 30 degrees, each at frequencies of 257, 300, and 385 MHz. The angle, θ, is a measure of azimuth; thus, each data plot is measured power in one plane for θ between 0 and 360 degrees. The

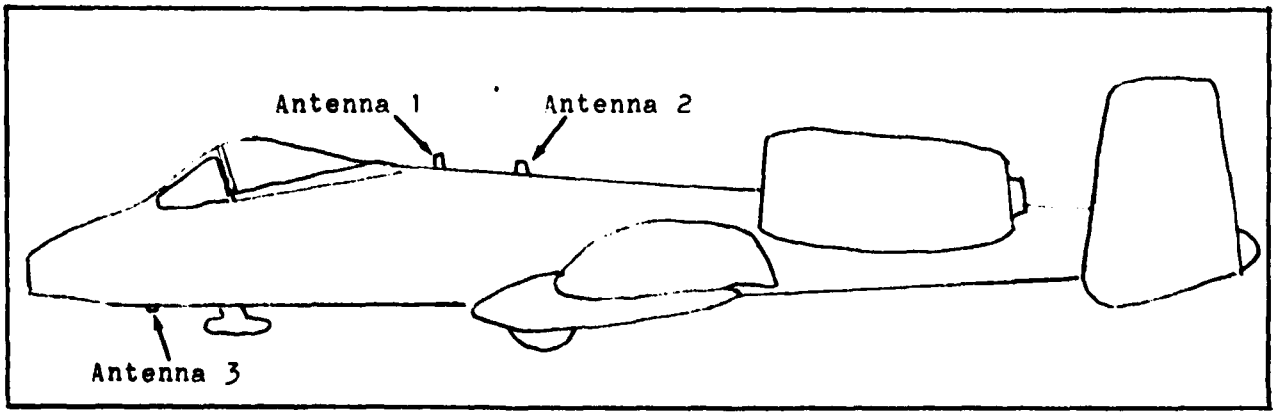

Figure 11. Antenna Locations for Measured Data on A-10 Aircraft.

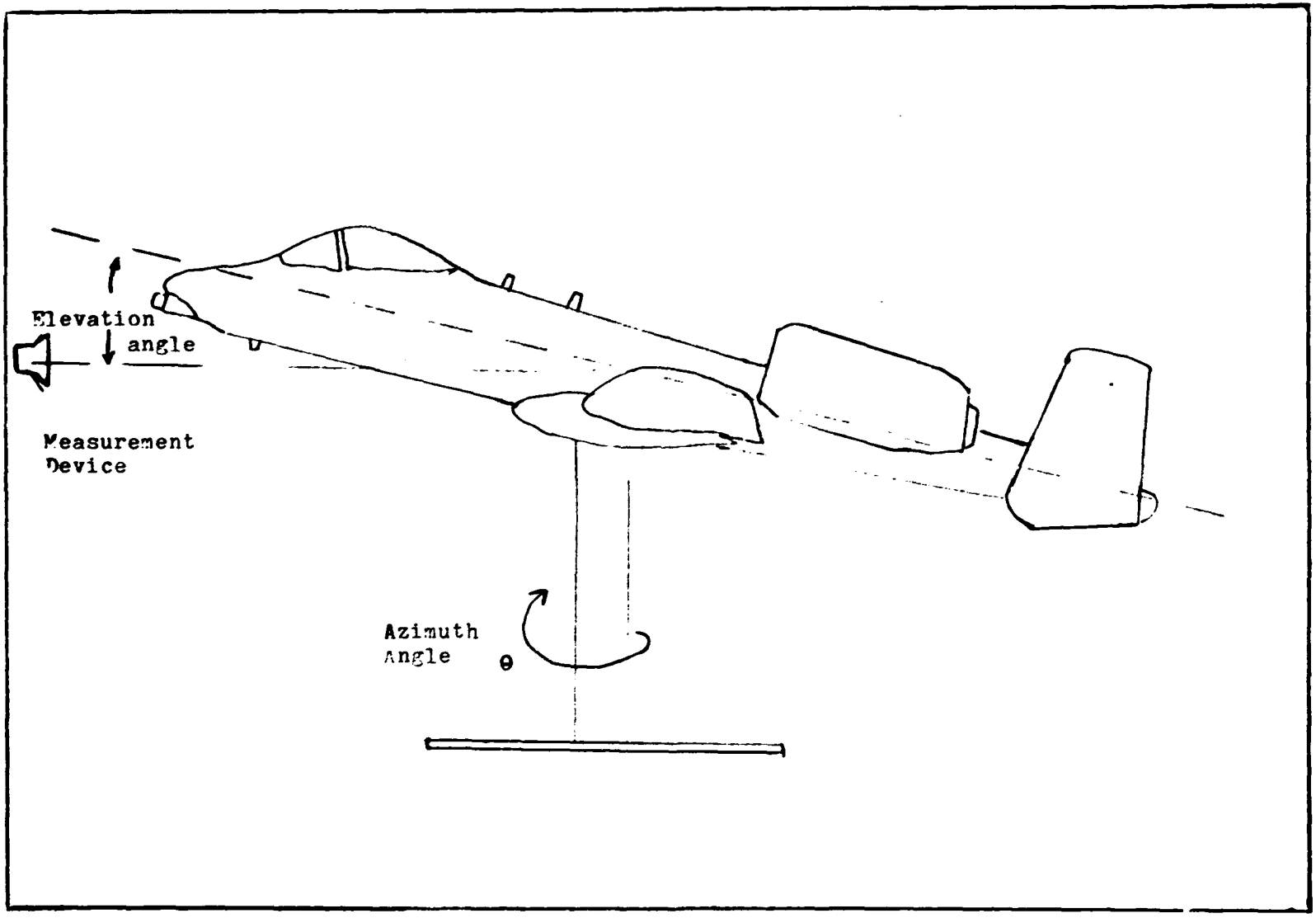

Figure 12. Physical Measurement Setting.

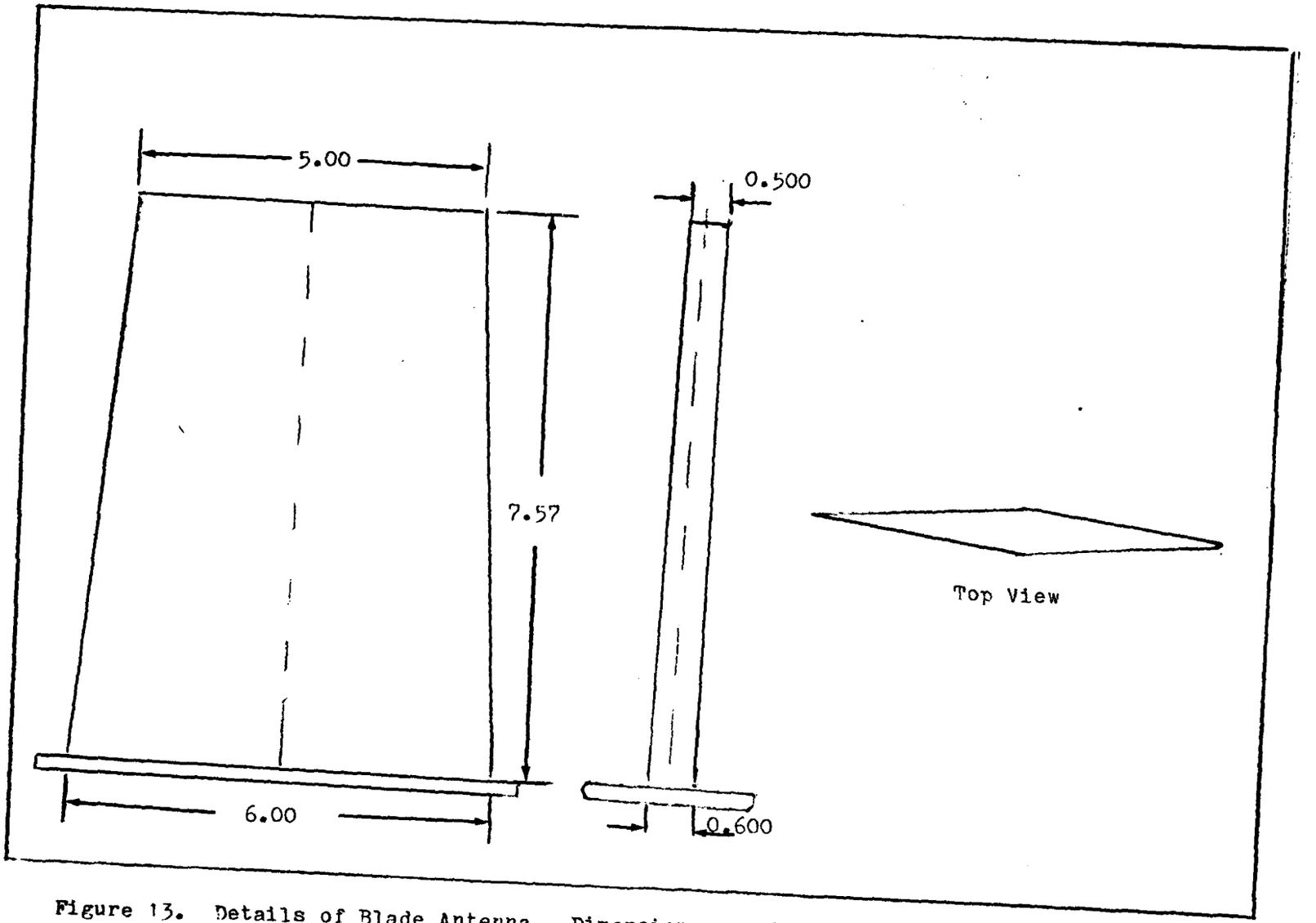

Figure 13. Details of Blade Antenna. Dimensions are in inches.

data plots are contained in Appendix C. The antenna used was a blade antenna. A diagram of this antenna is shown in Figure 13.

B. Mean and Variance

There are 12 plots available for each of the three elements. Each of these is a realization of the random process, $G_i(\Theta)$. Sampling the process at a given Θ yields an ensemble of 12 realizations of a random variable. This is because whenever the random process, $G_i(\Theta)$, has Θ fixed the result is a random variable. An illustration of the realizations of a random process is given in Figure 14. If p_i is a sample of one of the realizations at a given Θ, the mean of the random variable at a given Θ is estimated by

$$\hat{m} = \frac{1}{N} \sum_{i=1}^{N} p_i \qquad \text{(A-1)}$$

The variance of the data at a given Θ is estimated by

$$\hat{\sigma}^2 = \frac{1}{N-1} \sum_{i=1}^{N} (p_i)^2 - \frac{N}{N-1} (\hat{m})^2 \qquad \text{(A-2)}$$

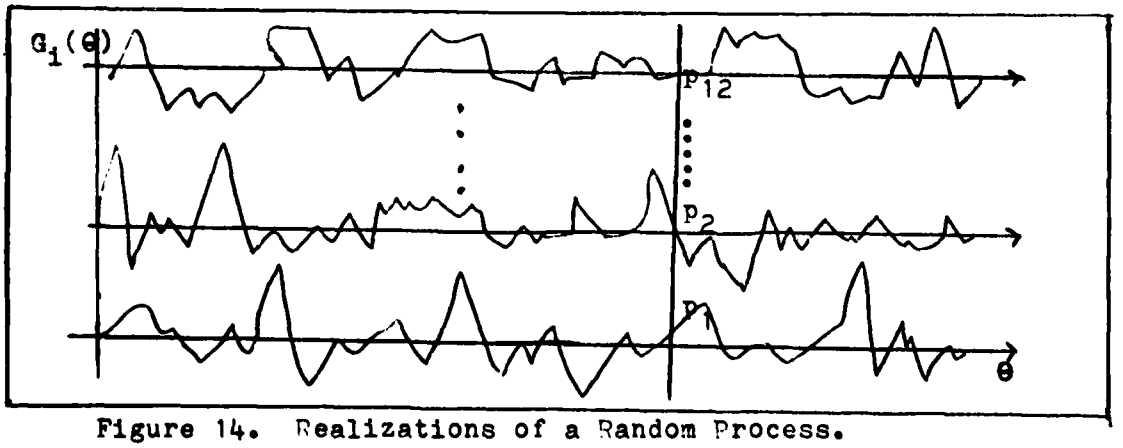

Figure 14. Realizations of a Random Process.

If each of the samples are identically independently distributed these two estimators are unbiased. The variances of the estimates vary approximately on the order of 1/N, so when evaluating the Tchebycheff inequality, given by

$$Pr\left\{|\hat{x} - x| \geq \epsilon\right\} \leq \left(\frac{var(\hat{x})}{\epsilon}\right)^2 \qquad (A-3)$$

the estimator does not become really accurate until N is on the order of several hundred. With 12 realizations, the estimators are not very good, but there are only twelve plots for each element. These calculations for mean and variance are made at every one degree and are plotted in Figures 15-23. Figures 15-17 are plots of the mean in db and Figures 18-20 are the plots of the algebraic mean. The variance plots are in Figures 21-23. These values for mean and variance can then be substituted into the performance measure equations to determine performance as in chapters III and IV. Clearly the mean and variance change with arrival angle to reflect the change in geometry caused by rotating the aircraft.

C. Correlation Distance

In order to calculate the probability that $|f(\Theta)|$ is greater than some threshold on an interval, some estimate of correlation distance is needed. To get the correlation distance one needs to look at the covariance of the data waveforms. The autocovariance of each waveform is given by

$$C_i(\Delta\Theta) = \frac{1}{T}\int_0^T (p_i(\Theta) - \hat{m}(\Theta))(p_i(\Theta + \Delta\Theta) - \hat{m}(\Theta + \Delta\Theta))\, d\Theta \qquad (A-4)$$

This function is a covariance assuming the process is stationary. T is the interval on which the function is observed and in this case it is 360 degrees. When using sampled data this can be approximated by a series of covariances for different values of shift in θ. Given a series of samples representing one waveform $A_1, A_2, \ldots, A_N$, for a shift of j, the autocovariance is given by (Ref 13:59)

$$R_j = \frac{1}{N-j+1} \sum_{m=1}^{N-j+1} (A_m - AVER)(A_{m+j-1} - AVER) \qquad (A-5)$$

where

$$AVER = \frac{1}{N} \sum_{i=1}^{N} A_i \qquad (A-6)$$

N = the number of sample points in A

j = 1, 2, 3, ... L representing $\Delta\theta$ of 0, 1, 2, ... L-1

The R_j can be plotted versus $\Delta\theta$ for the covariance of each waveform. R_j is autocovariance not to be confused with autocorrelation. The function depicted by R_j versus theta shift is $C_i(\theta)$, the autocovariance of the single waveform. What is needed is an estimate of autocovariance for the entire process and not just each waveform, however. The total autocovariance is then estimated by

$$C(\Delta\theta) = \frac{1}{12} \sum_{i=1}^{12} C_i(\Delta\theta) \qquad (A-7)$$

This estimate is unbiased and it has the same problem as the previous estimates: not enough waveforms. From these autocovariances the correlation distances can be found by the angle

where the covariance reaches 1/10 of its peak value (1/10 is an arbitrary assignment depending on the definition of correlation distance). This works out to about 15 or 20 degrees. This can then be used in calculating the probability that $|f(\theta)|$ is greater than a threshold on some interval. Sample autocovariance for each of the three elements are plotted in Figures 24-26.

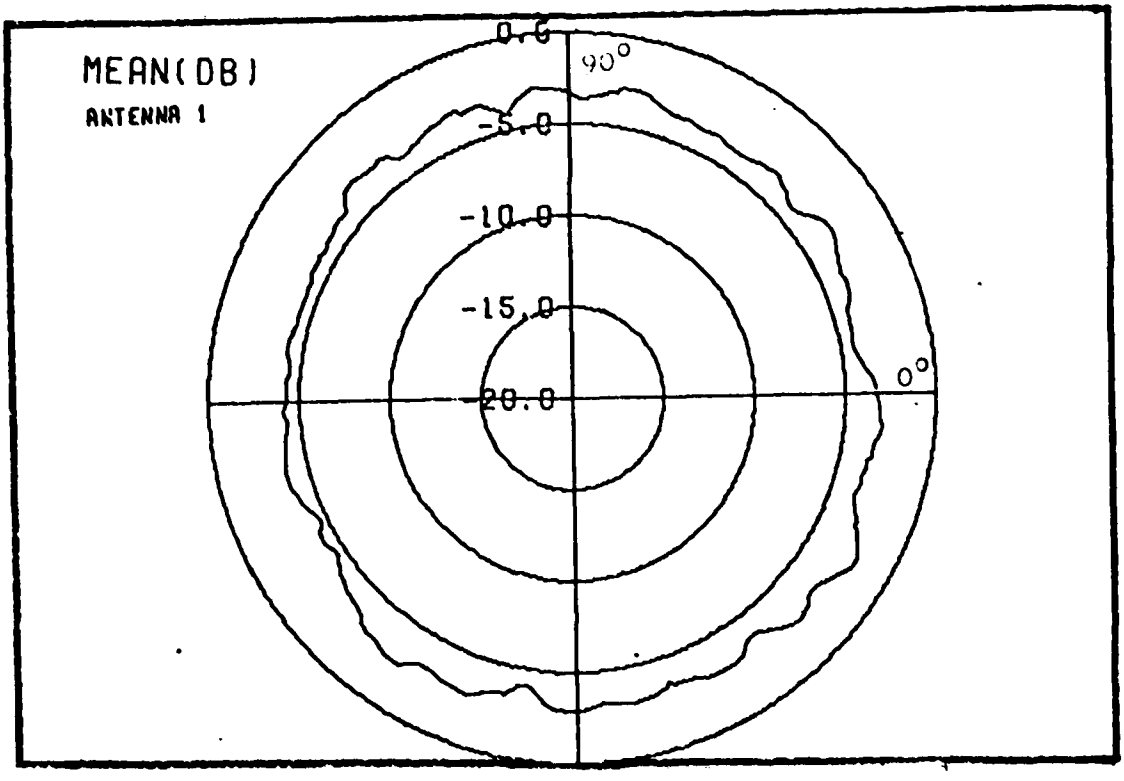

Figure 15. Sample Mean in db; Antenna 1

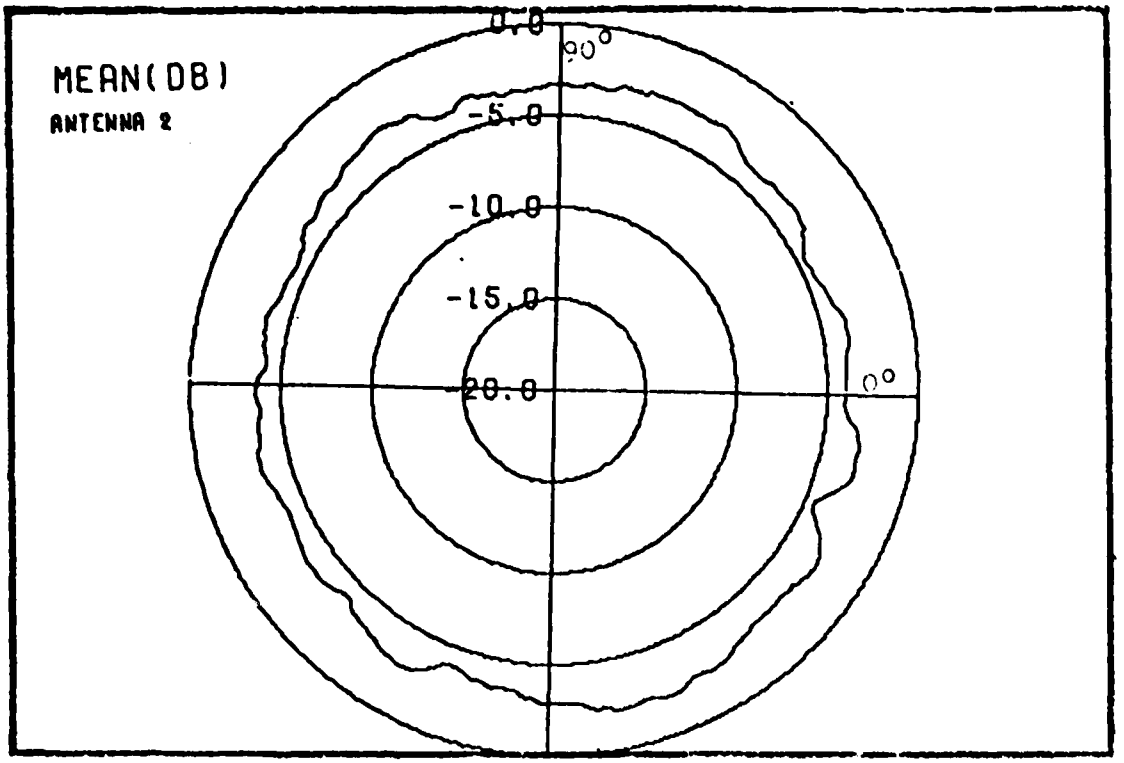

Figure 16. Sample Mean in db: Antenna 2

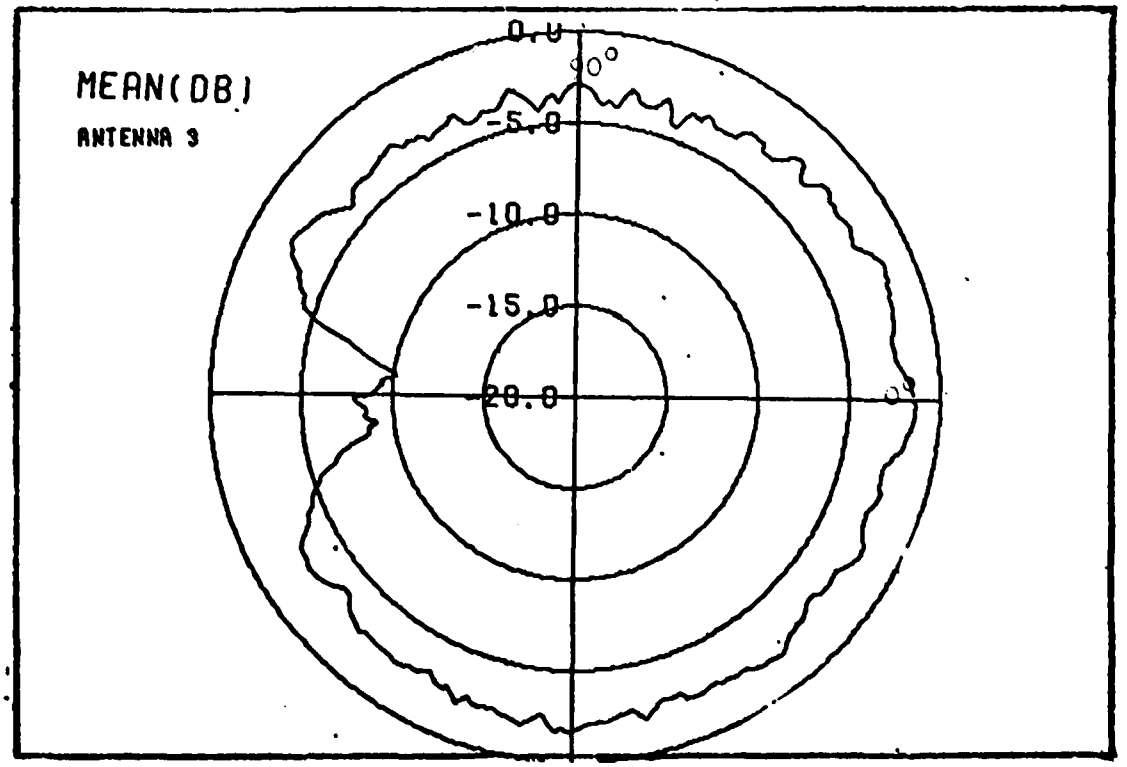

Figure 17. Sample Mean in db: Antenna 3

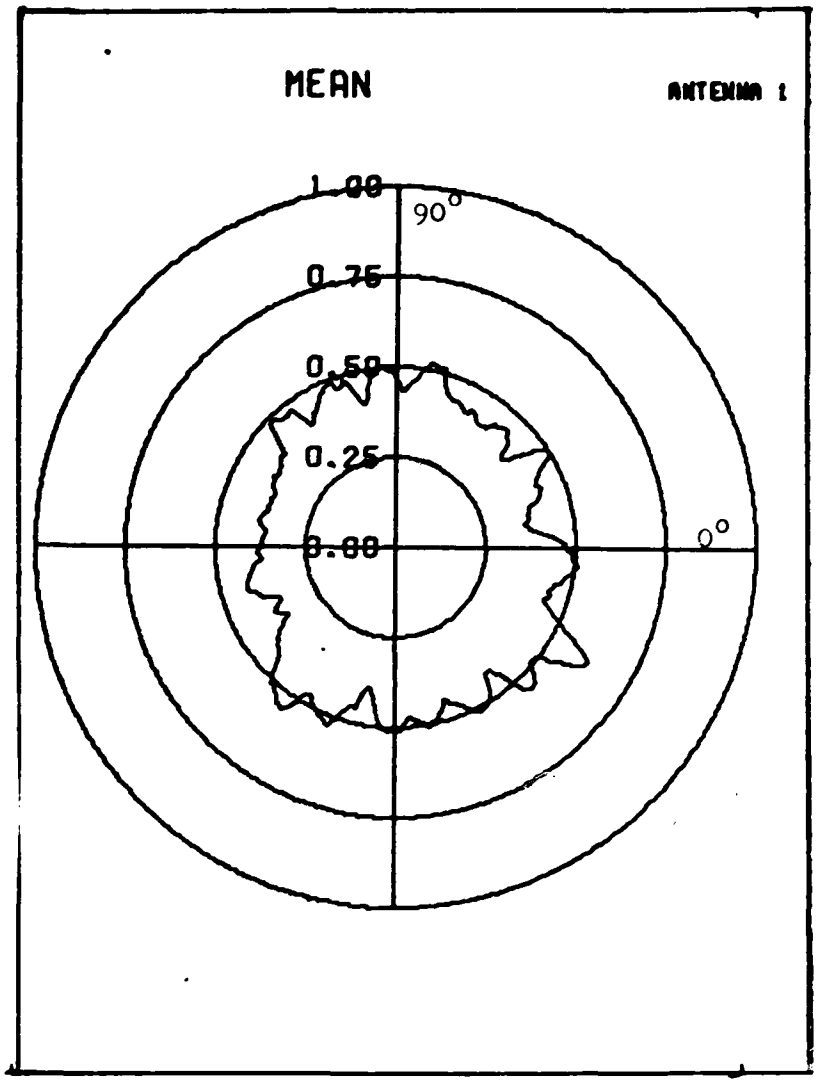

Figure 18. Sample Mean(algebraic): Antenna 1

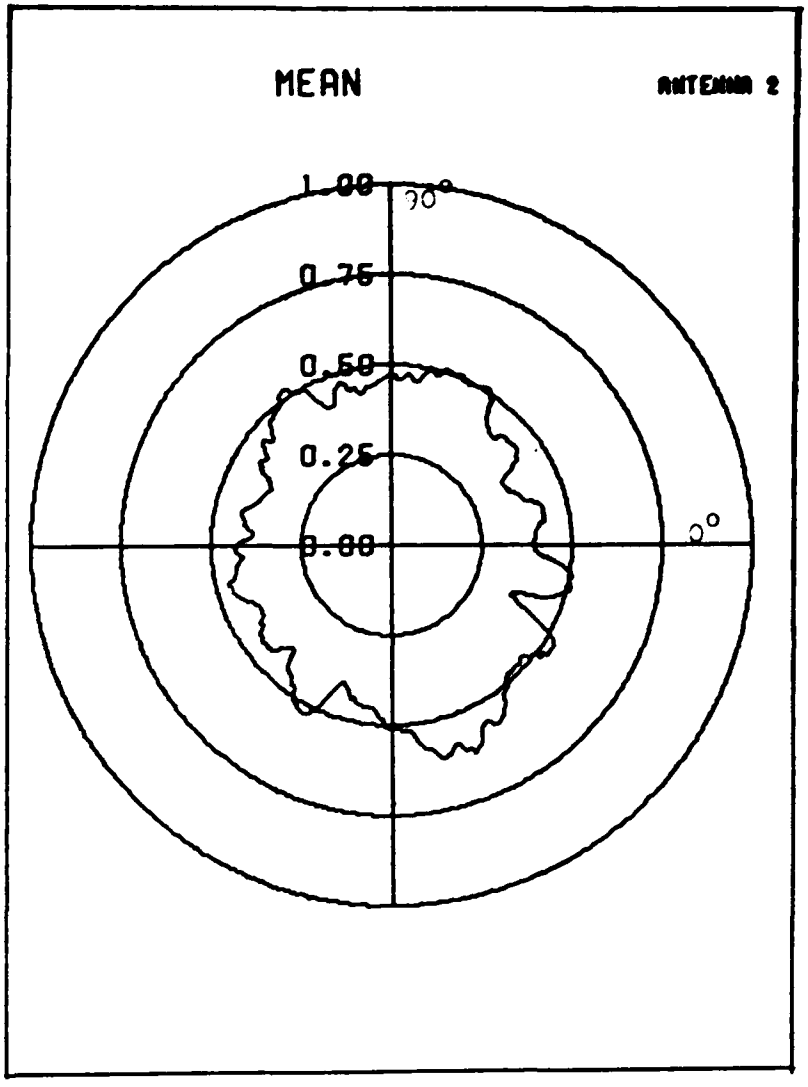

Figure 19. Sample Mean(algebraic): Antenna 2

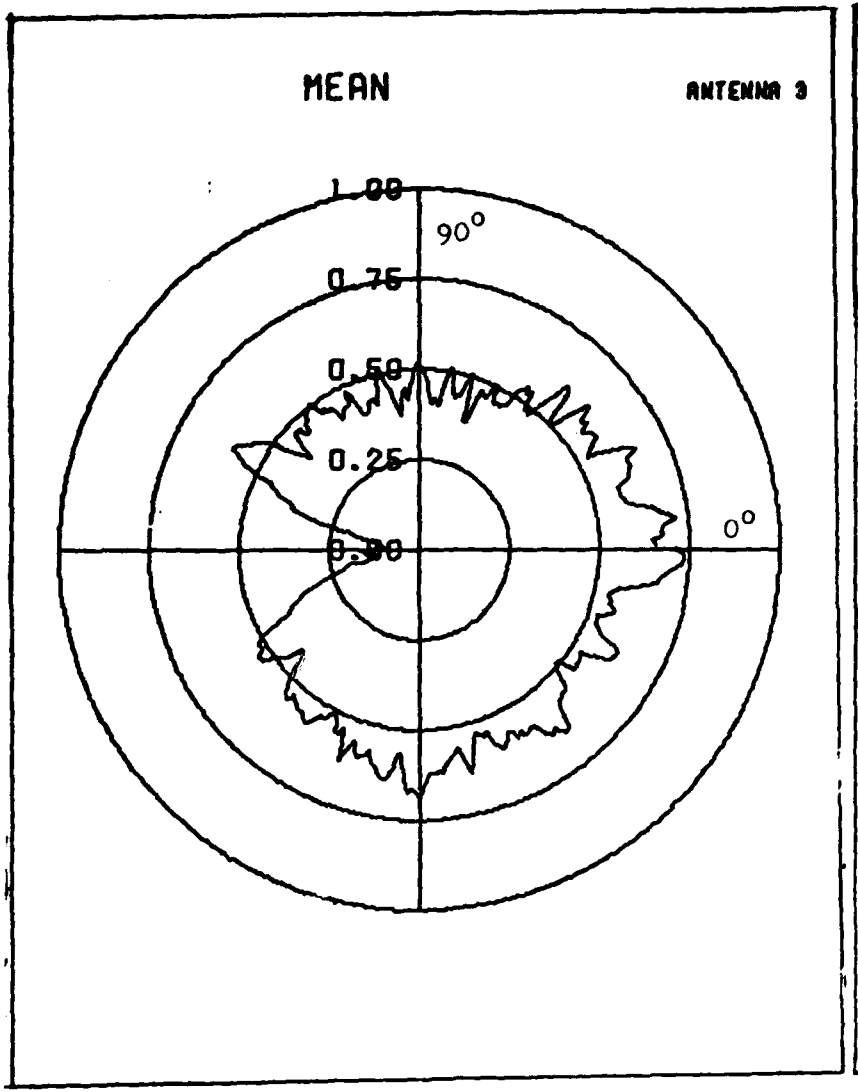

Figure 20. Sample Mean(algebraic):Antenna 3

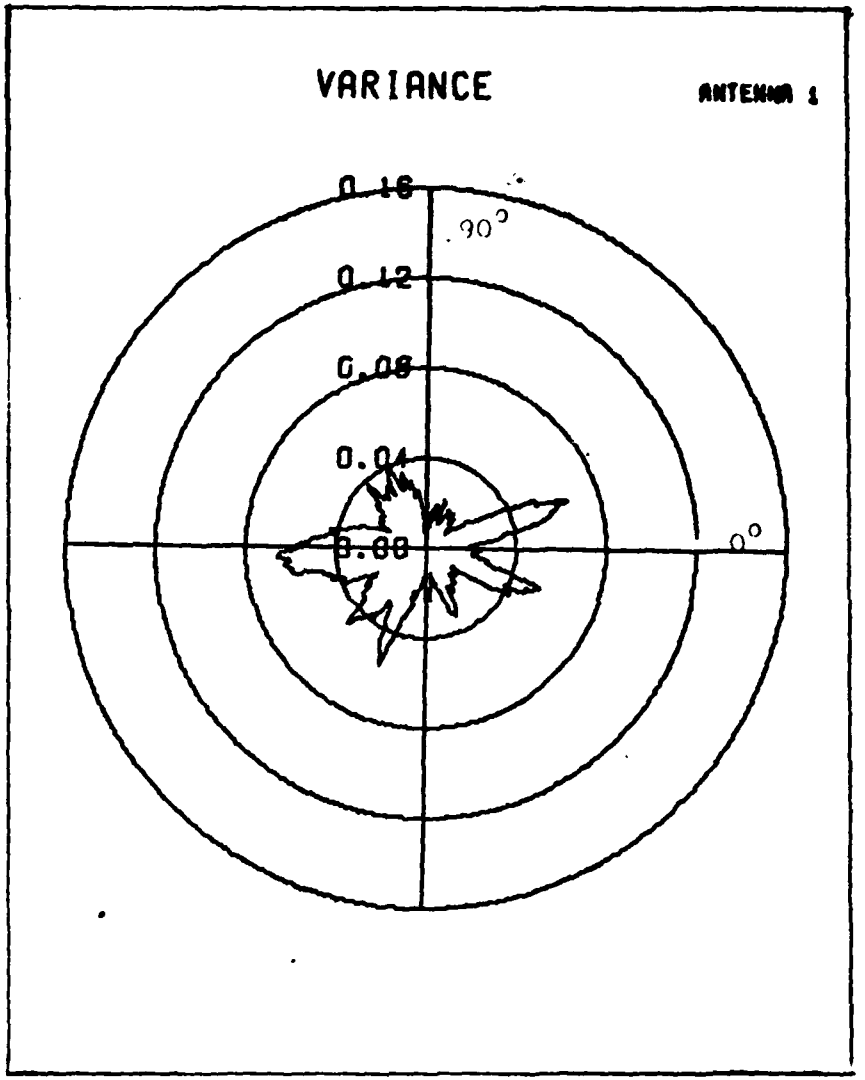

Figure 21. Sample Variance: Antenna 1

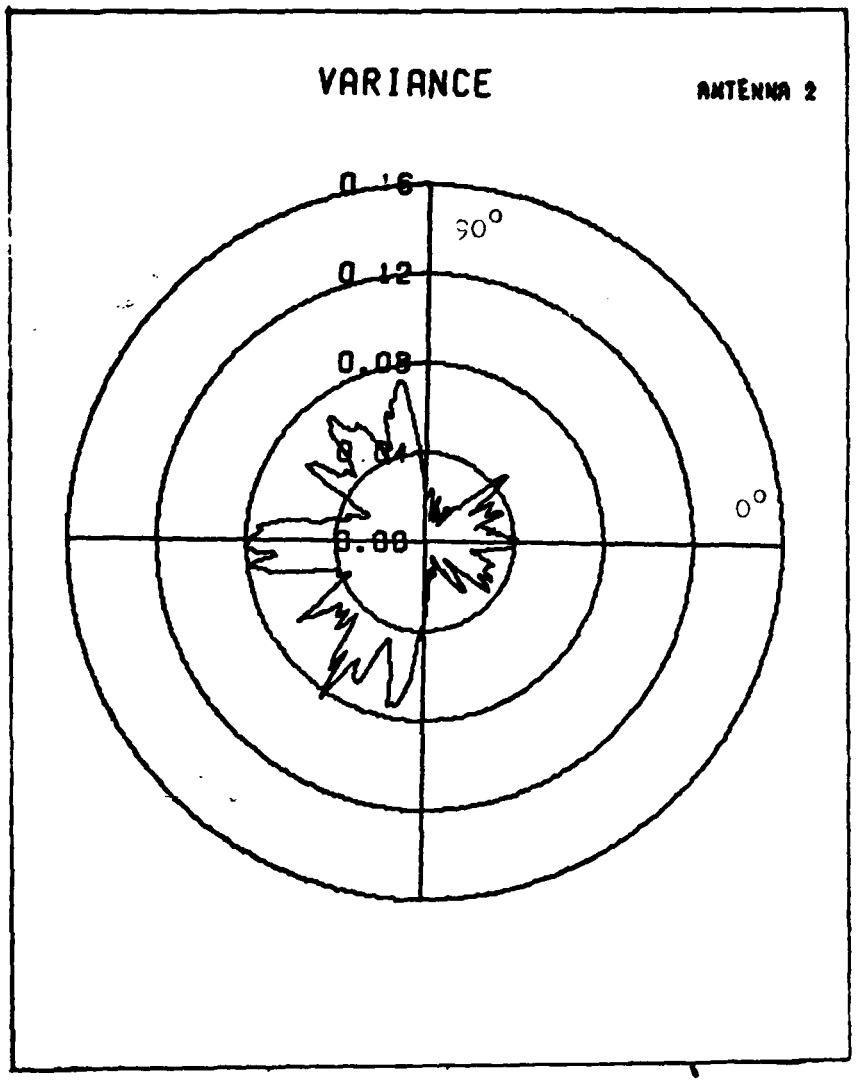

Figure 22. Sample Variance: Antenna 2

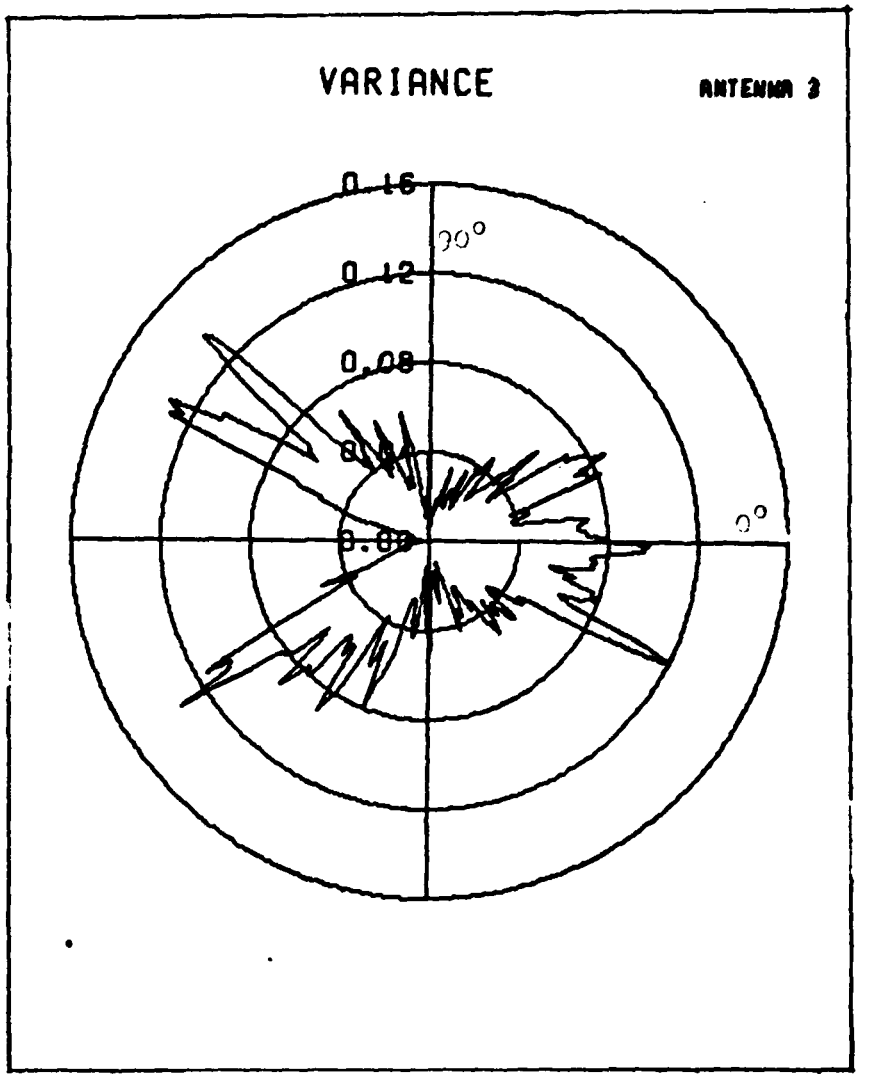

Figure 23. Sample Variance: Antenna 3

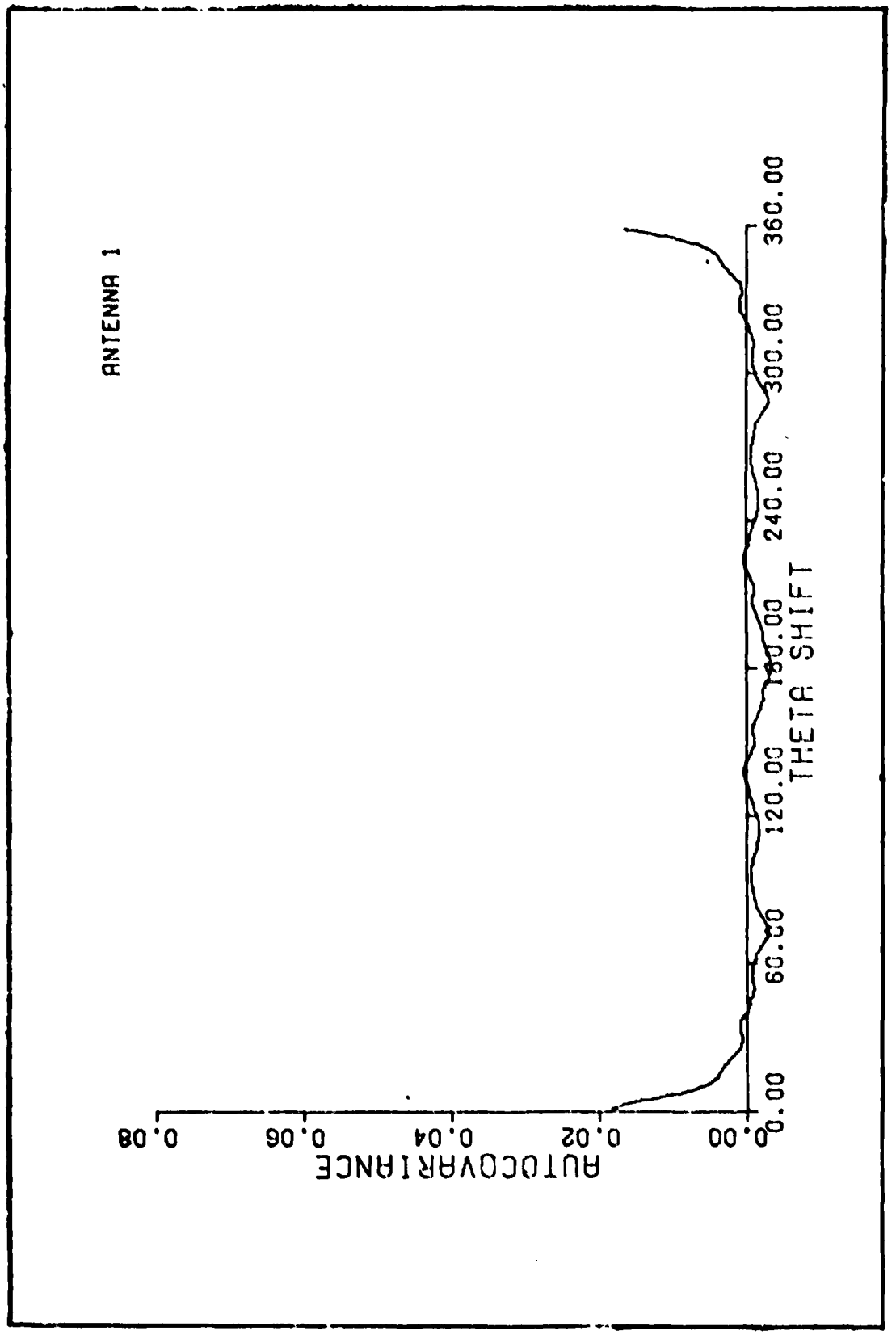

Figure 24. Autocovariance from measured data: Antenna 1.

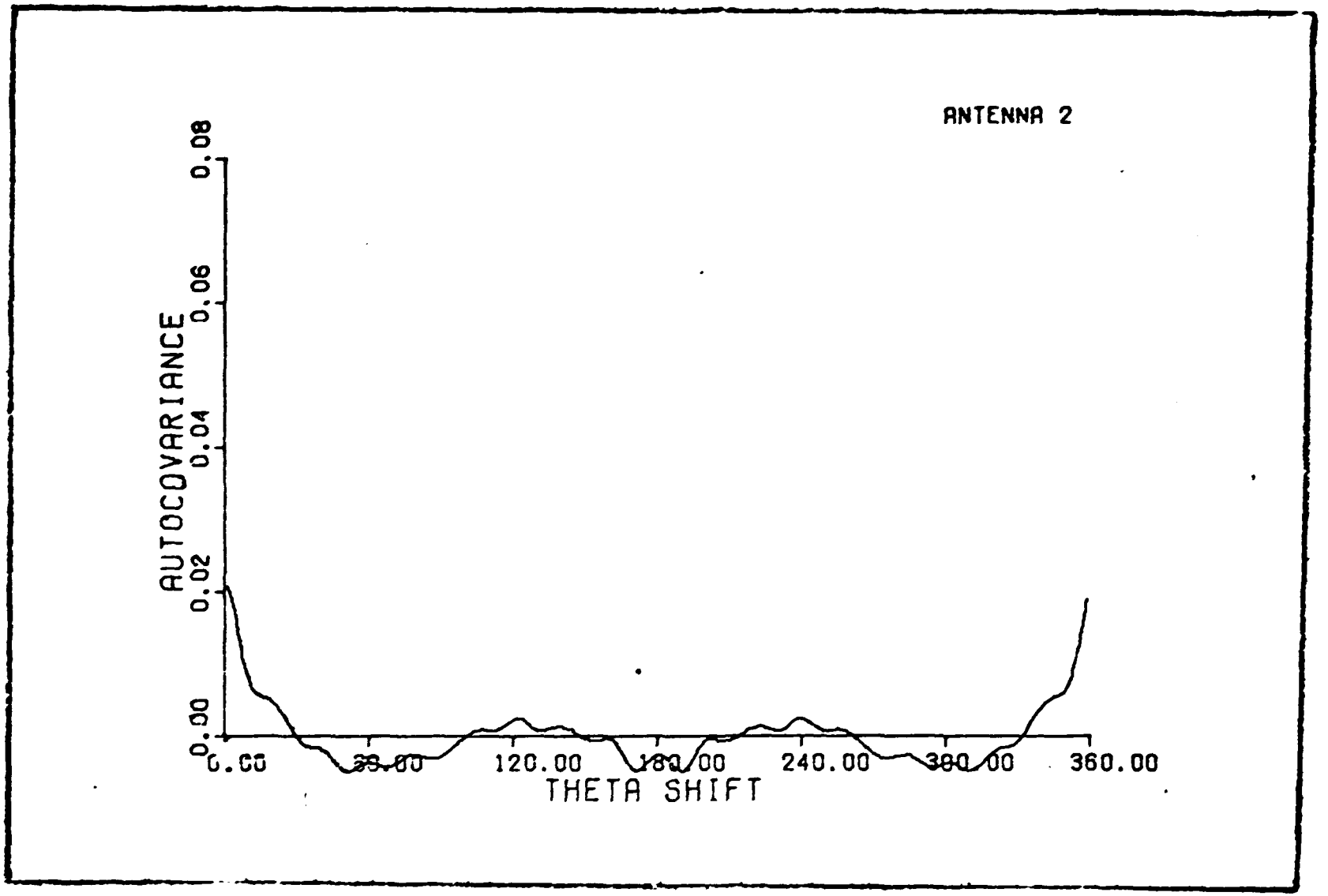

Figure 25. Autocovariance from Measured Data: Antenna 2

Appendix B: Supplementary Probability Plots

This appendix contains plots for the first performance measure determined in chapter III and plotted in chapter IV. These plots are the probability that the magnitude of $f(\theta)$ is greater than a threshold R, for R=1,2,3 at four different variances for the array. Figure 27 is for var=0.075 ; Figure 28 is for var=0.150 ; Figure 29 is for var=0.225 ; and Figure 30 is for var=0.300.

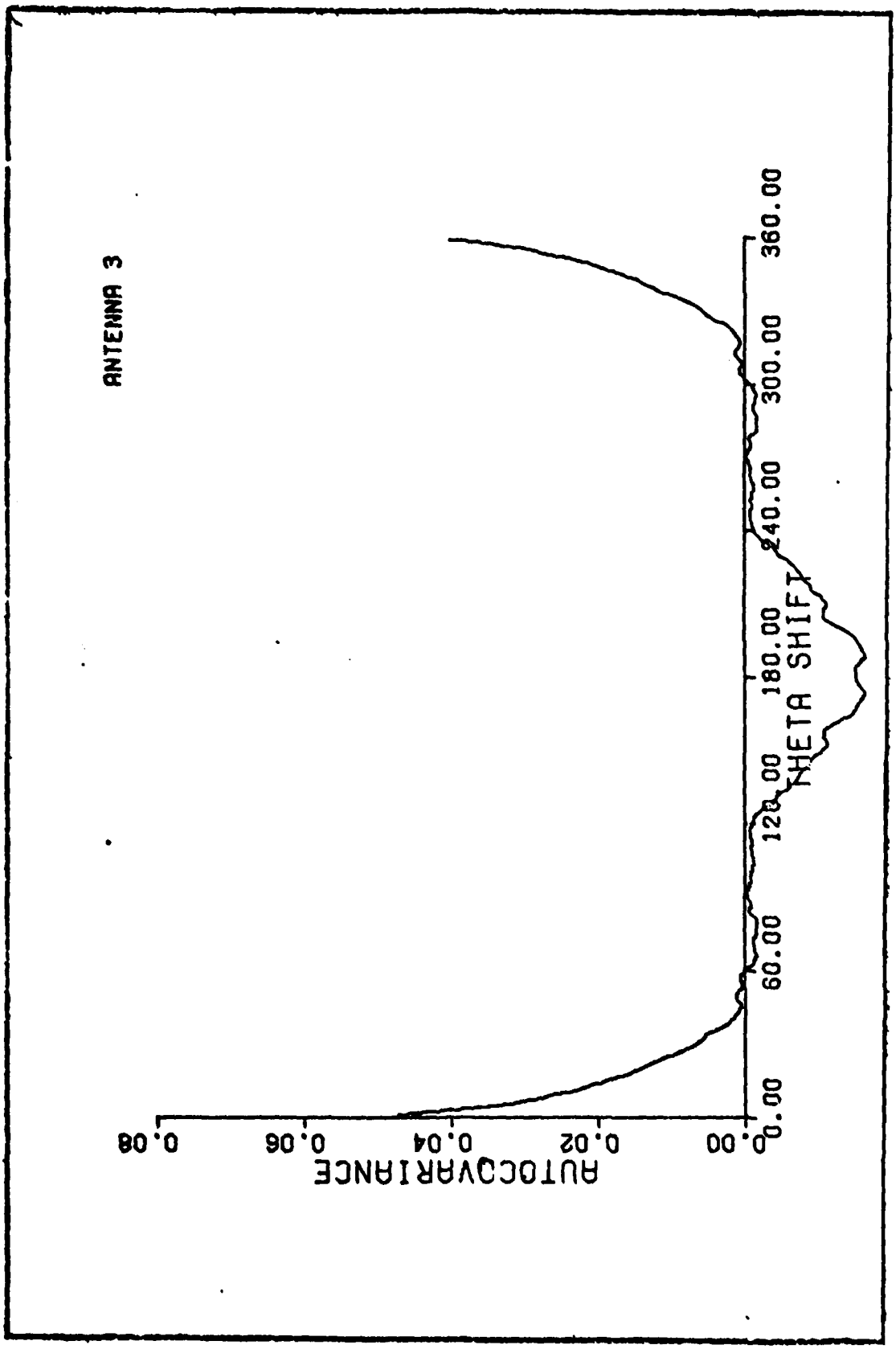

Figure 26. Autocovariance from Measured Data: Antenna 3.

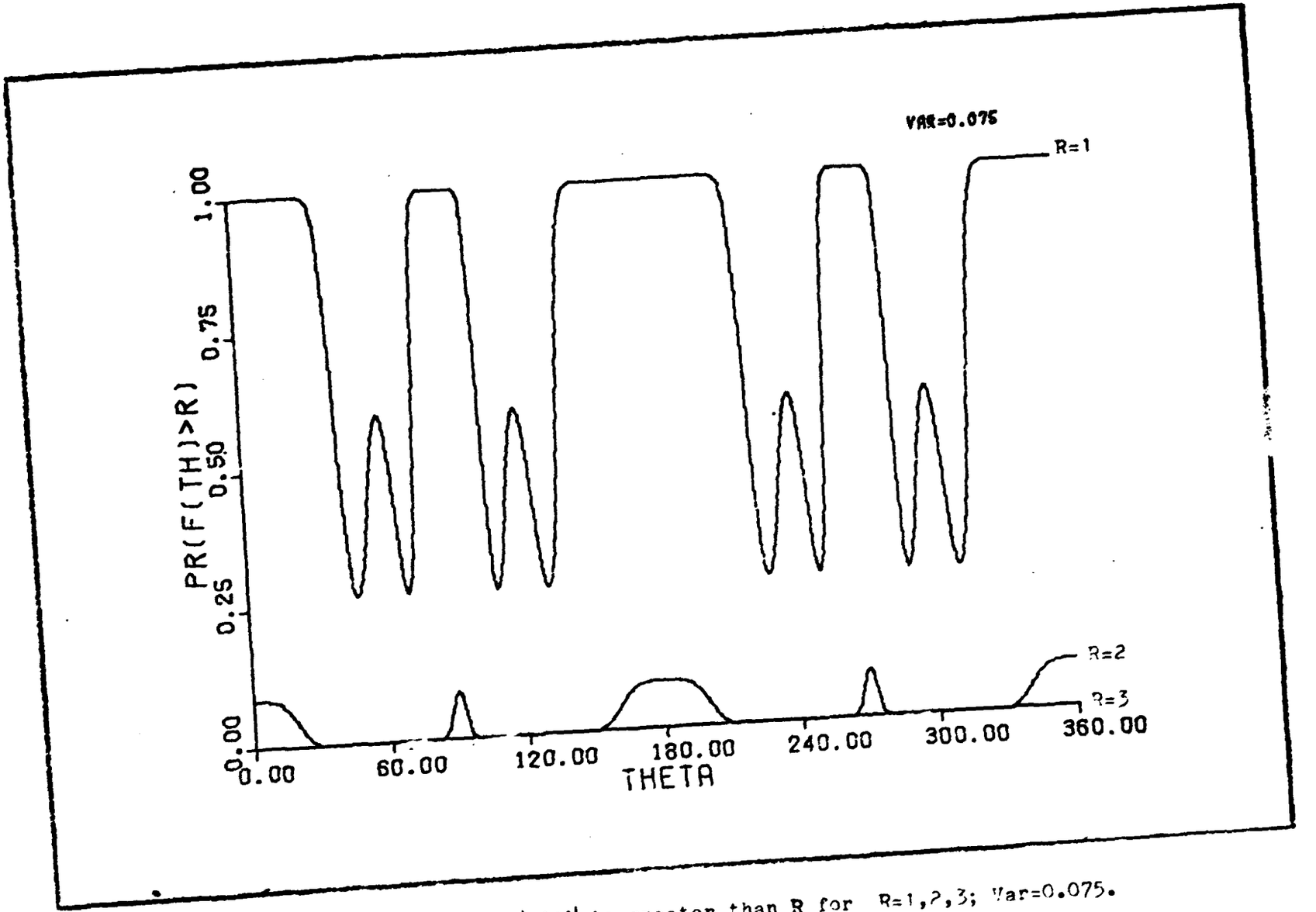

Figure 27. Probability that $|f(\theta)|$ is greater than R for R=1,2,3; Var=0.075.

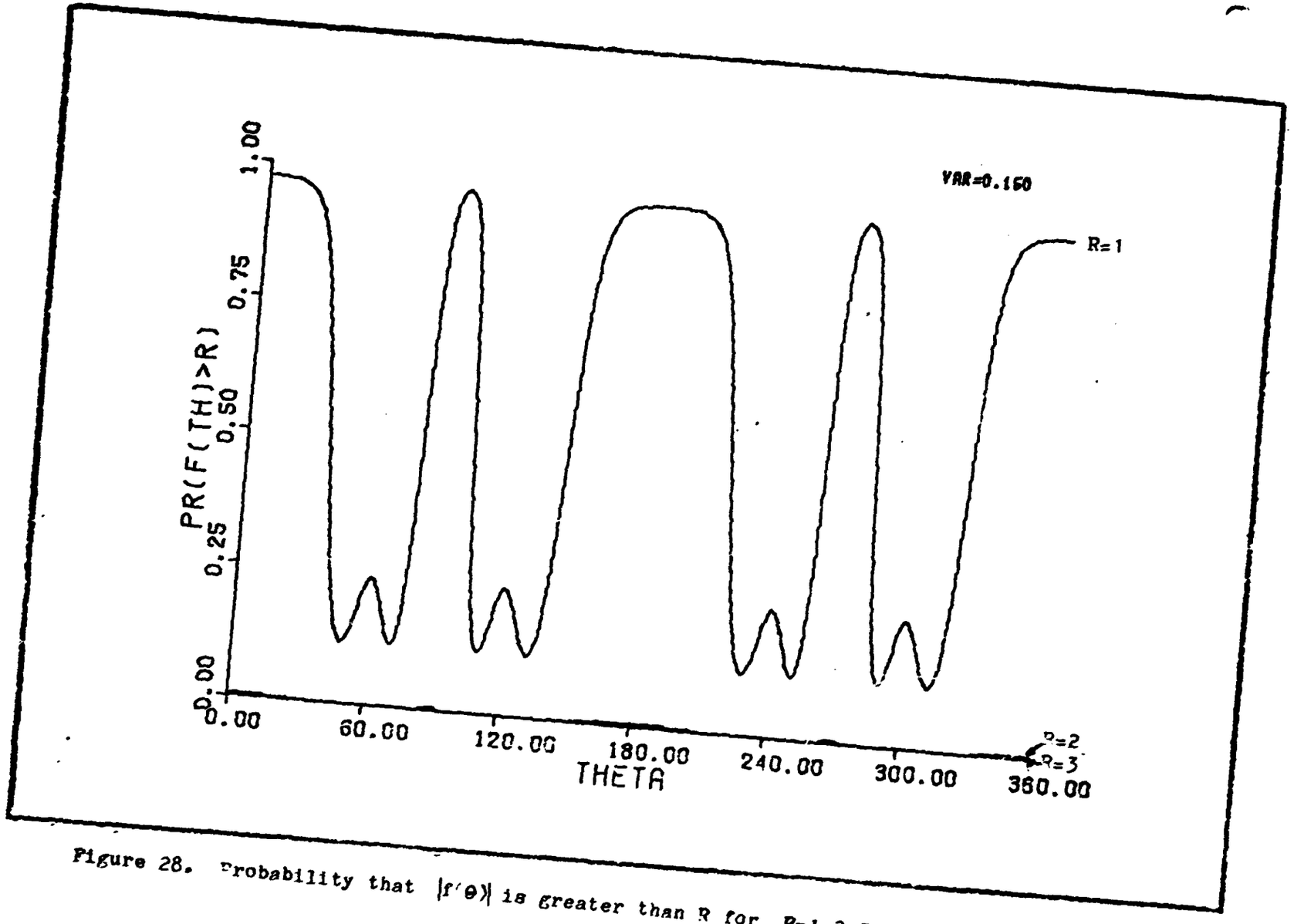

Figure 28. Probability that $|f(\theta)|$ is greater than R for R=1,2,3; Var=0.150.

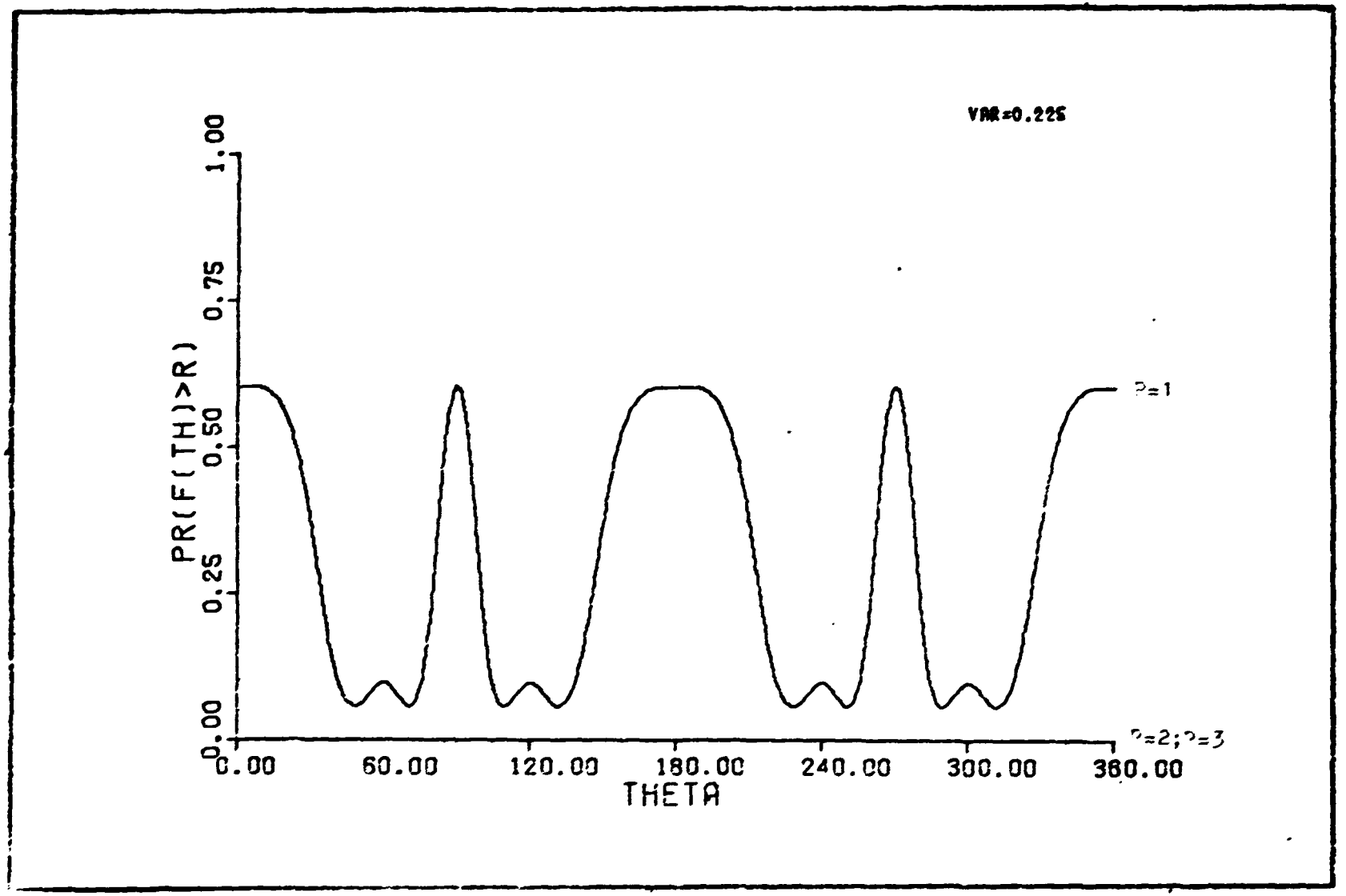

Figure 29. Probability that $|f(\theta)|$ is greater than R for R=1,2,3; Var=0.225.

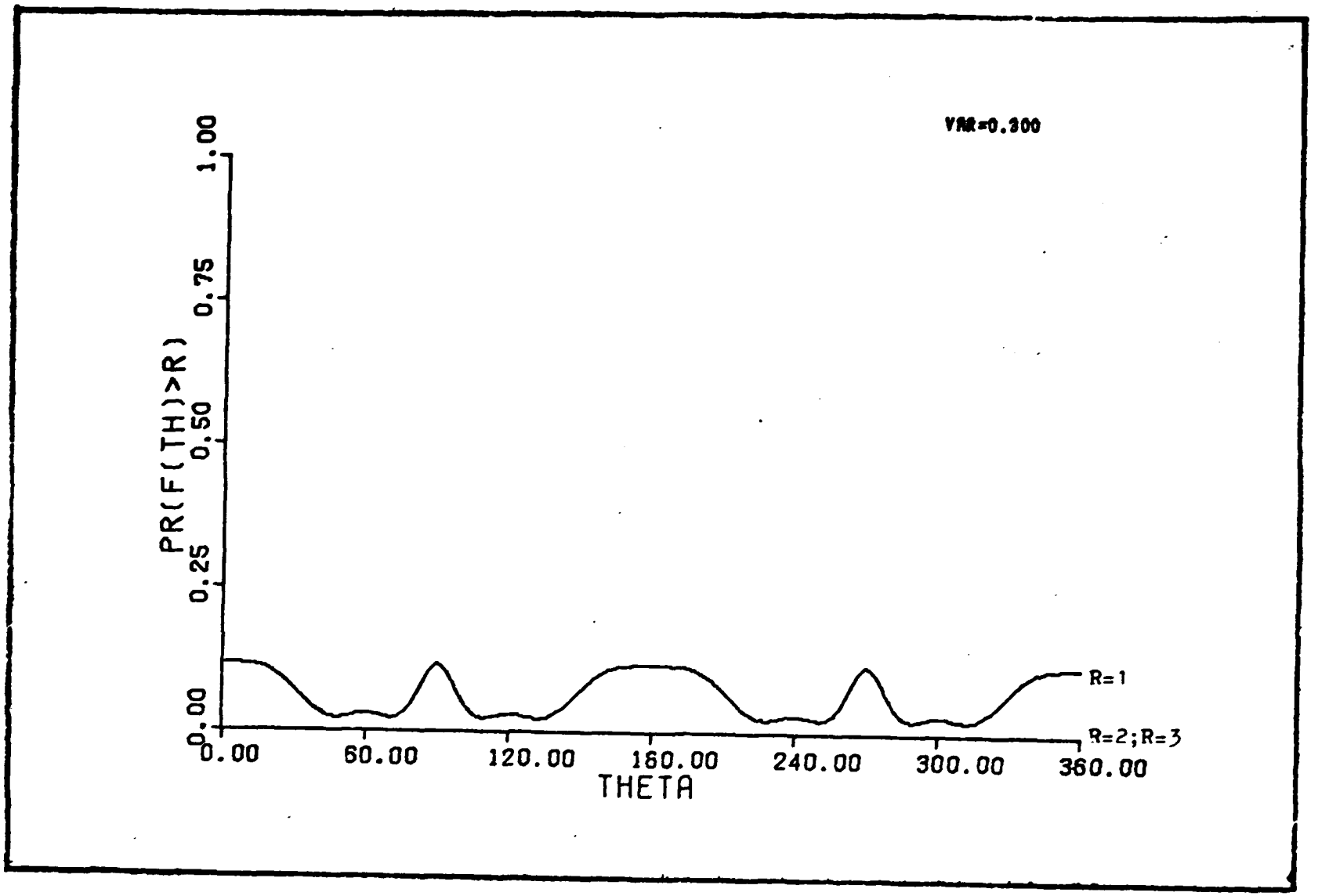

Figure 30. Probability that $|f(\theta)|$ is greater than R for R=1,2,3; Var=0.300.

Appendix C: Data Plots

This appendix contains the data plots used for determining the statistics of the array elements as outlined in Appendix A. All the plots are for vertical polarization and they are plots of measured power in one plane. Figures 31-42 are the plots for Antenna 1 ; Figures 43-54 are the plots for Antenna 2; and Figures 55-66 are the plots for Antenna 3. The plots for each element are for elevations of -15, 0, 15, and 30 degrees each at frequencies of 257, 300, and 385 MHz. The letters "SGH" found on each plot refer to Standard Gain Horn. The SGH level marked on each plot refers to 0 db of relative gain.

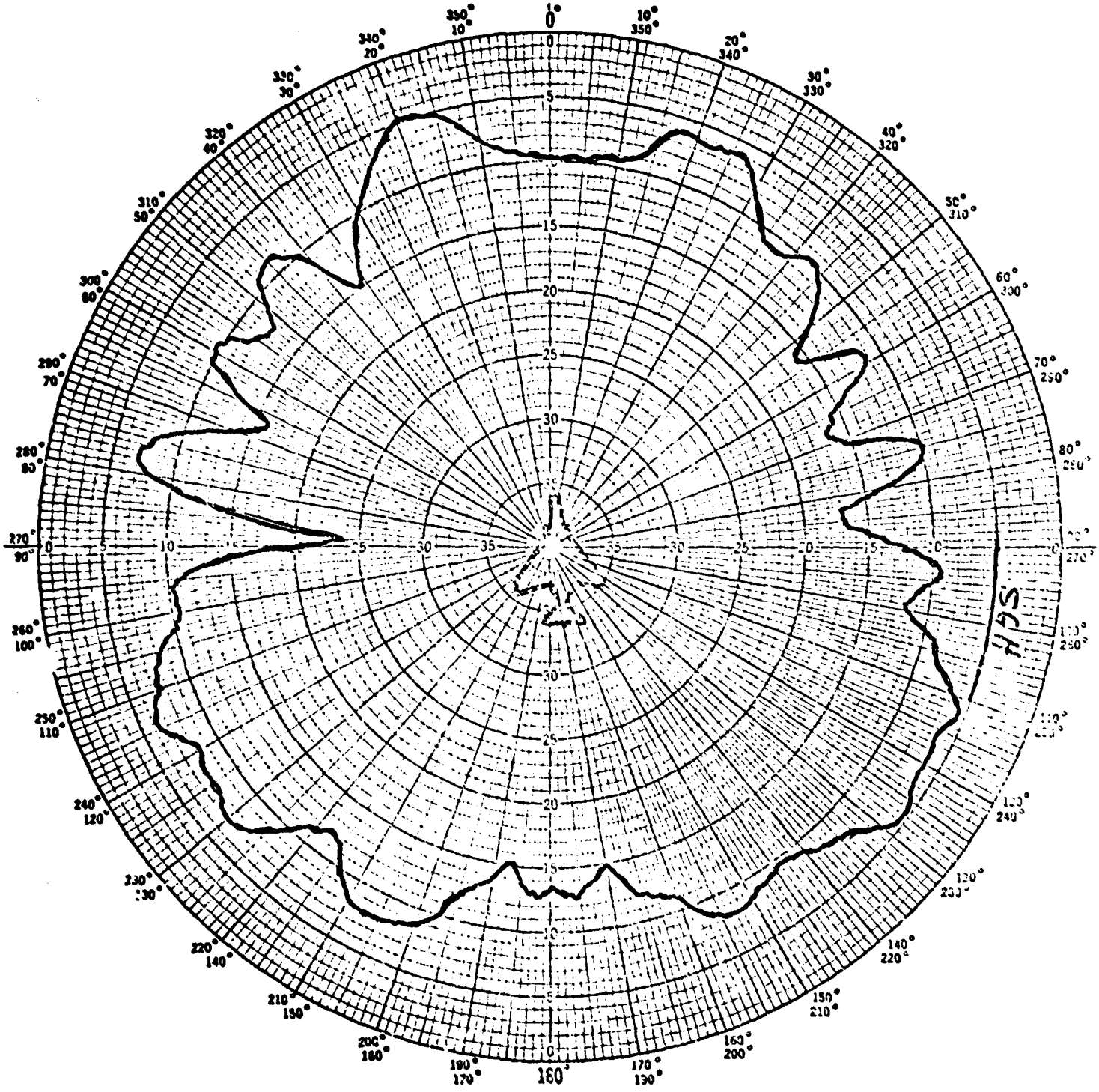

Figure 31. Data Plot: Antenna 1; elevation=30°; frequency=257 MHz.

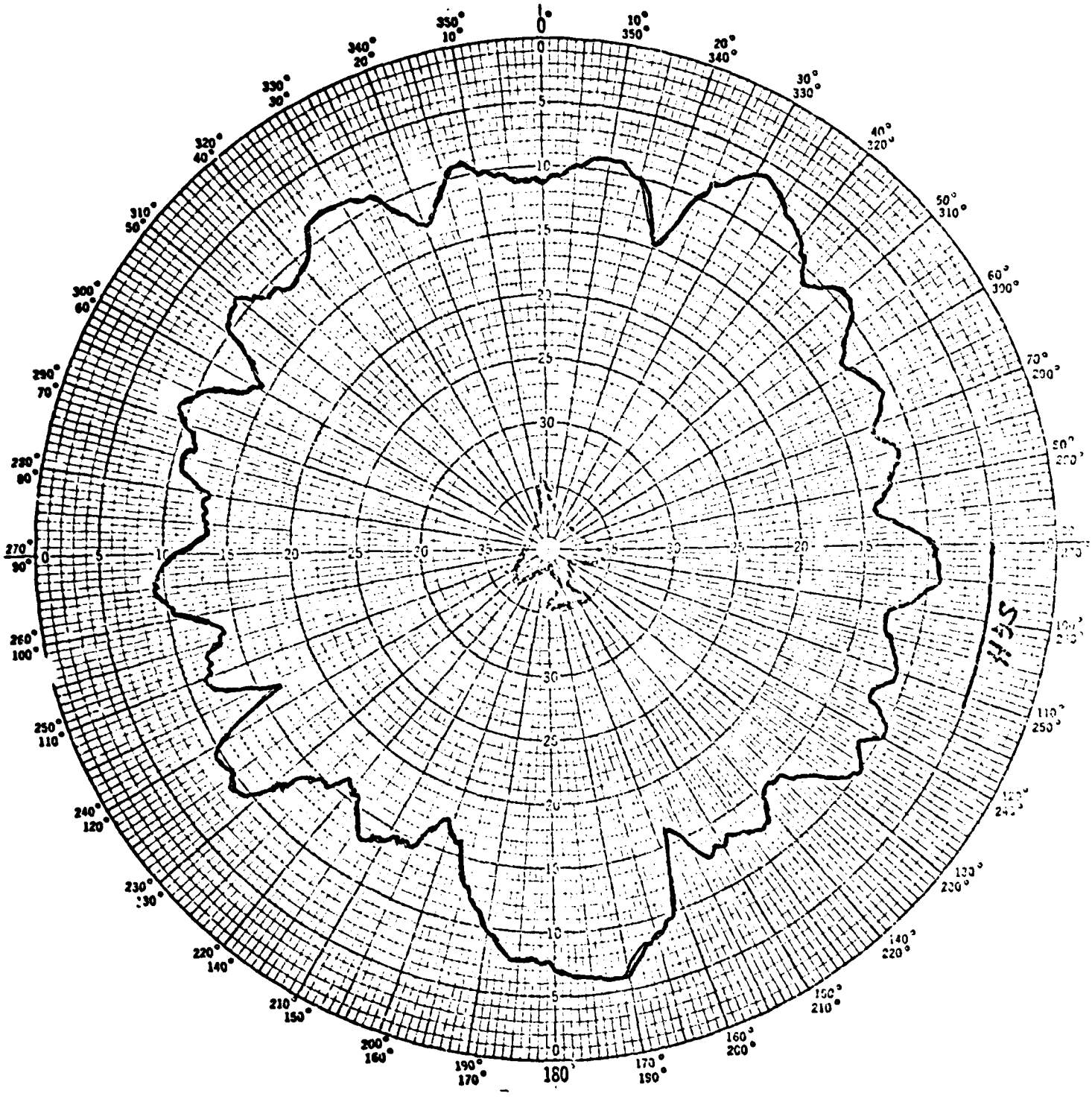

Figure 32. Data Plot: Antenna 1; elevation=15°; frequency=257MHz.

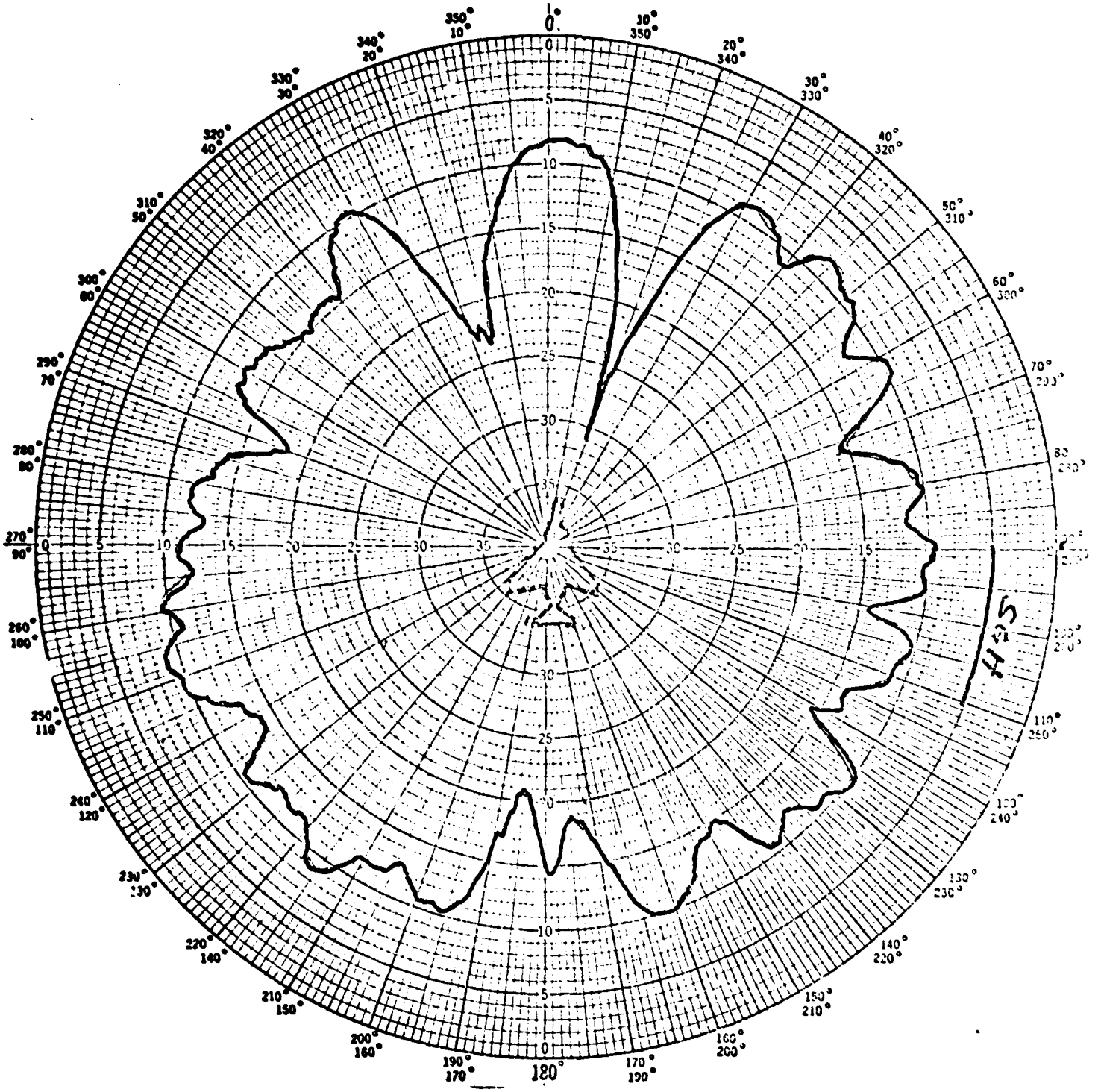

Figure 33. Data Plot: Antenna 1; elevation=0°; frequency=257MHz.

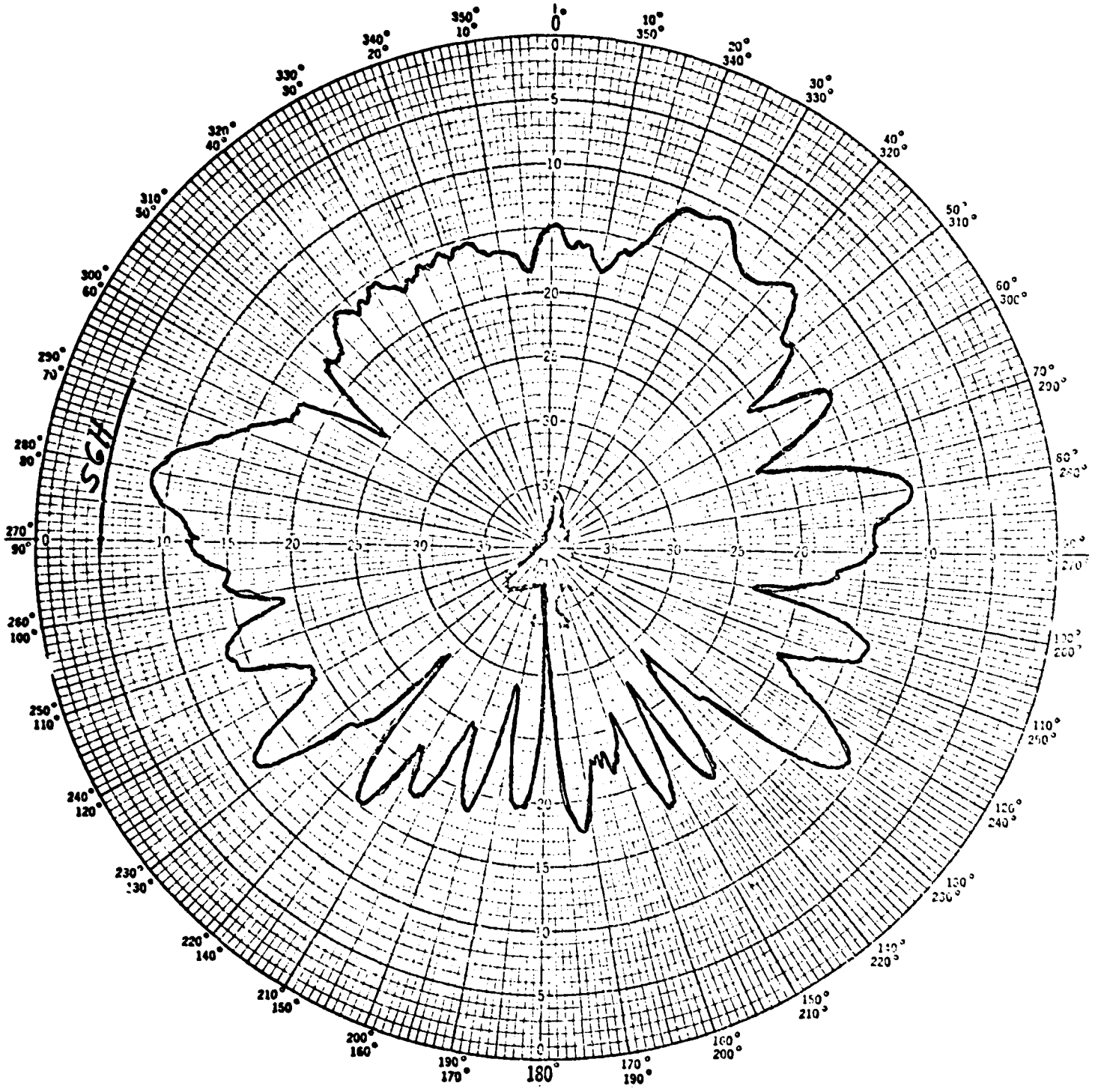

Figure 34. Data Plot: Antenna 1; elevation=-15°; frequency=257MHz.

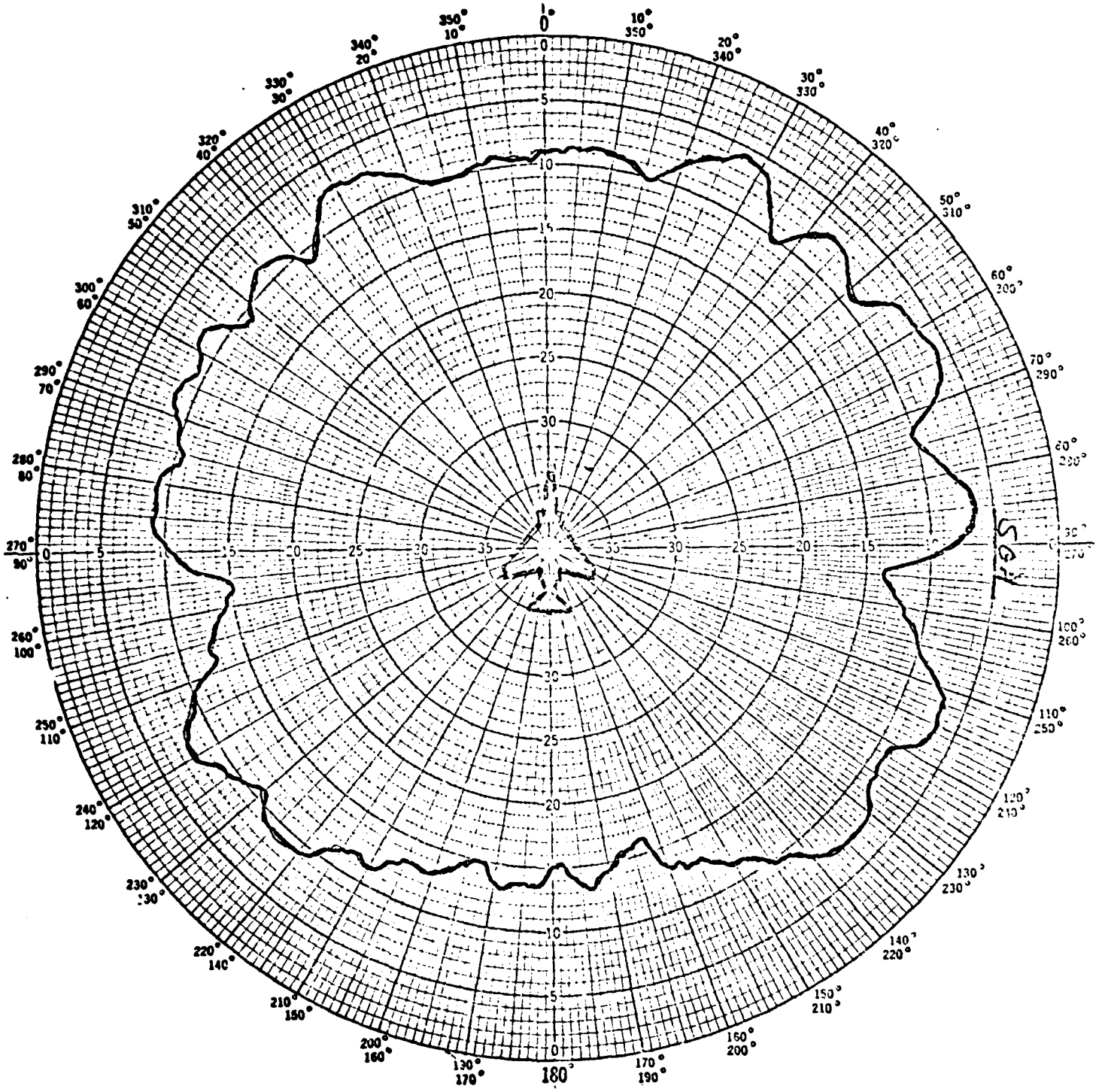

Figure 35. Data Plot: Antenna 1; elevation=30°; frequency=300MHz.

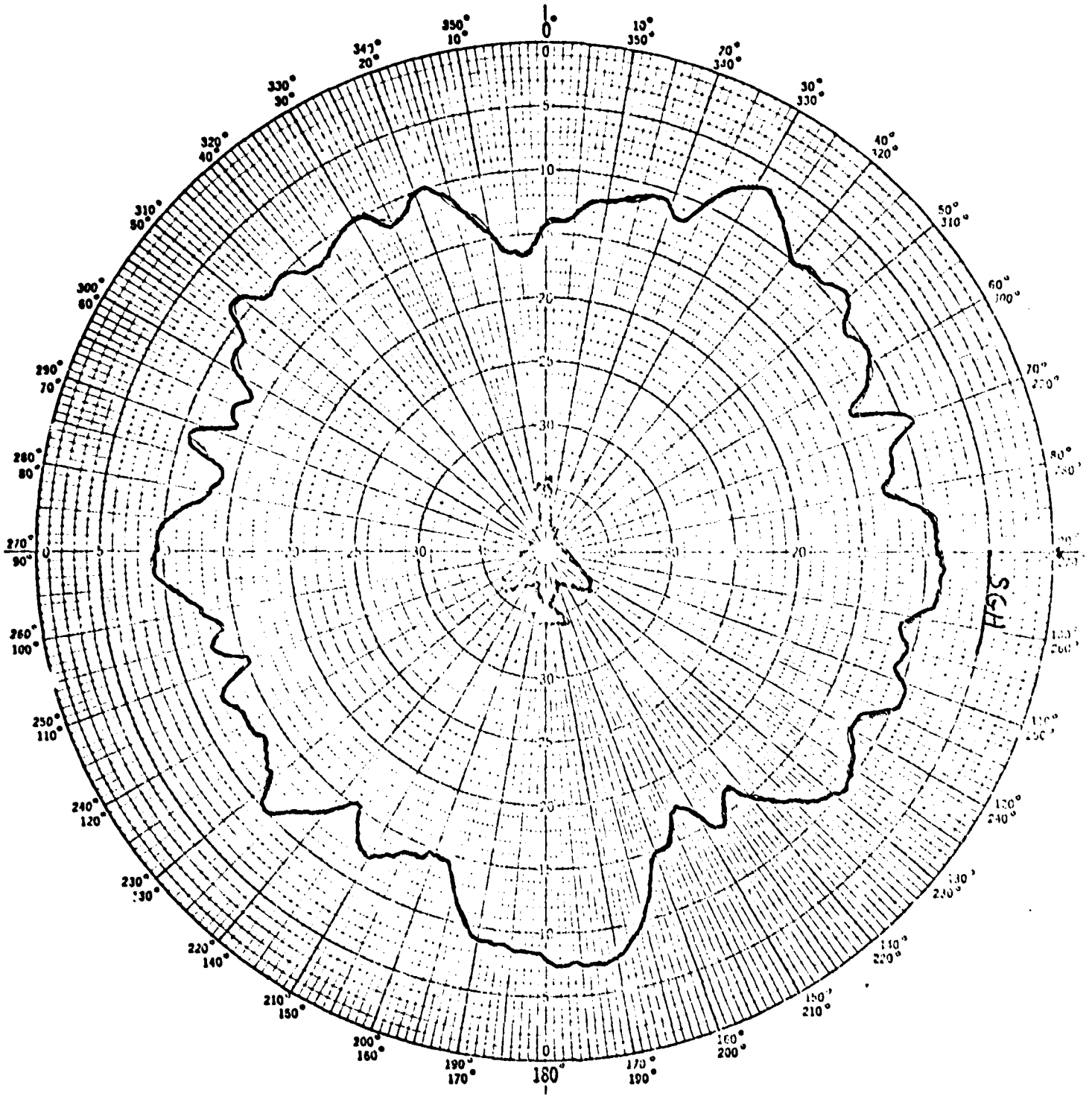

Figure 36. Data Plot: Antenna 1; elevation=15°; frequency=300MHz.

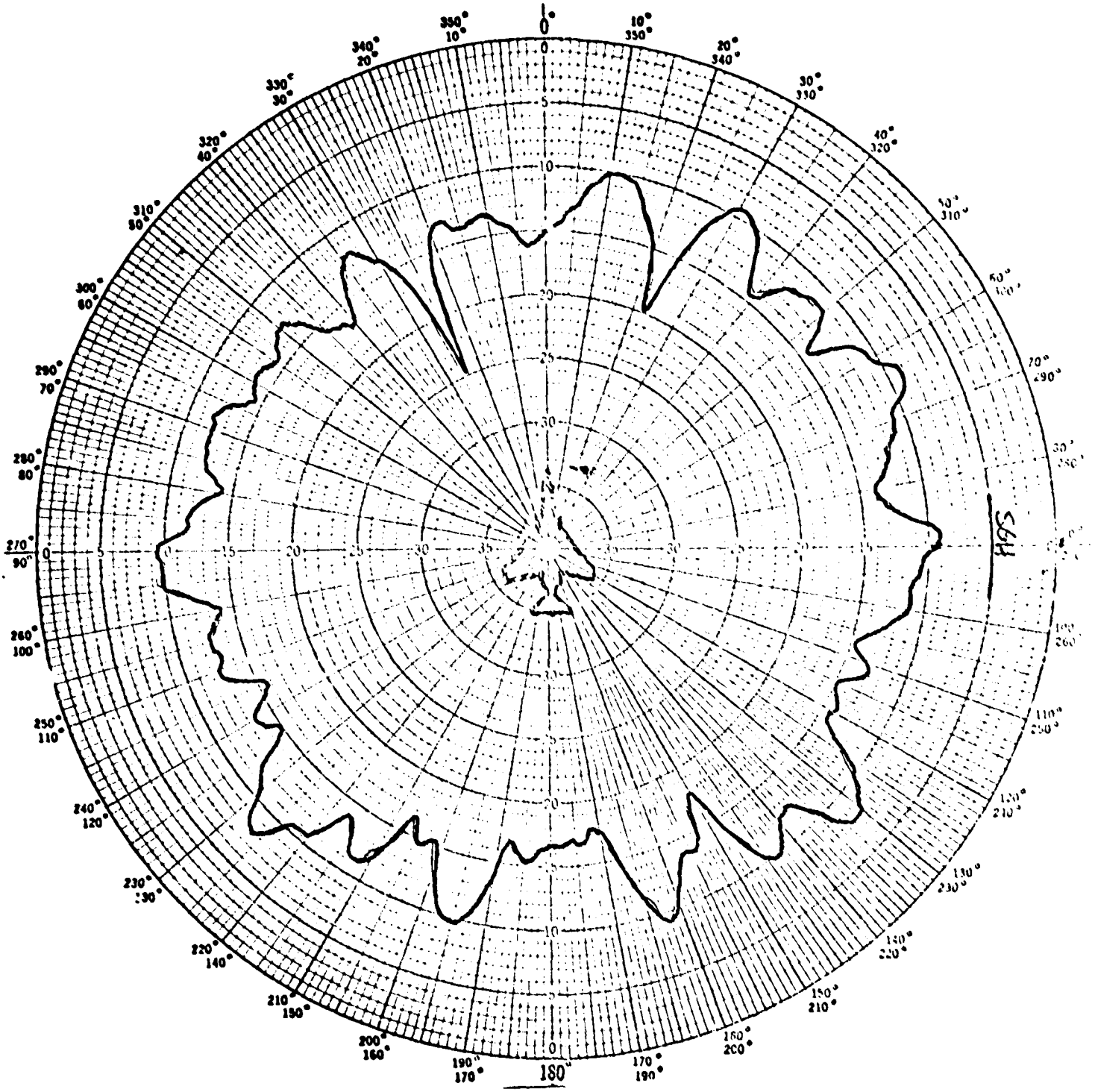

Figure 37. Data Plot: Antenna 1; elevation=0°; frequency=300MHz.

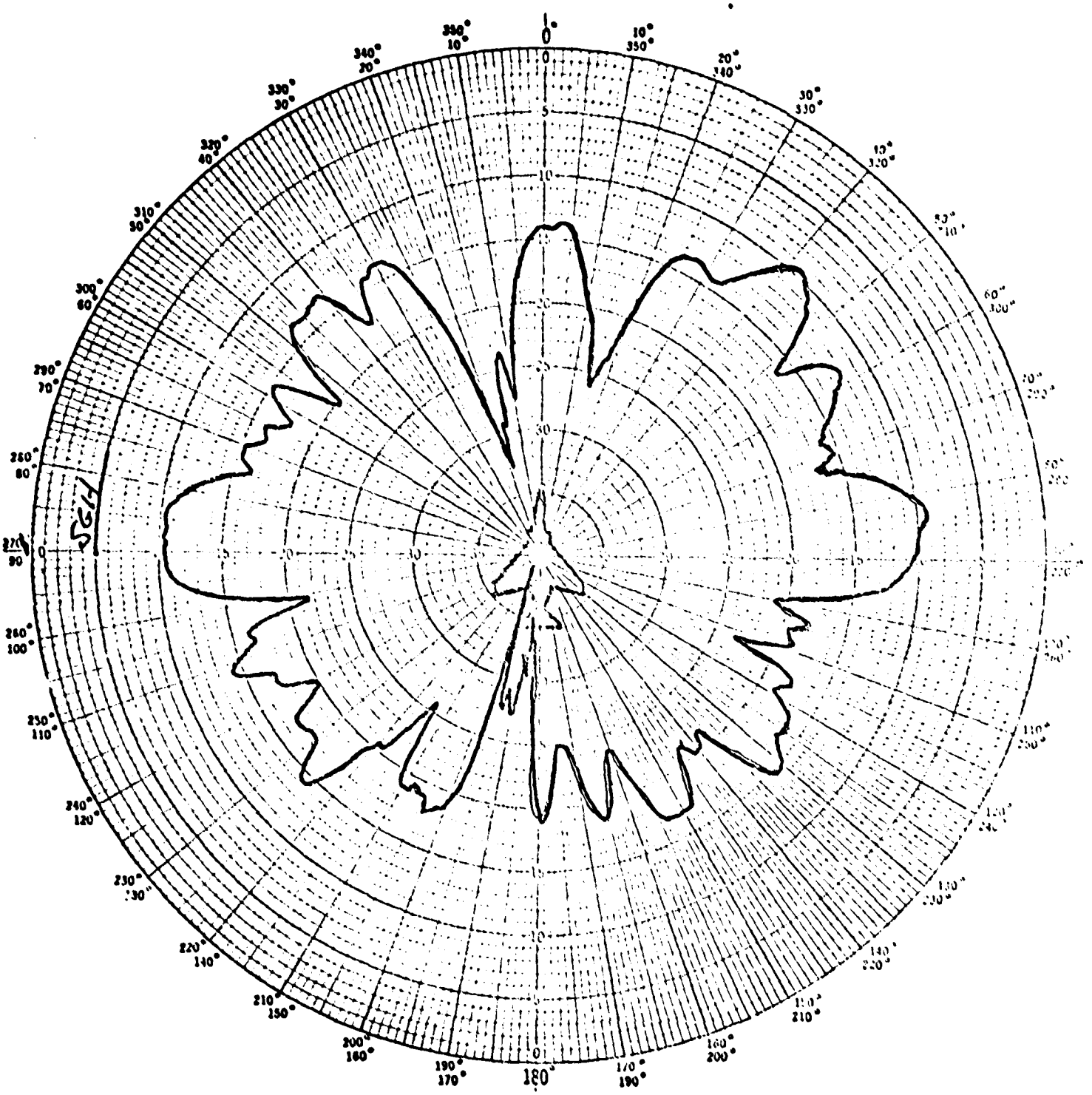

Figure 38. Data Plot: Antenna 1; elevation=-15°; frequency=300 MHz.

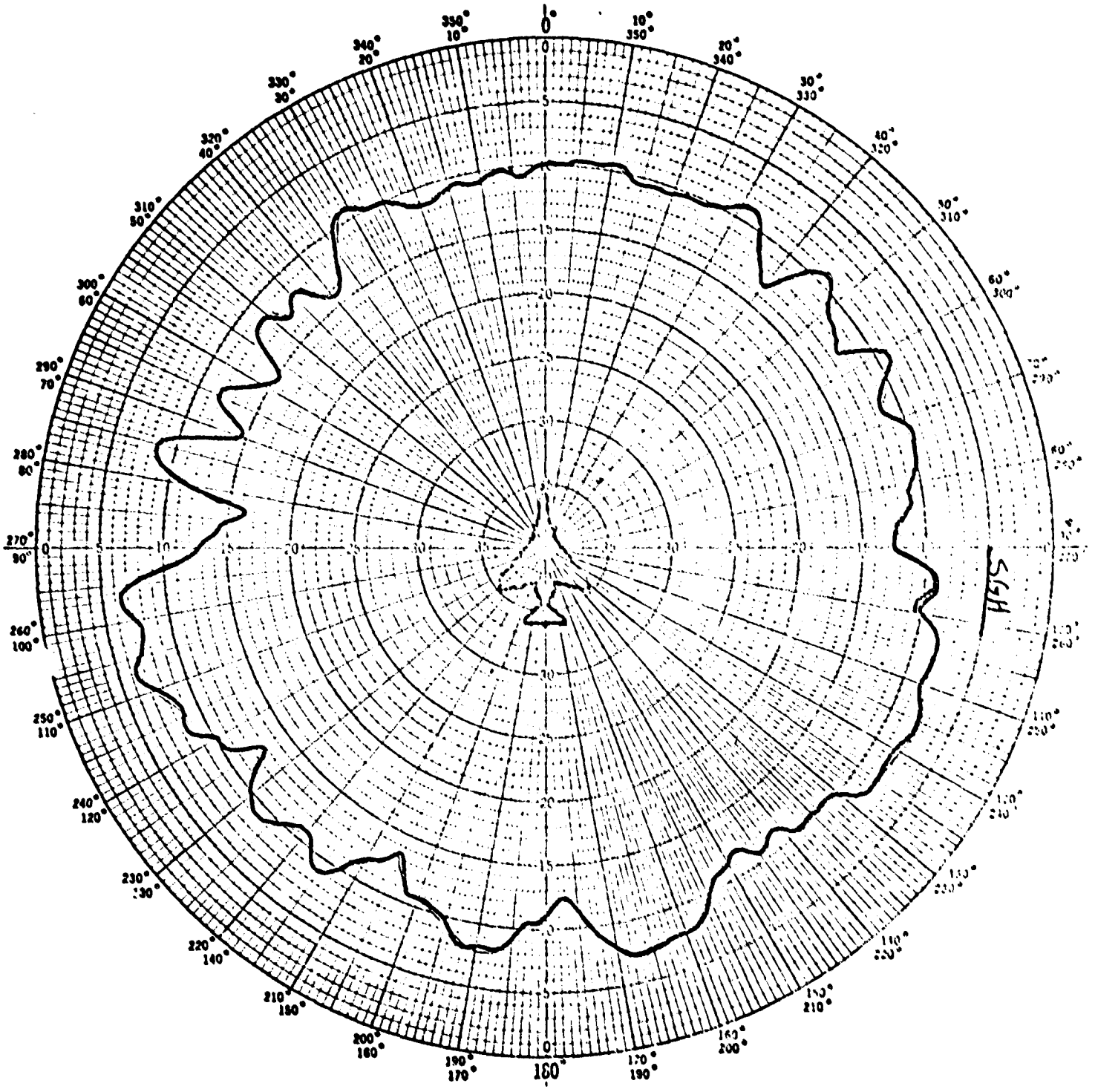

Figure 39. Data Plot: Antenna 1; elevation=30°; frequency=385MHz.

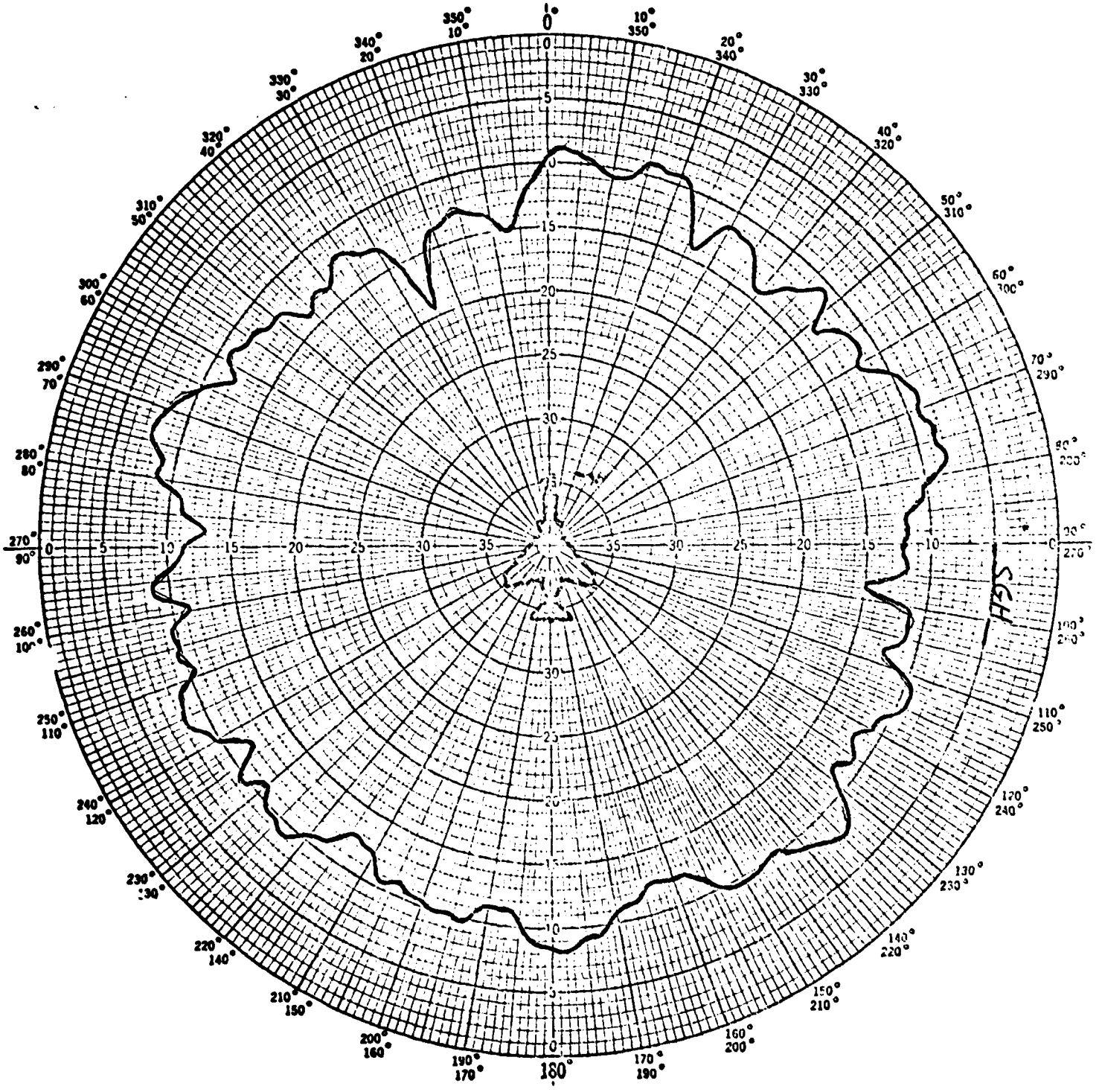

Figure 40. Data Plot: Antenna 1; elevation=15°; frequency=385Mhz.

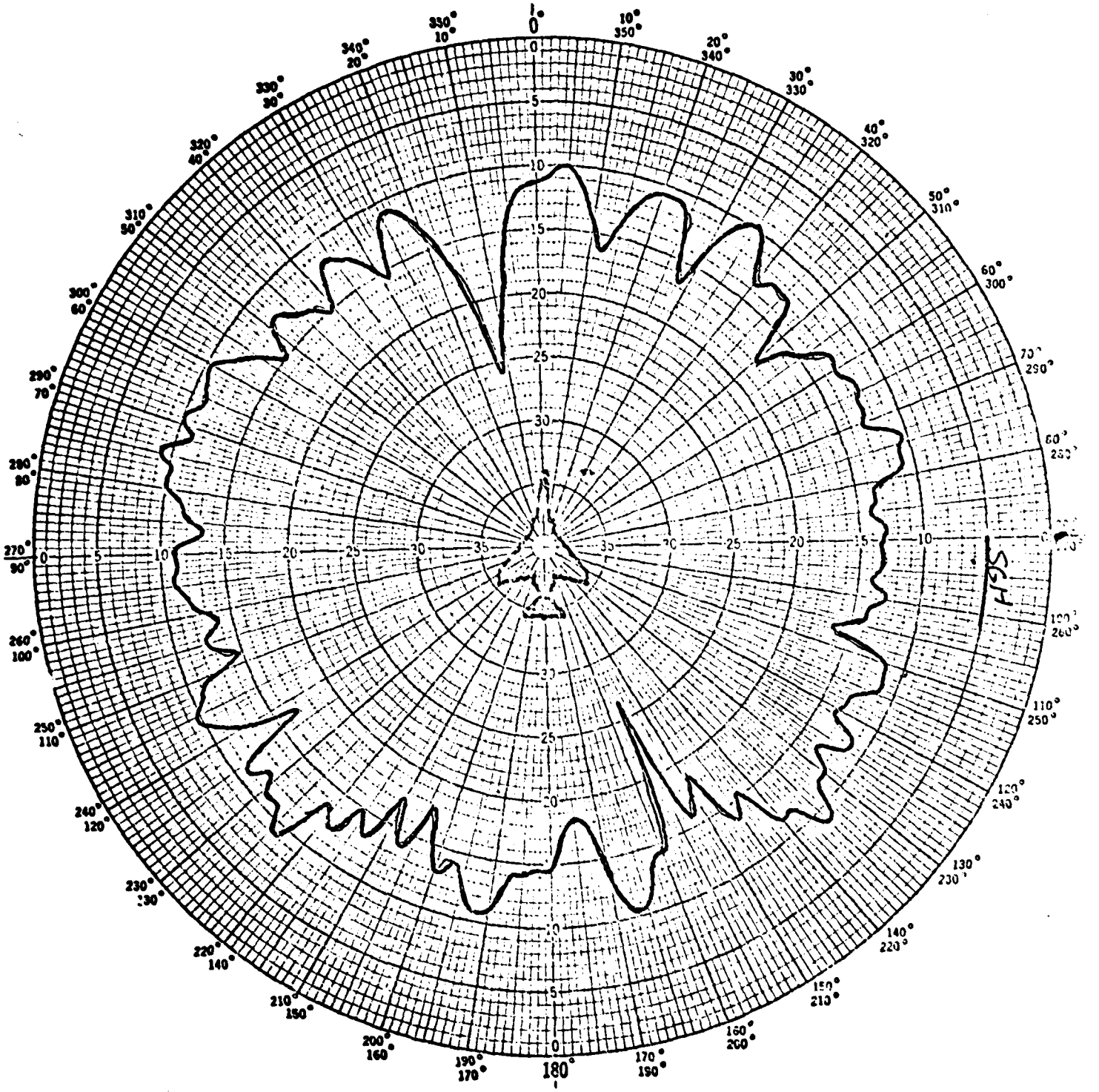

Figure 41. Data Plot: Antenna 1; elevation=0°; frequency=385MHz.

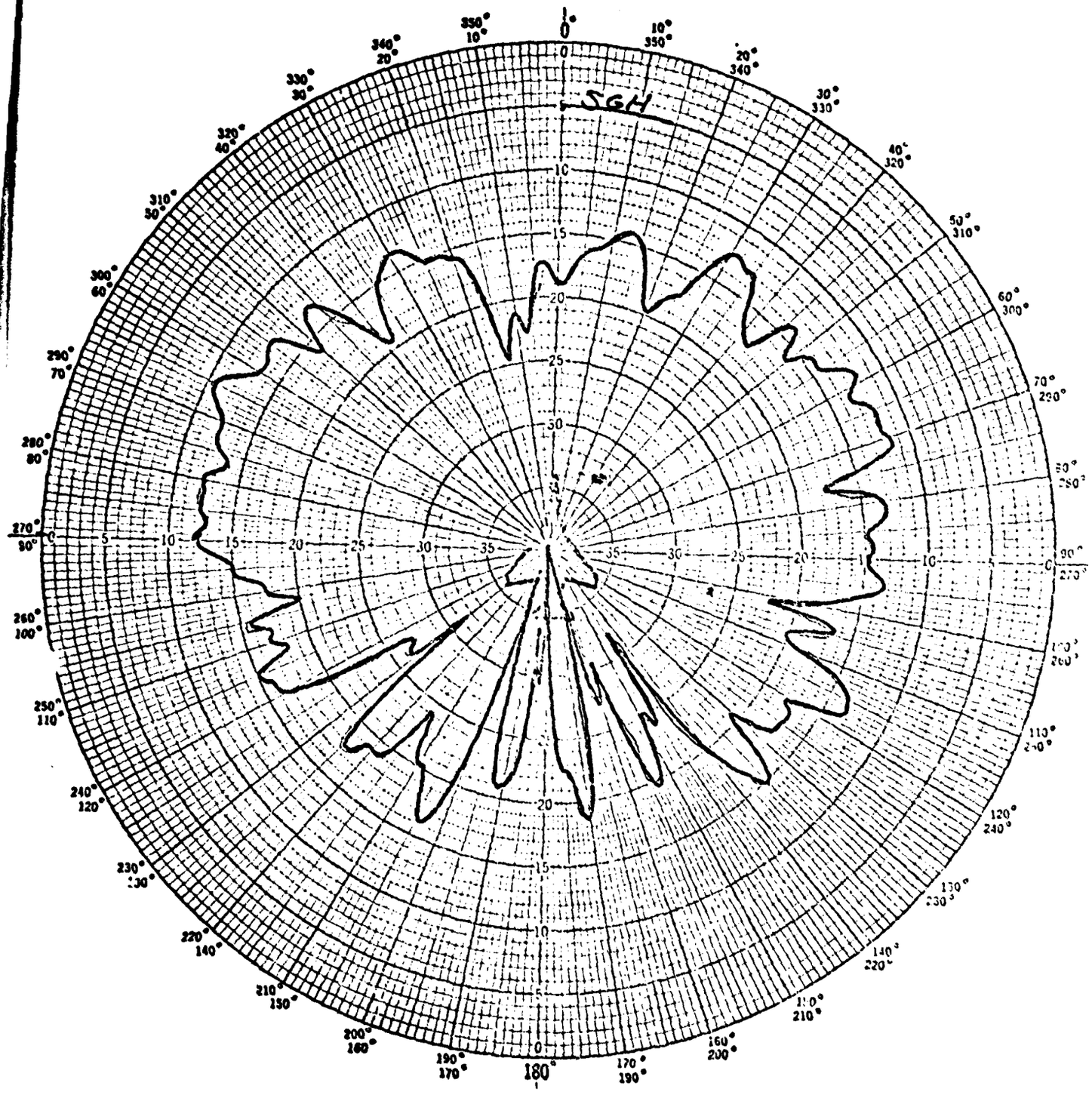

Figure 42. Data Plot: Antenna 1; elevation=-15°; frequency=385MHz.

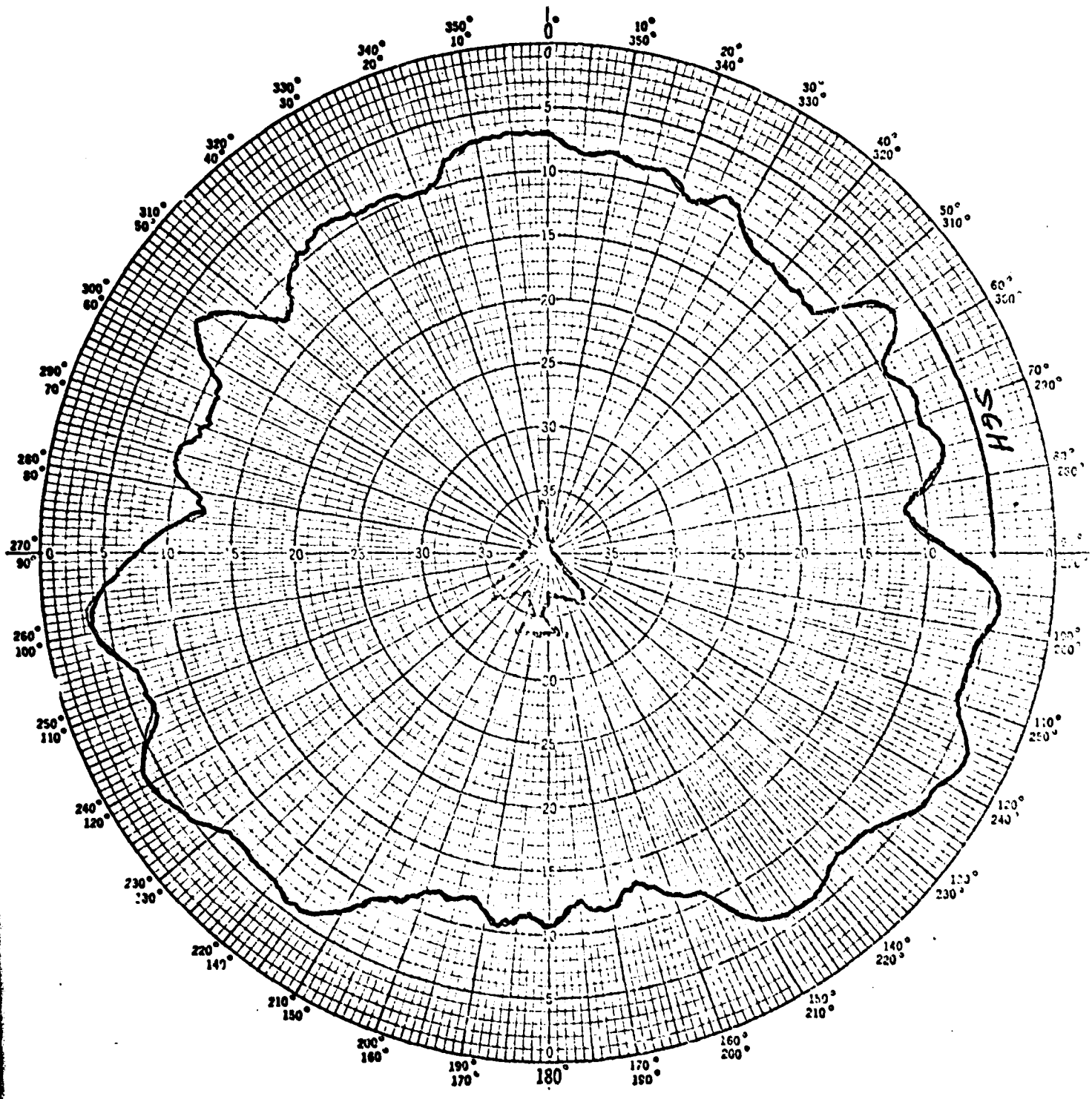

Figure 43. Data Plot: Antenna 2; elevation=30°; frequency=257MHz.

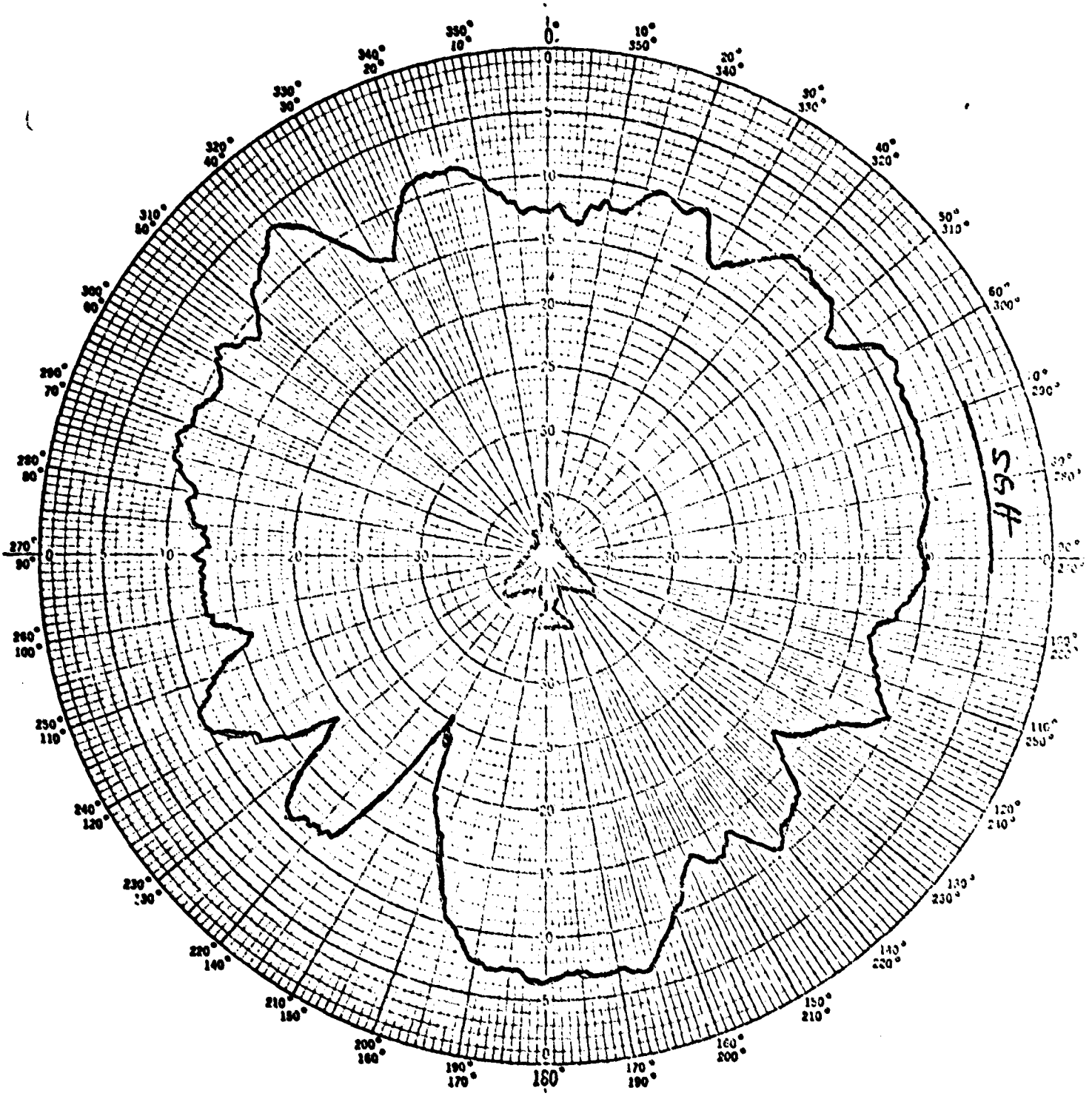

Figure 44. Data Plot: Antenna 2; elevation=15°; frequency=257MHz.

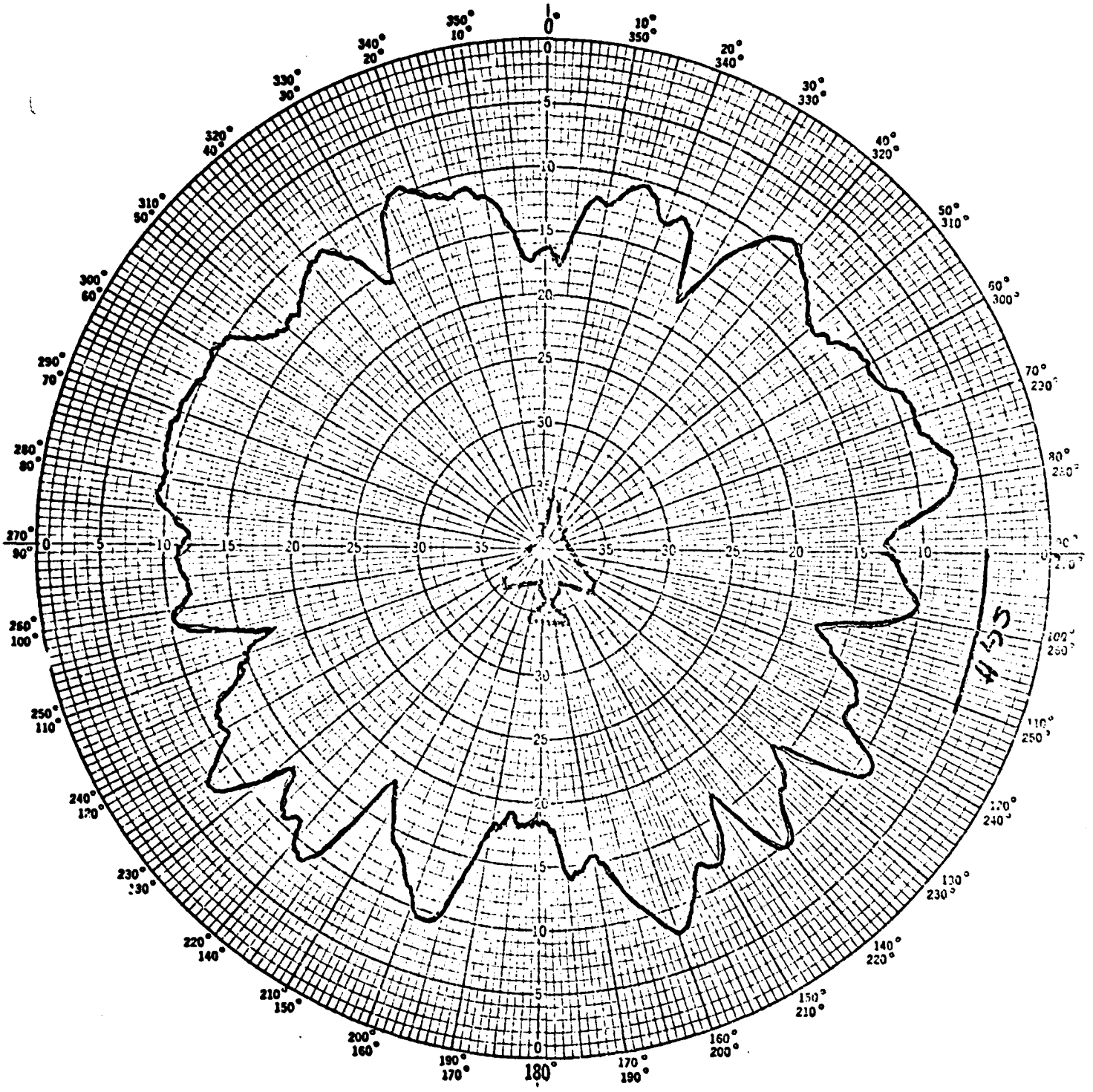

Figure 45. Data Plot: Antenna 2; elevation=0°; frequency=257MHz.

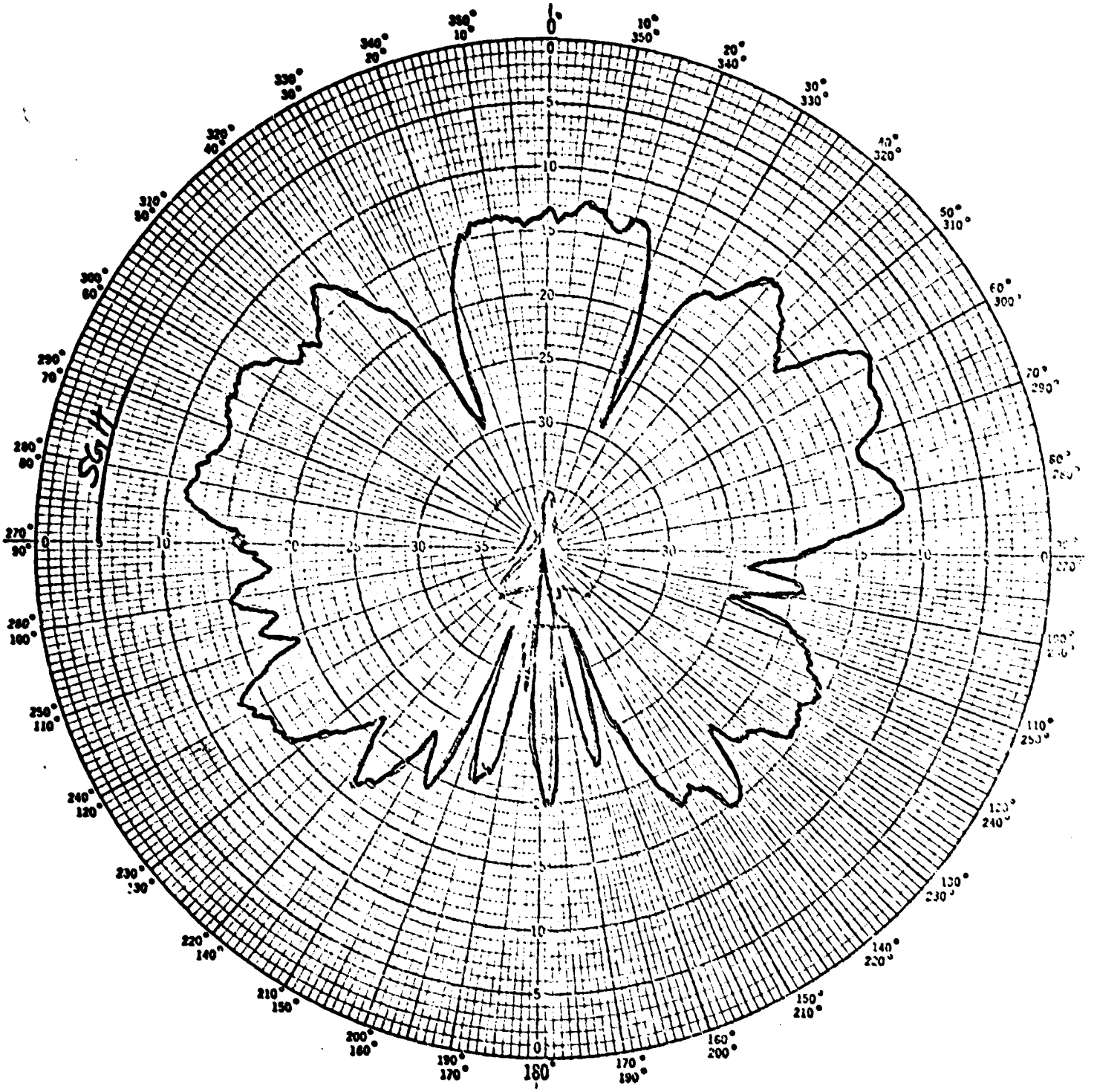

Figure 46. Data Plot: Antenna 2; elevation=-15°; frequency=257MHz.

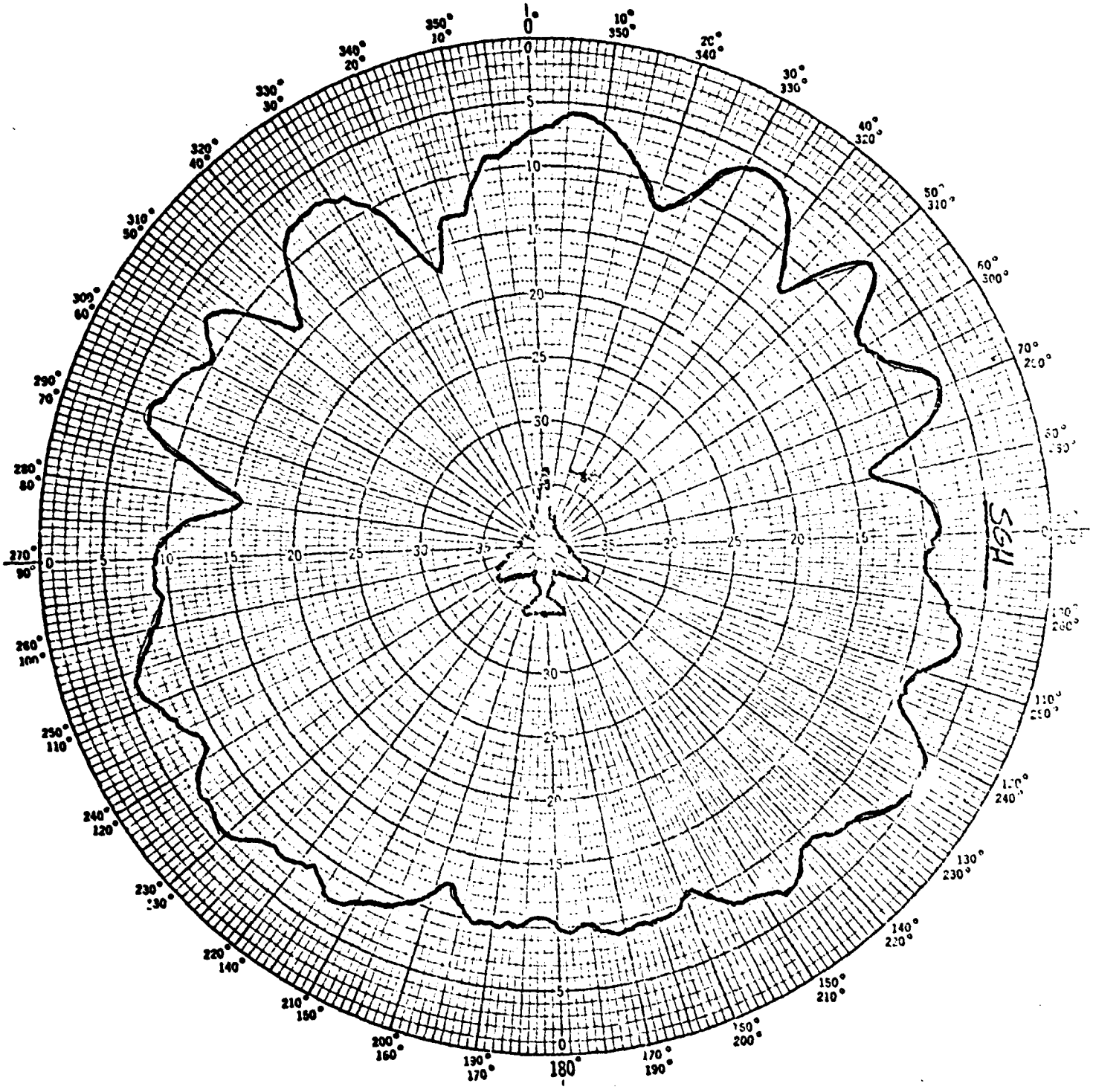

Figure 47. Data Plot: Antenna 2; elevation=30°; frequency=300MHz.

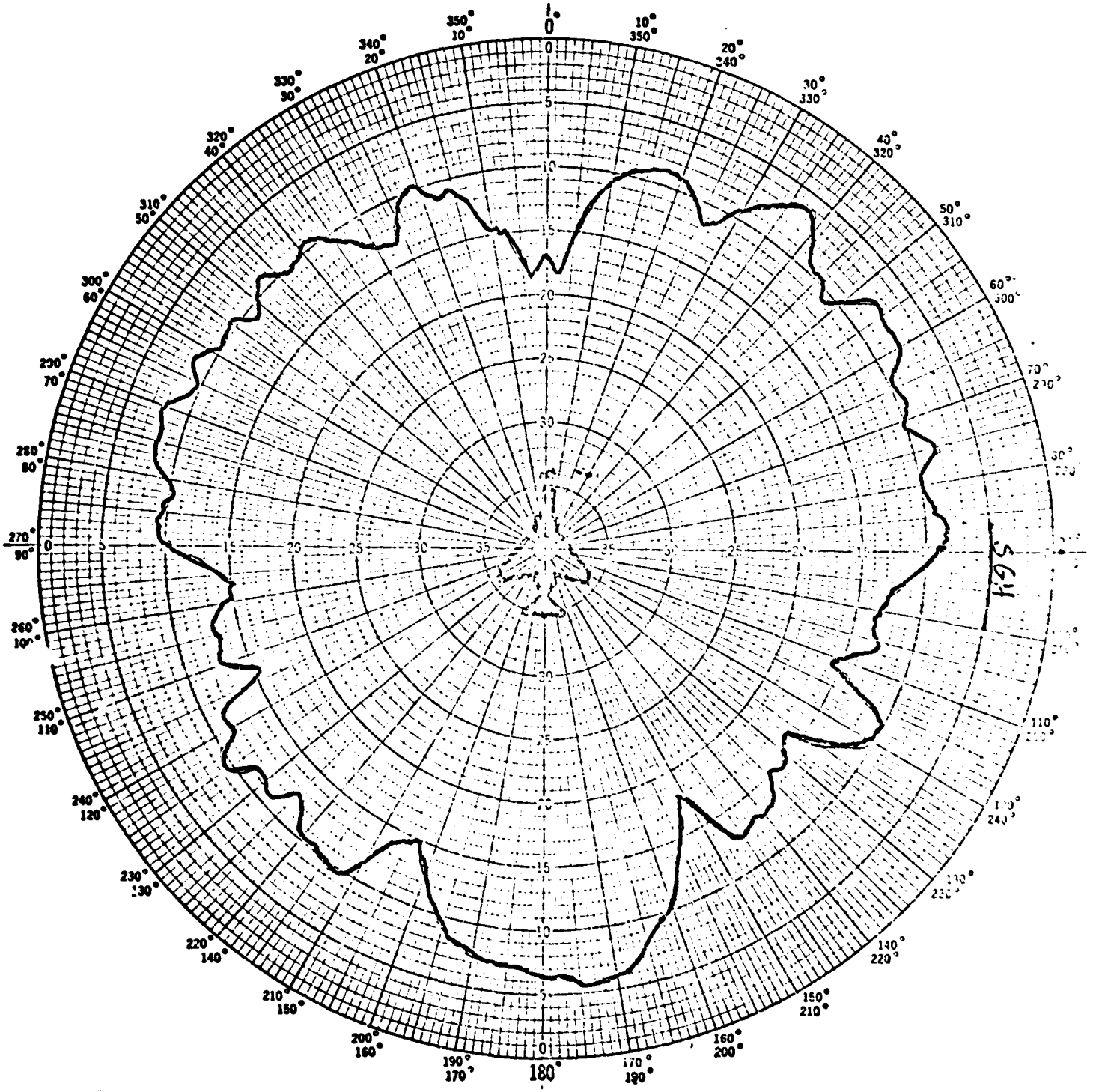

Figure 48. Data Plot: Antenna 2; elevation= 15°; frequency=300MHz.

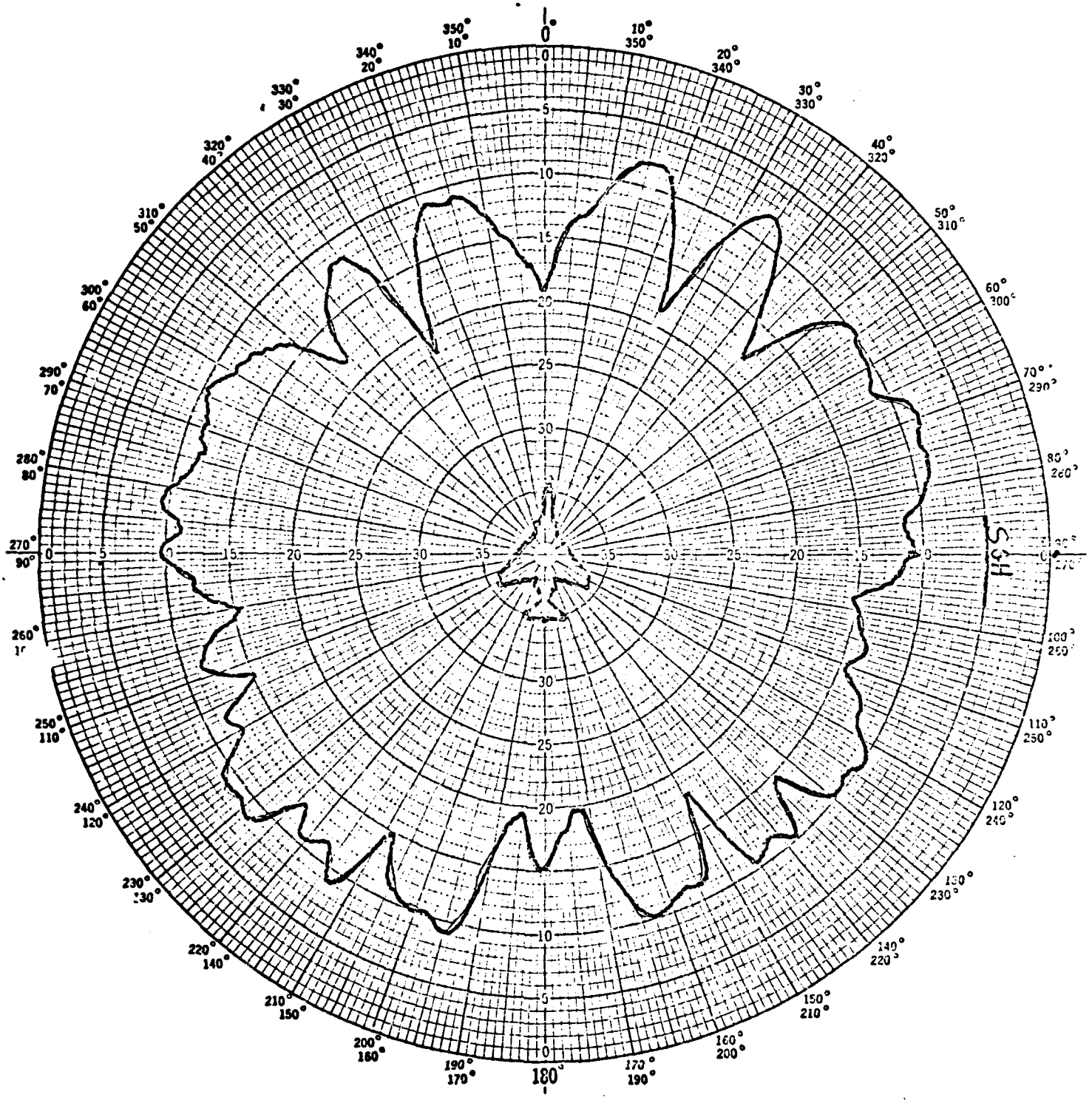

Figure 49. Data Plot: Antenna 2; elevation=0°; frequency=300MHz.

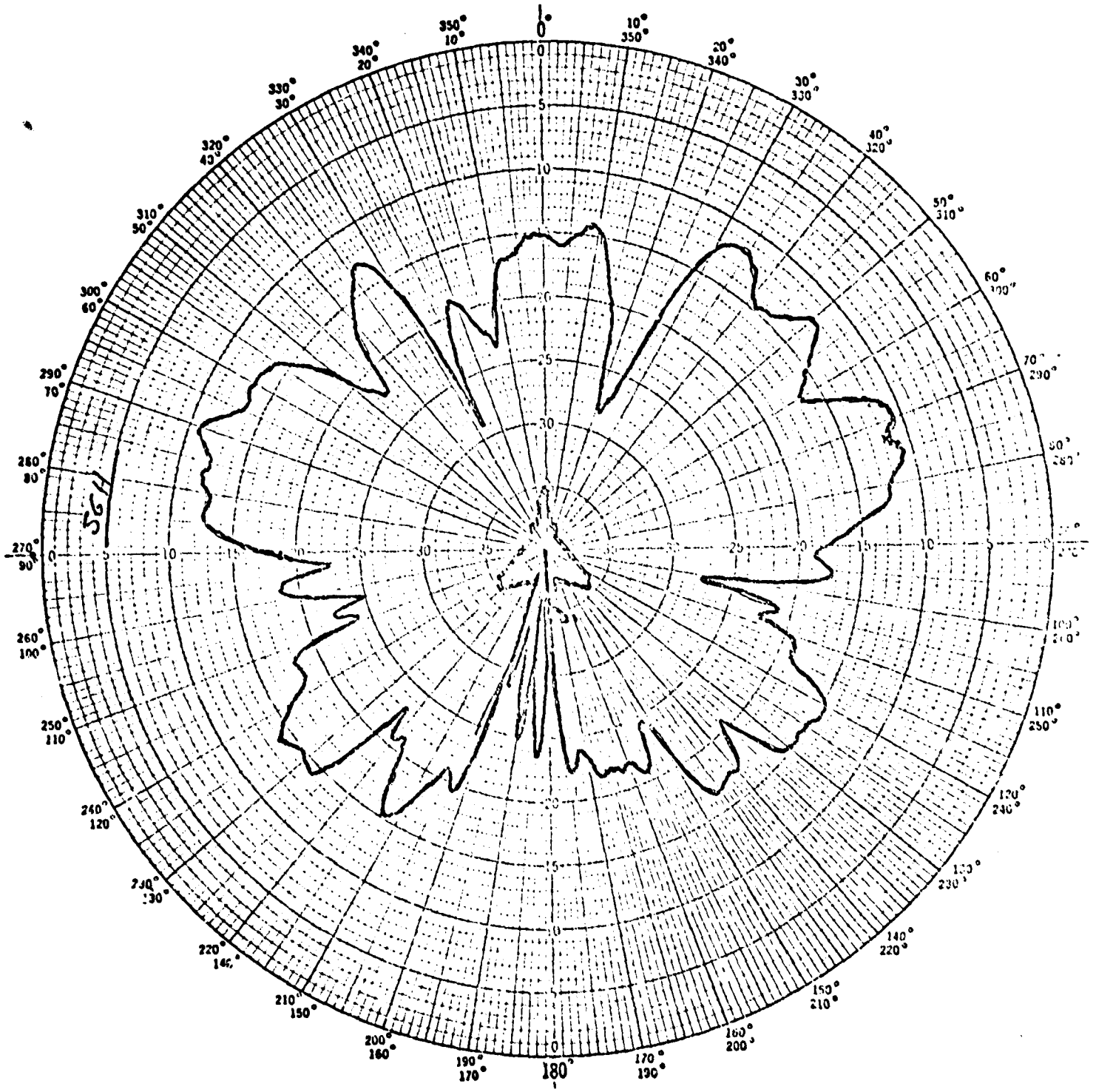

Figure 50. Data Plot: Antenna 2; elevation=-15°; frequency=300MHz.

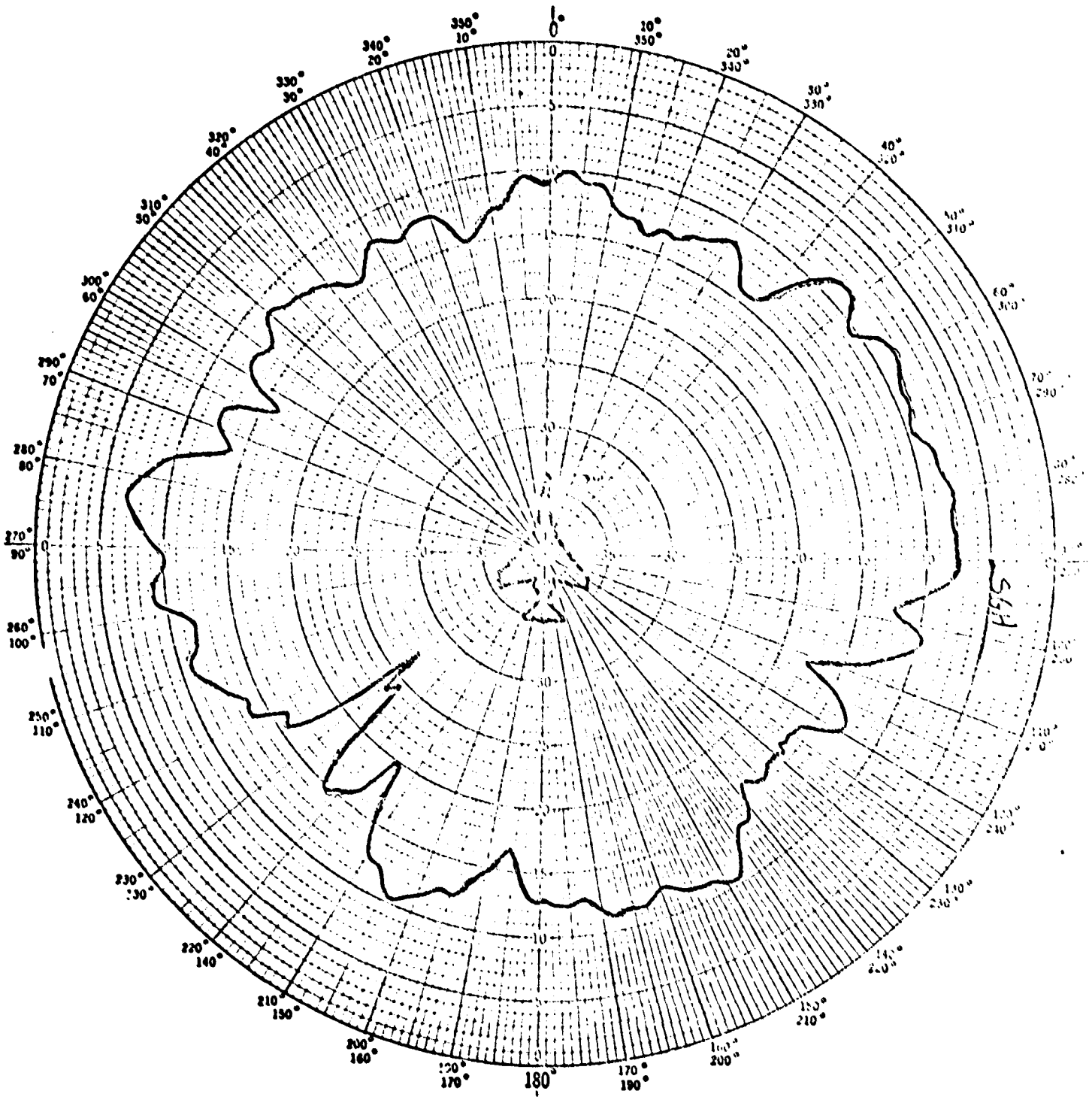

Figure 51. Data Plot: Antenna 2; elevation=30°; frequency=385MHz.

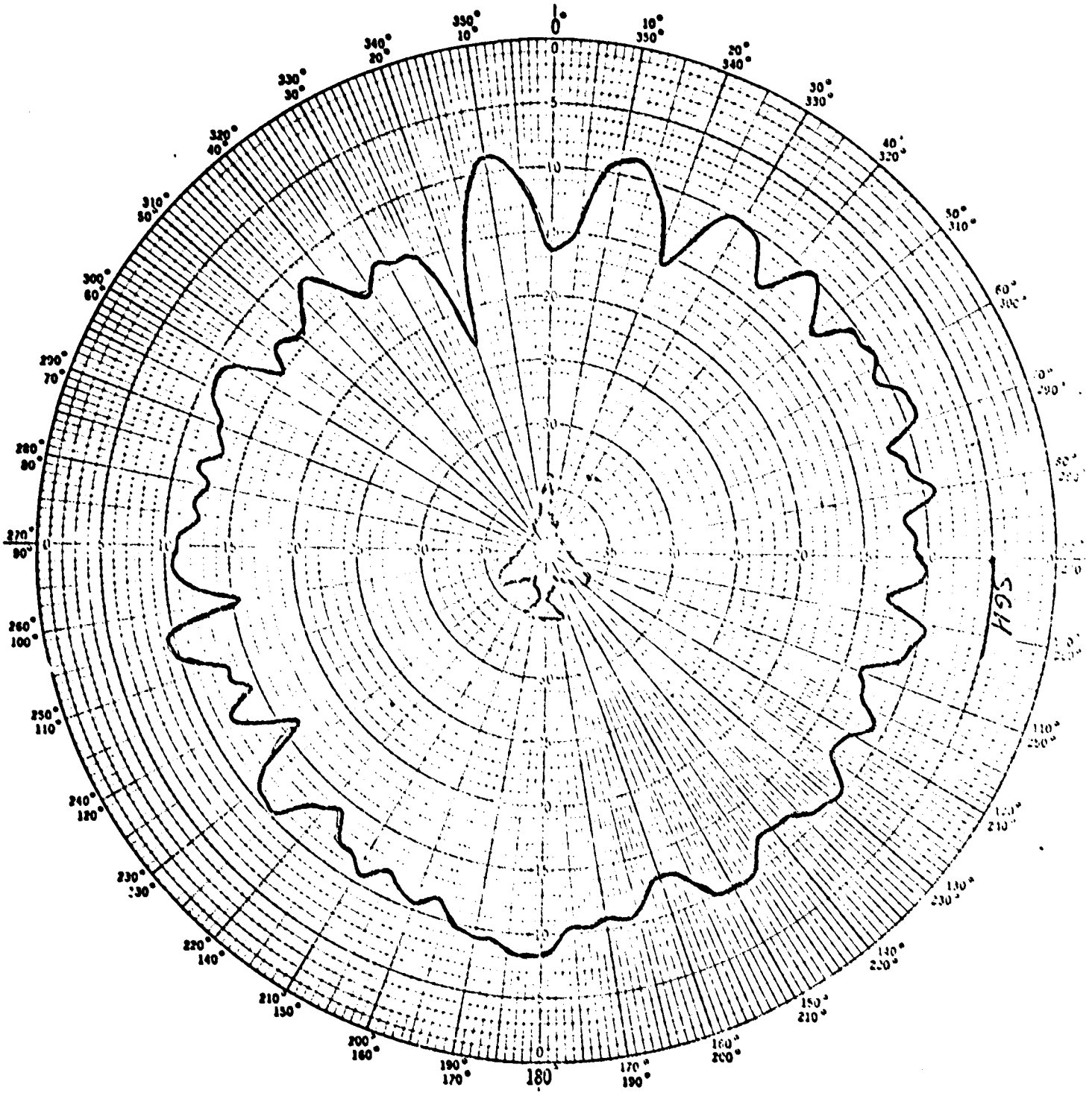

Figure 52. Data Plot: Antenna 2; elevation=15°; frequency=385MHz.

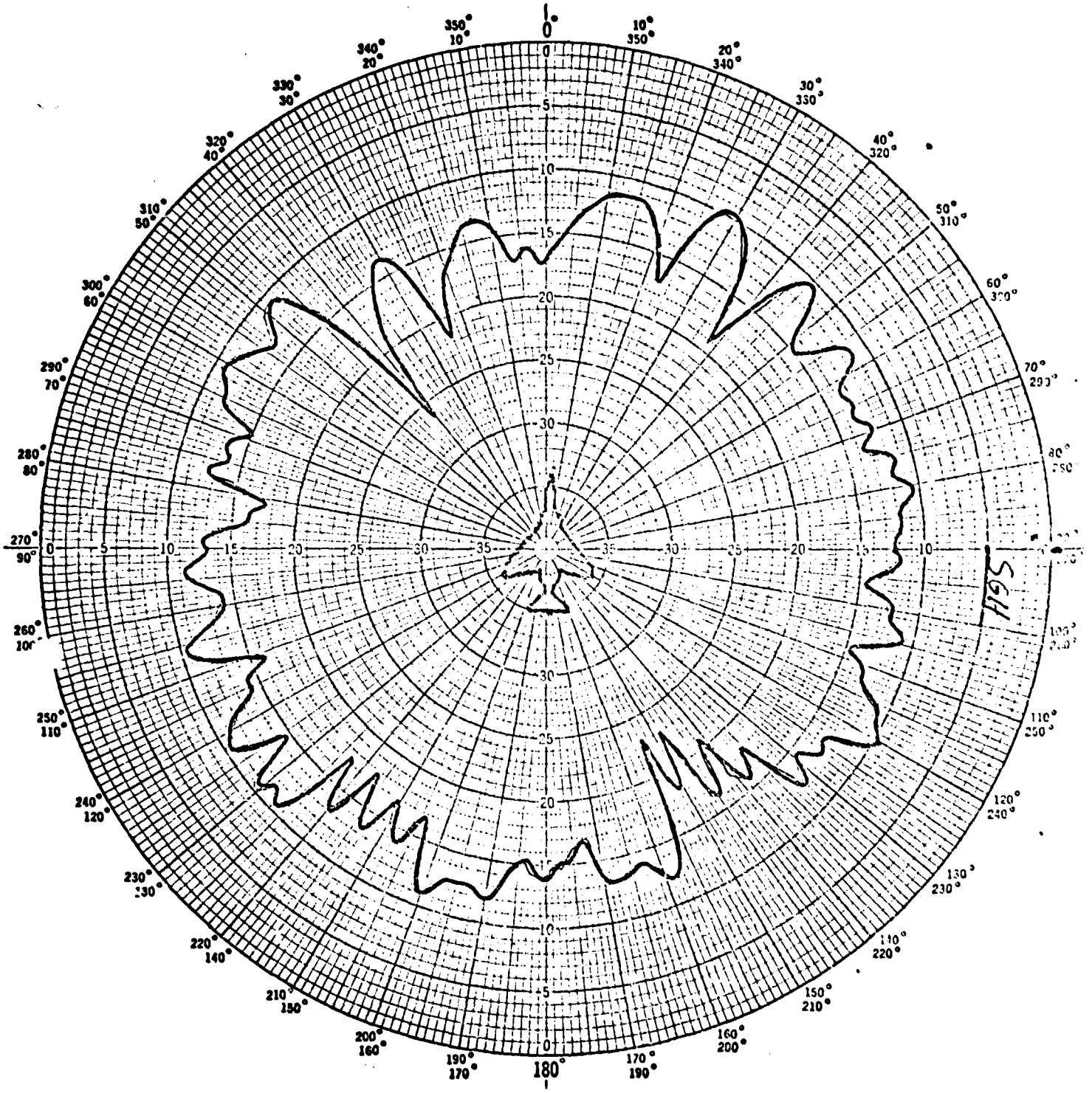

Figure 53. Data Plot: Antenna 2; elevation=0°; frequency=385MHz.

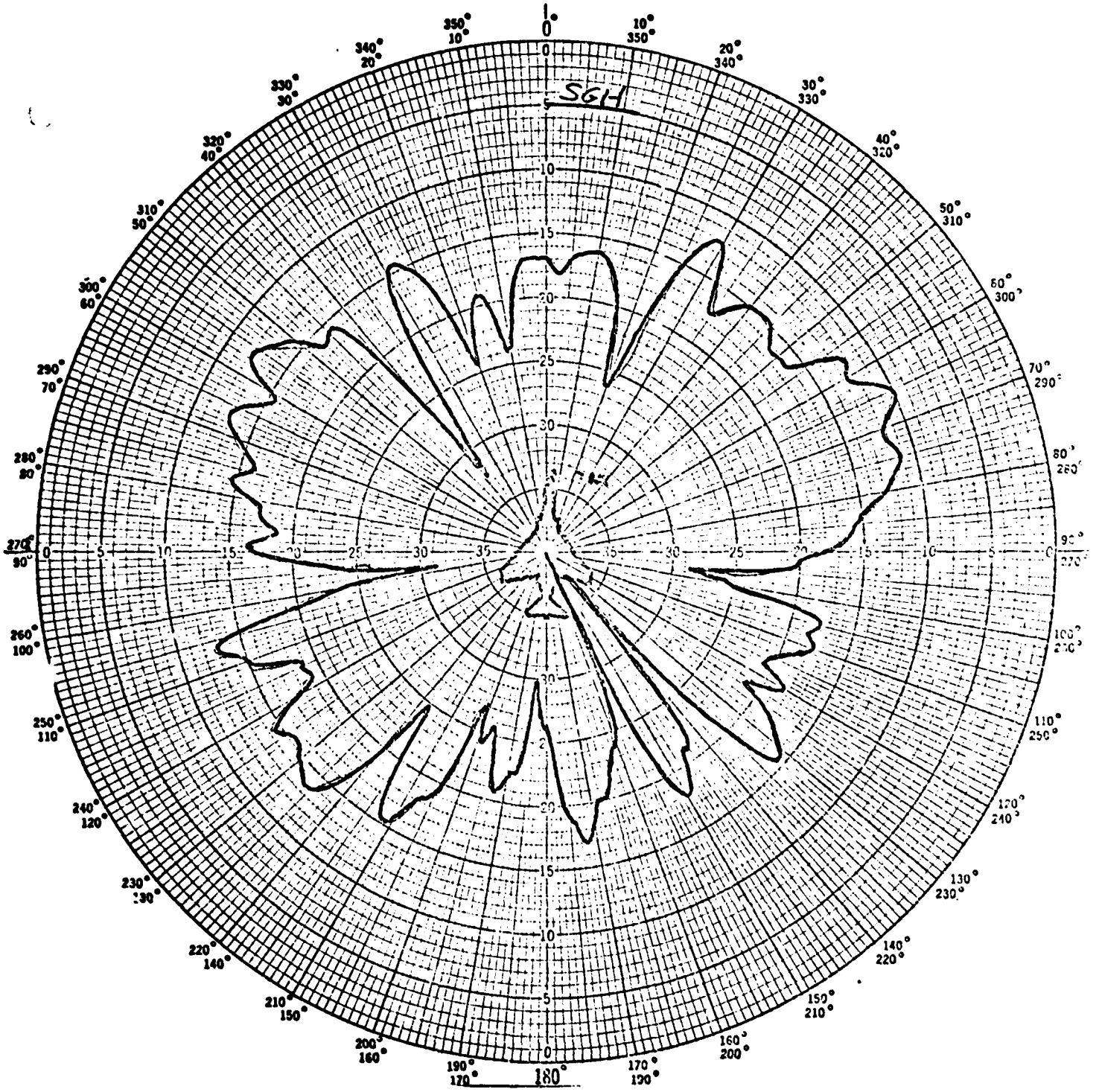

Figure 54. Data Plot: Antenna 2; elevation=-15°; frequency=385MHz.

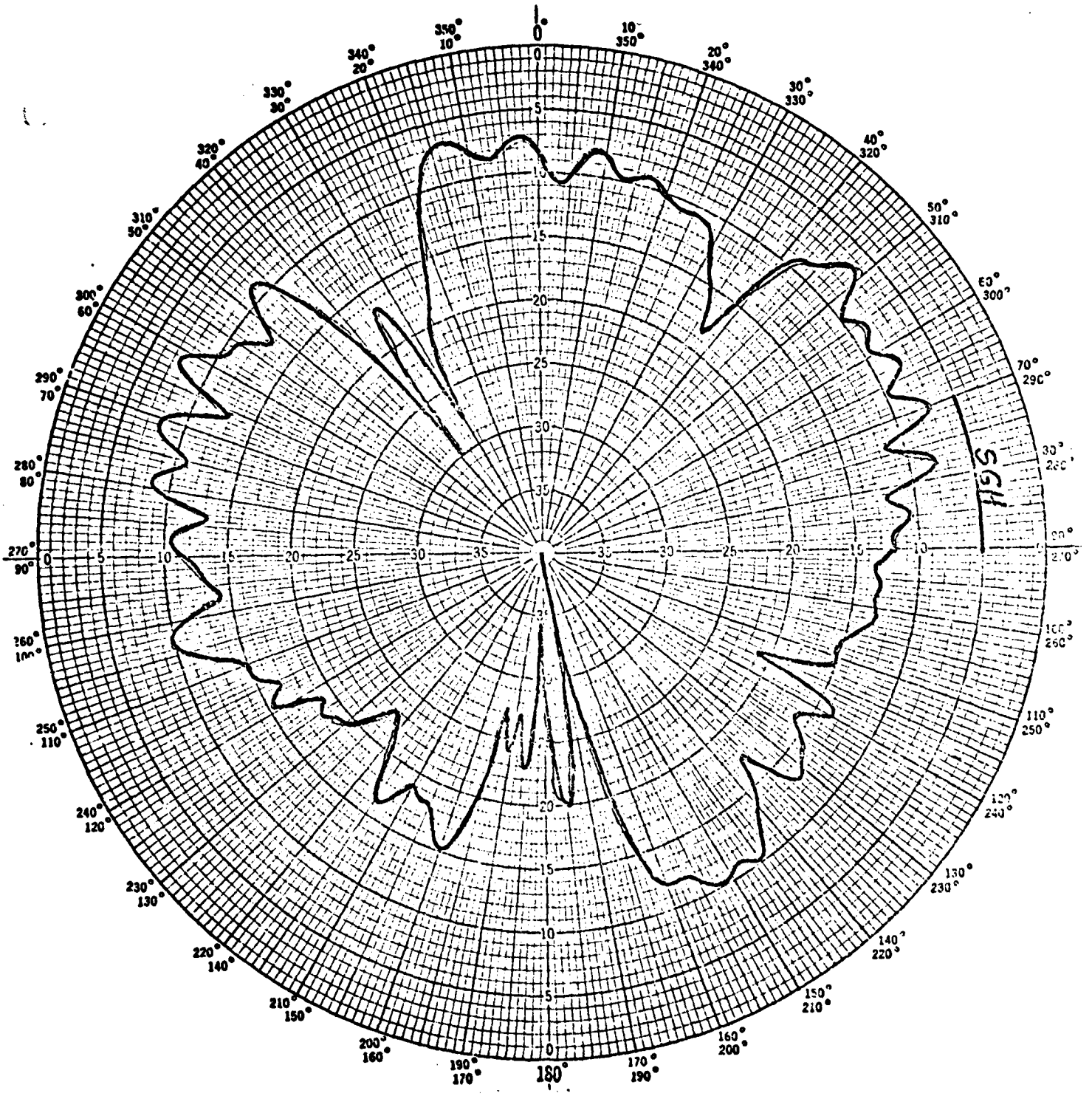

Figure 55. Data Plot: Antenna 3; elevation=30°; frequency=257MHz.

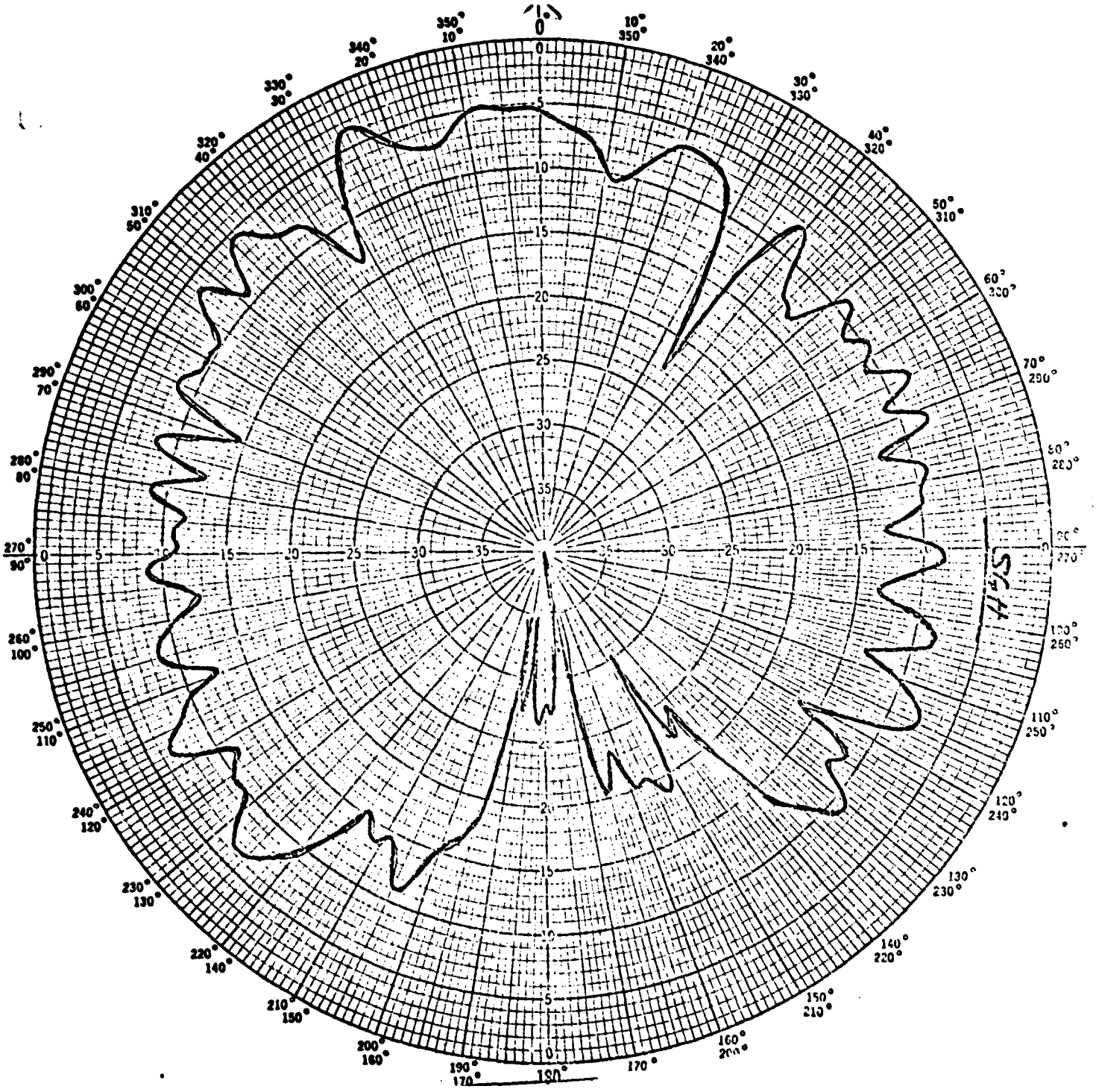

Figure 56. Data Plot: Antenna 3; elevation=15°; frequency=257MHz.

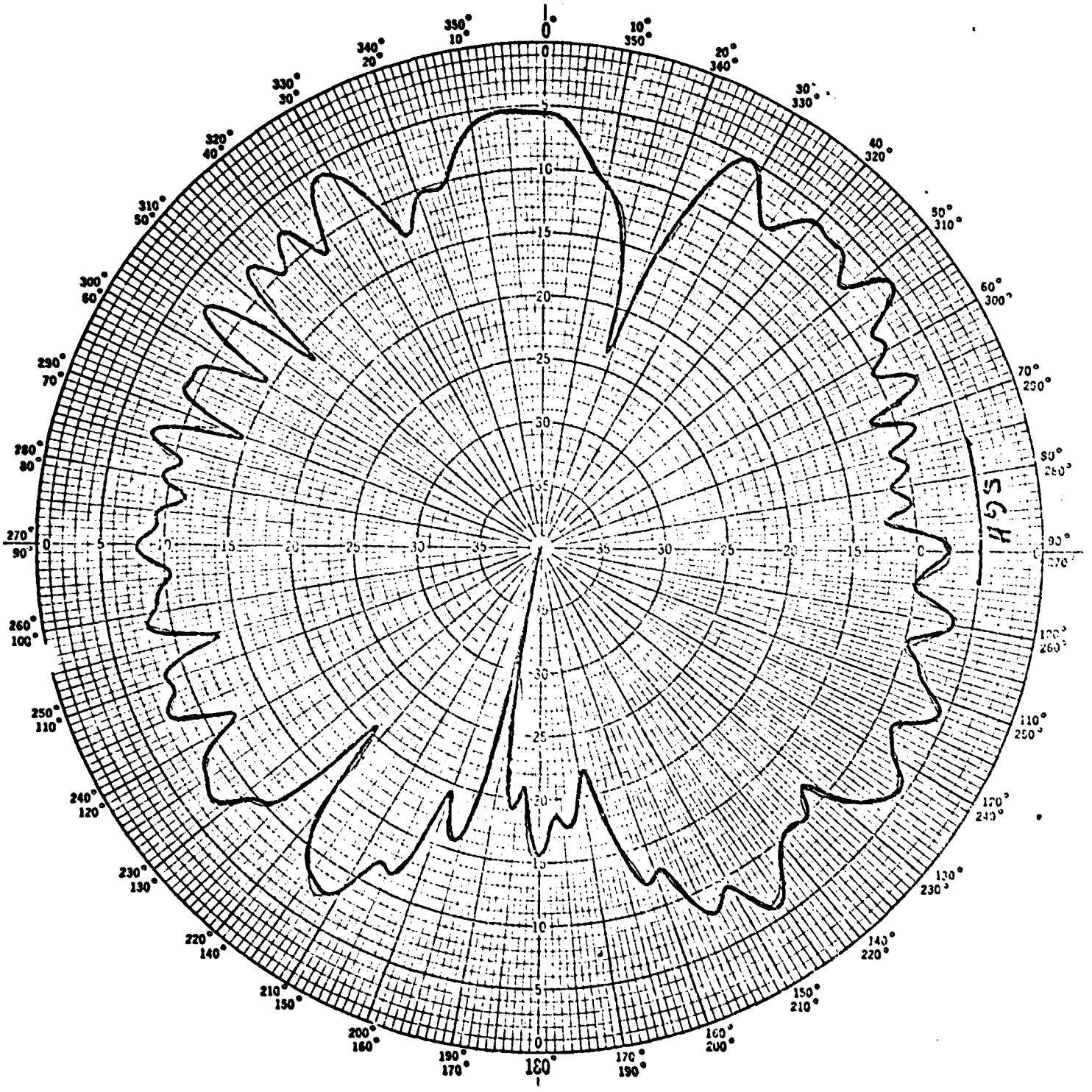

Figure 57. Data Plot:Antenna 3;elevation=0°;frequency=257MHz.

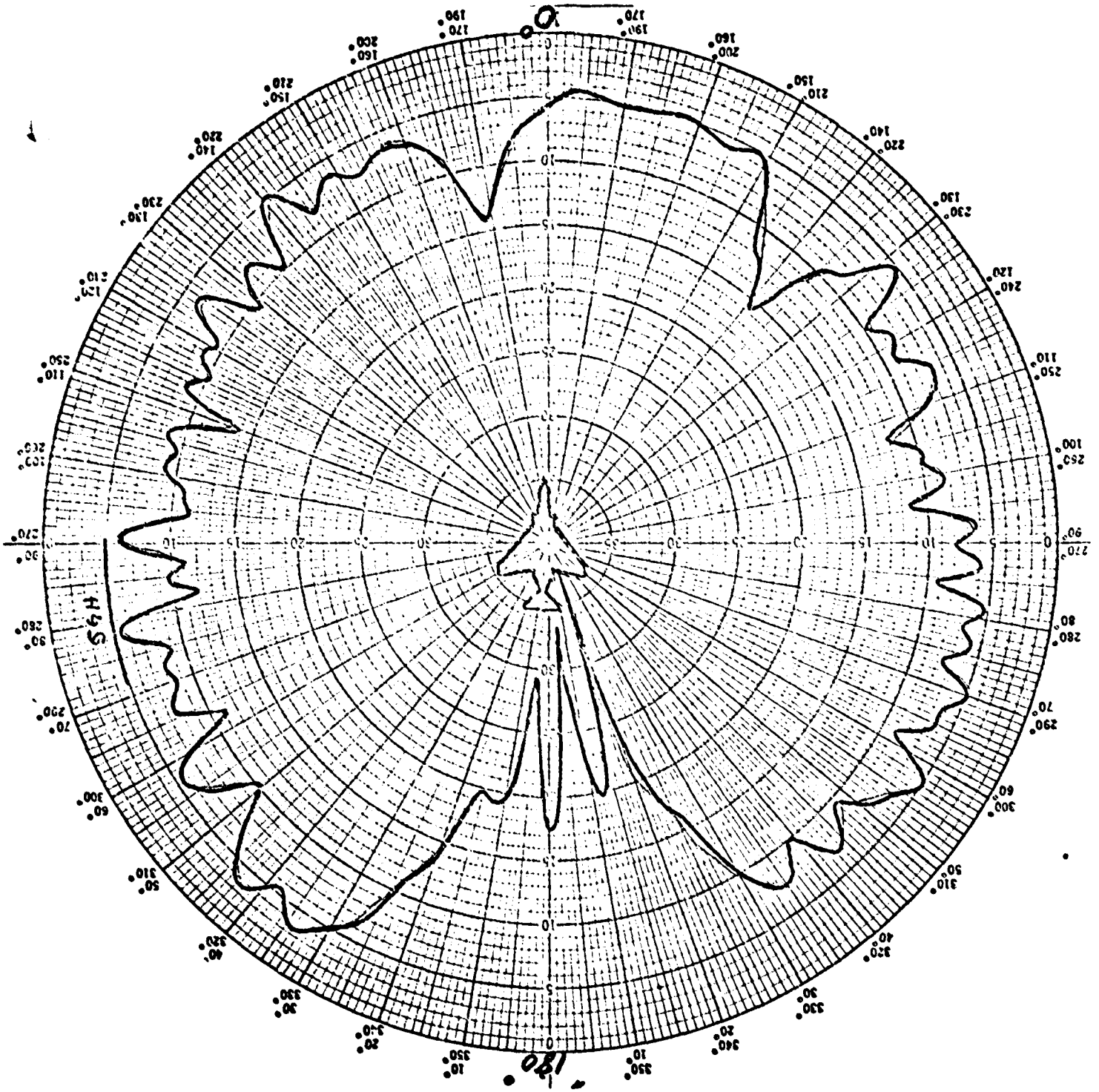

Figure 58. Data Plot: Antenna 3; elevation=-15°; frequency=257MHz.

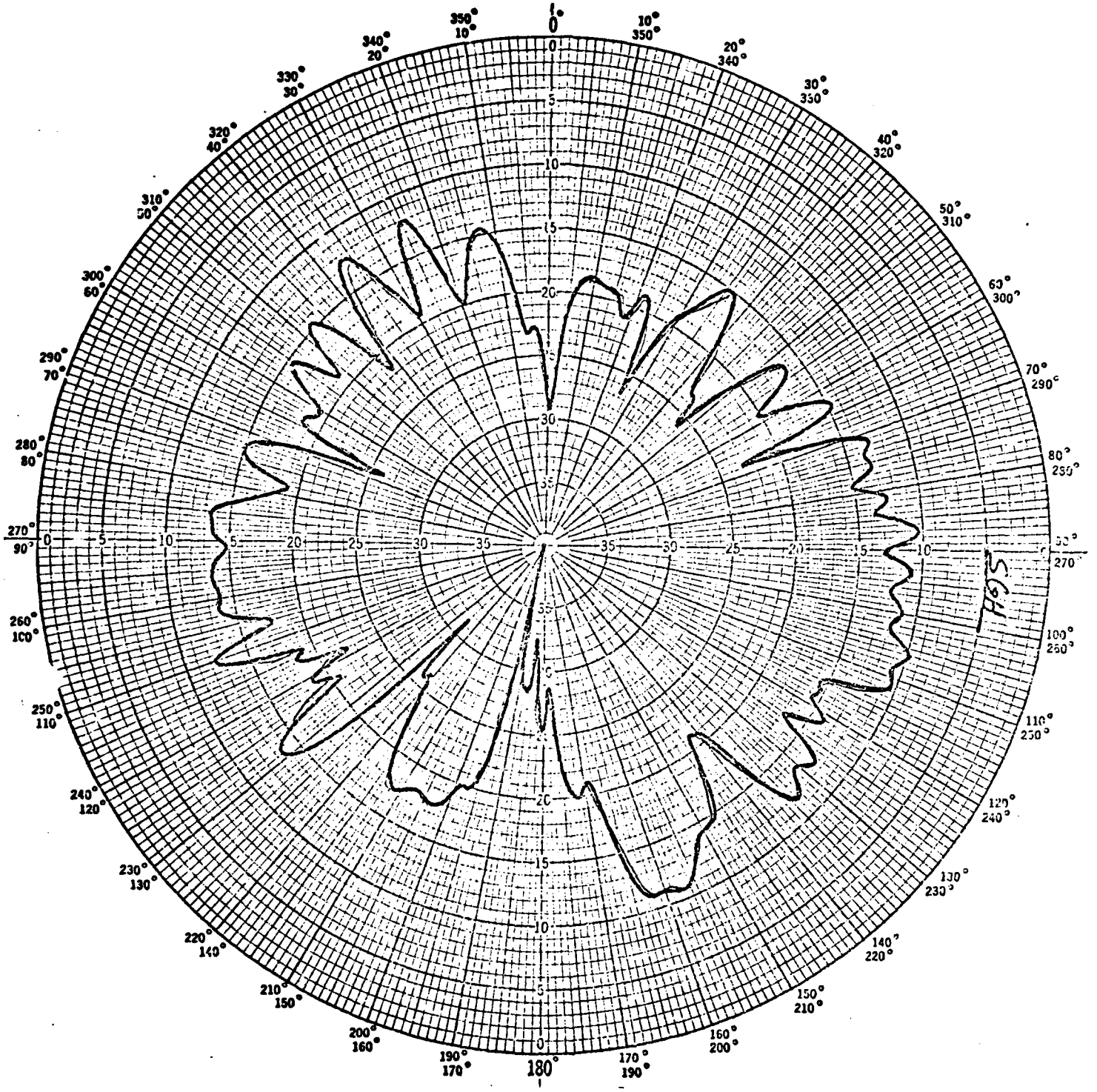

Figure 59. Data Plot: Antenna 3; elevation=30°; frequency=300MHz.

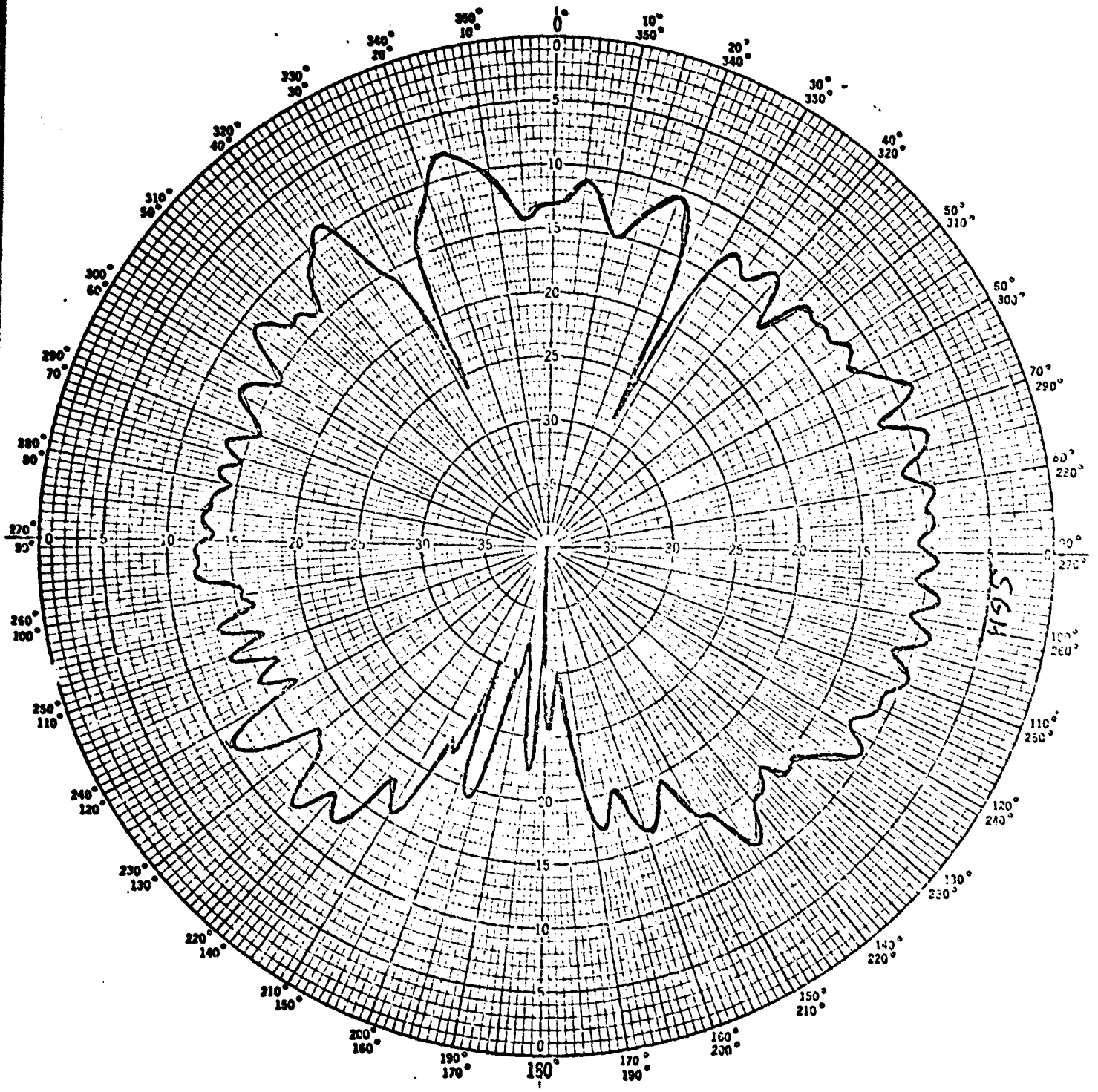

Figure 60. Data Plot: Antenna 5; elevation=15°; frequency=300MHz.

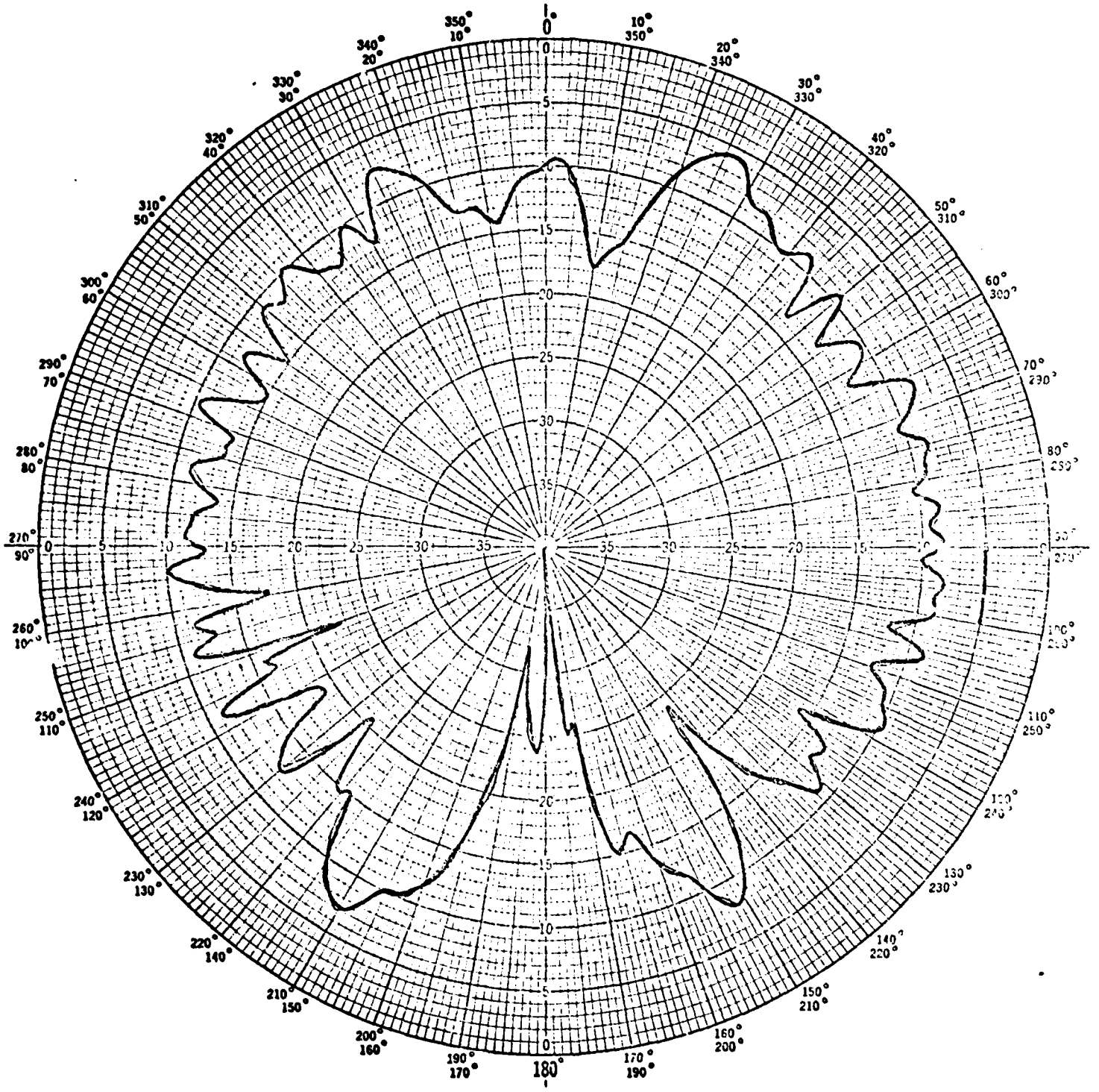

Figure 61. Data Plot: Antenna 3; elevation=0°; frequency=300MHz.

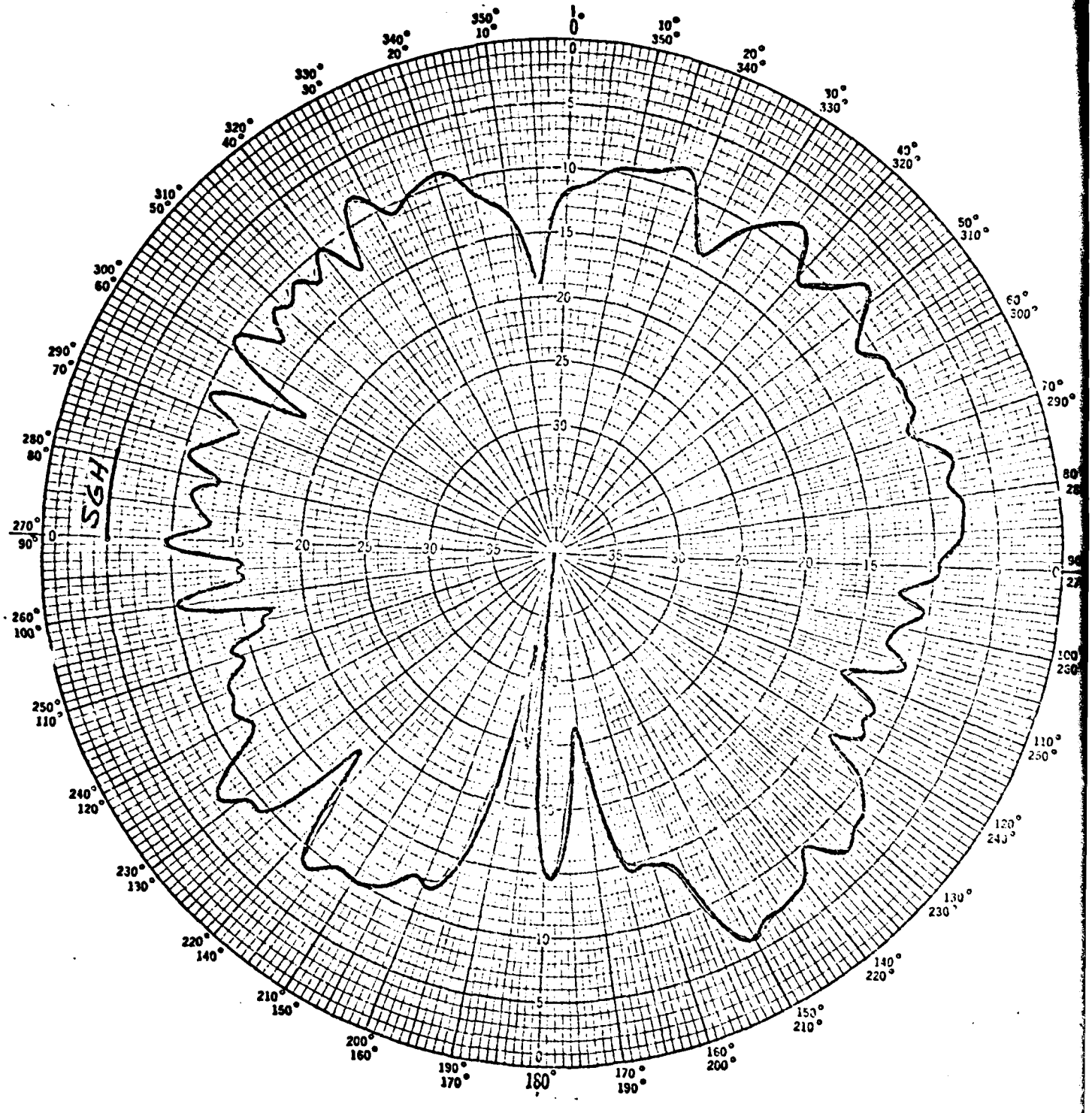

Figure 62. Data Plot: Antenna 3; elevation=-15°; frequency=300MHz.

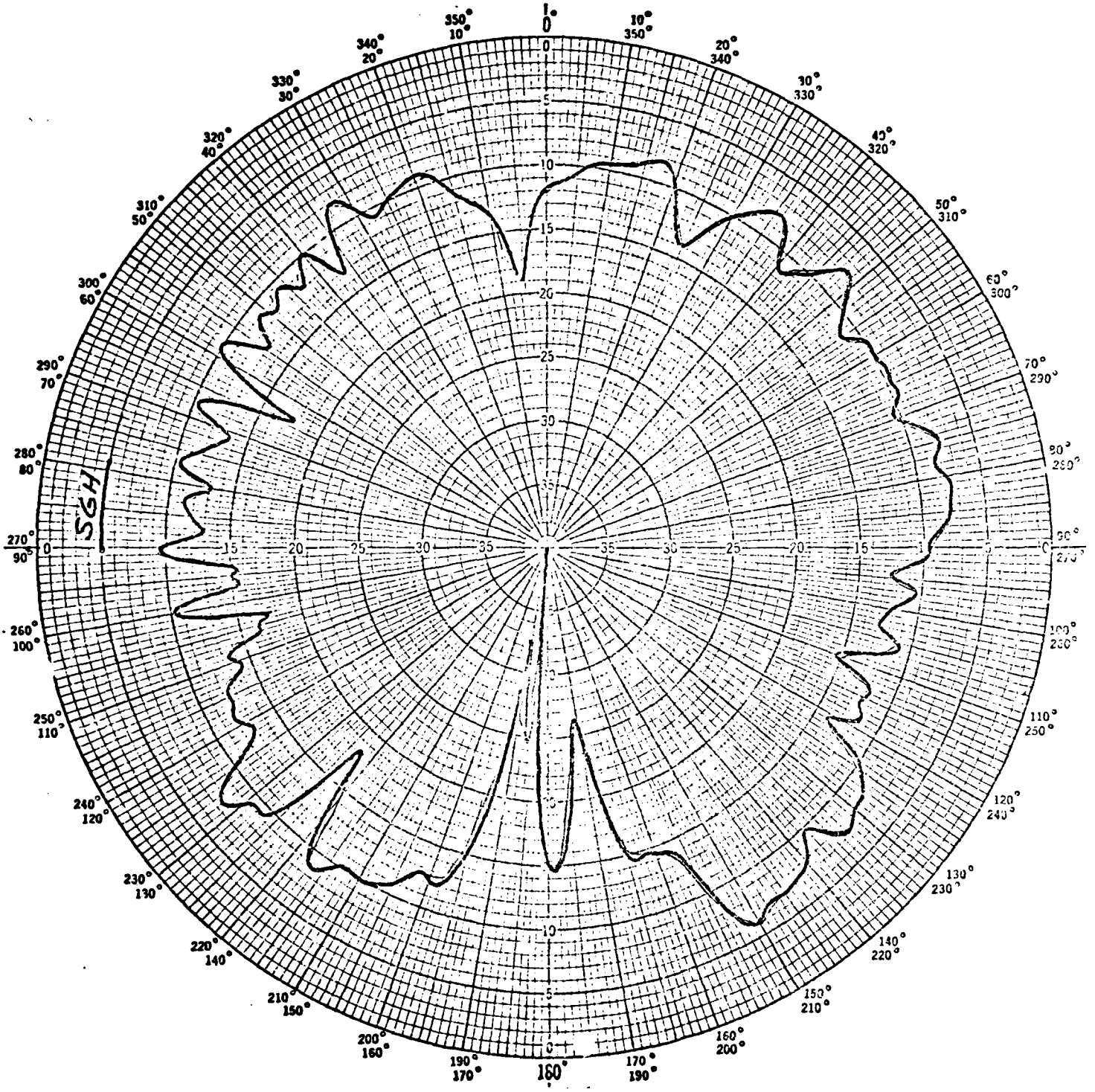

Figure 62. Data Plot: Antenna 3; elevation=-15°; frequency=300MHz.

AD-A080 369 AIR FORCE INST OF TECH WRIGHT-PATTERSON AFB OH SCHOO--ETC F/G 9/5
A STATISTICAL MODEL FOR MULTIPATH REFLECTION EFFECTS OF ANTENNA--ETC(U)
DEC 79 J L FRACK
UNCLASSIFIED AFIT/GE/EE/79-14 NL

2 OF 2
AD A080369

END
DATE FILMED
3-80
DDC

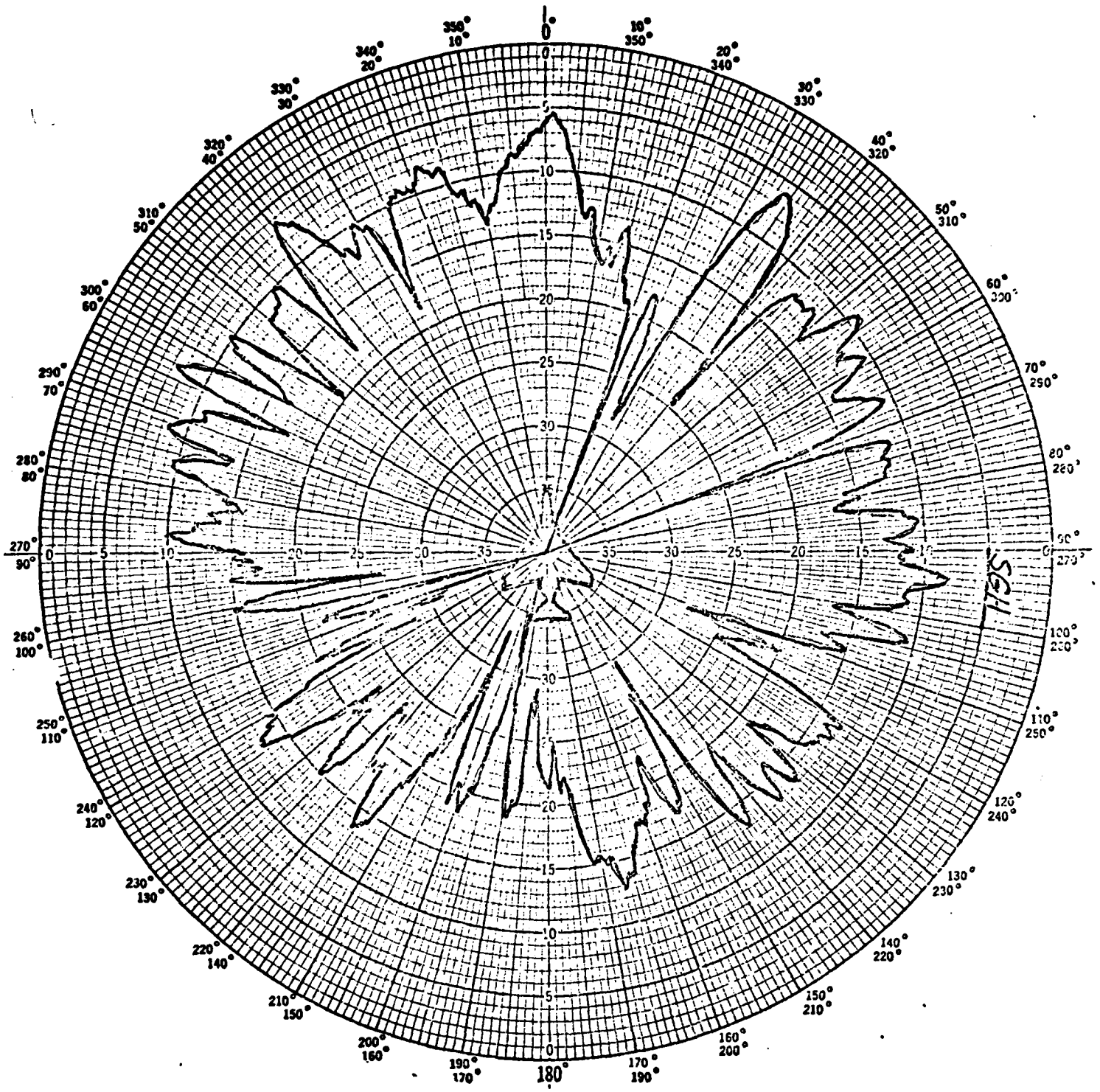

Figure 63. Data Plot: Antenna 3; elevation=30°; frequency=385MHz.

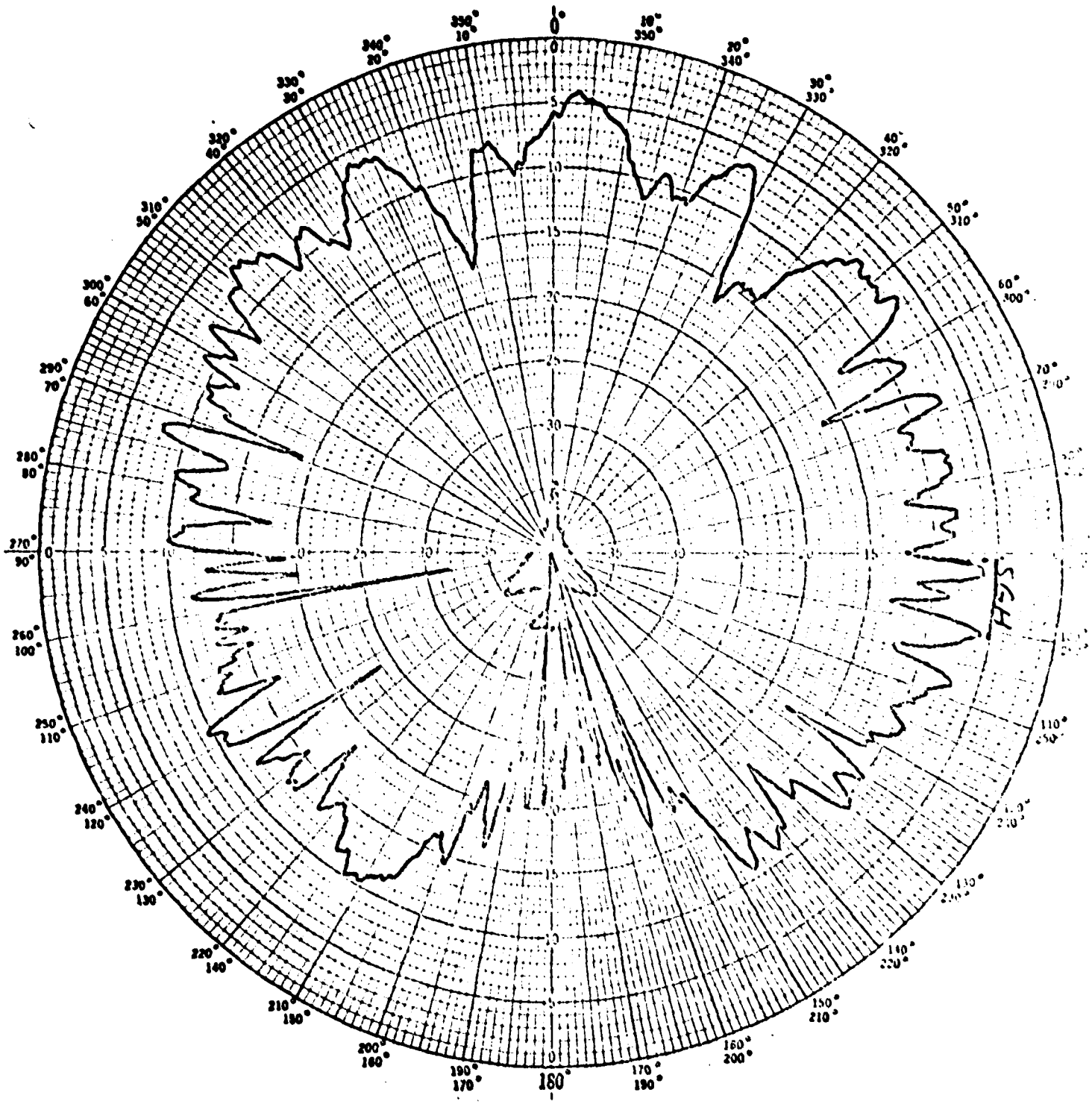

Figure 64. Data Plot; elevation=15°; frequency=385MHz.

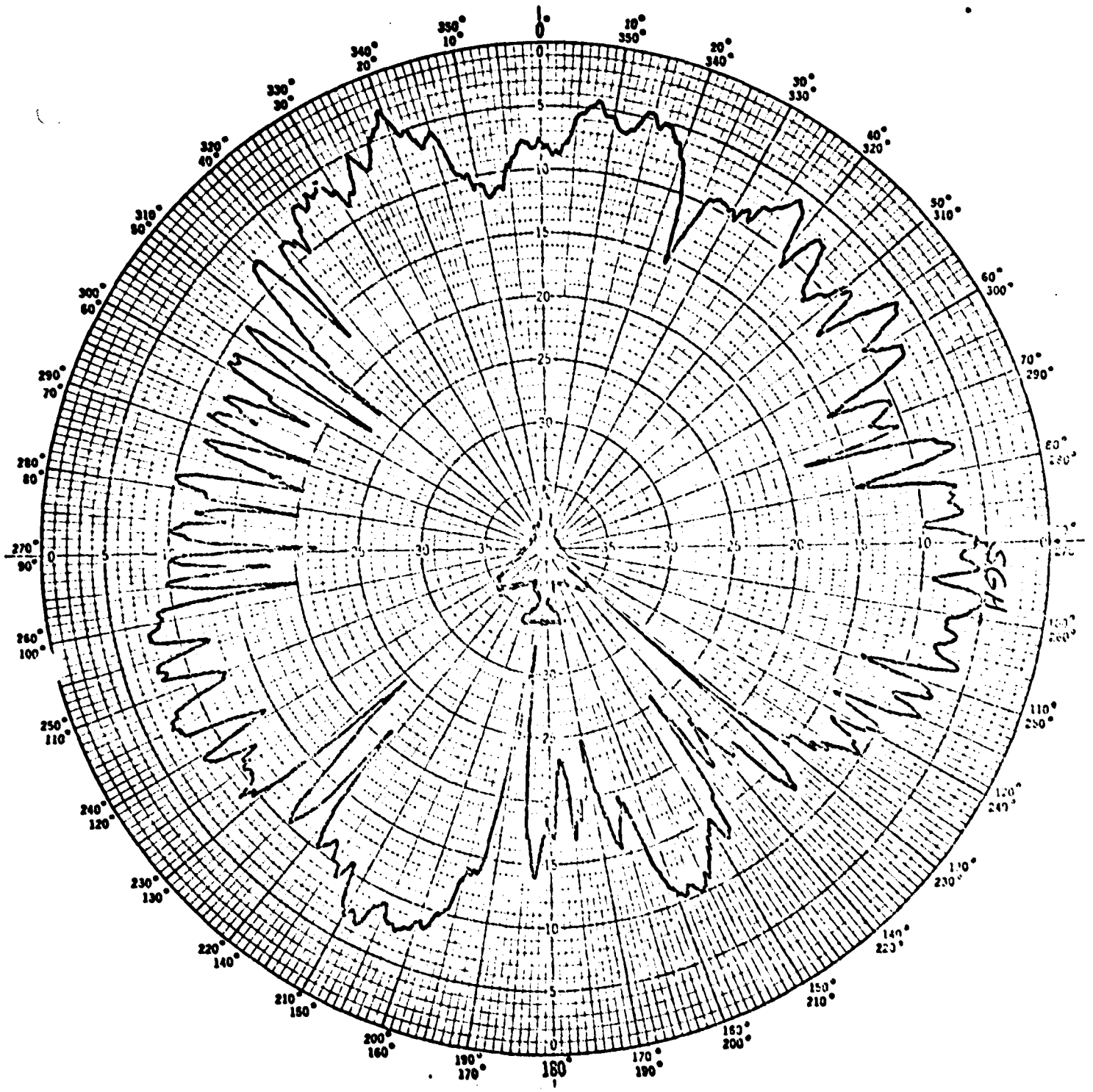

Figure 65. Data Plot: Antenna 3; elevation=0°; frequency=385MHz.

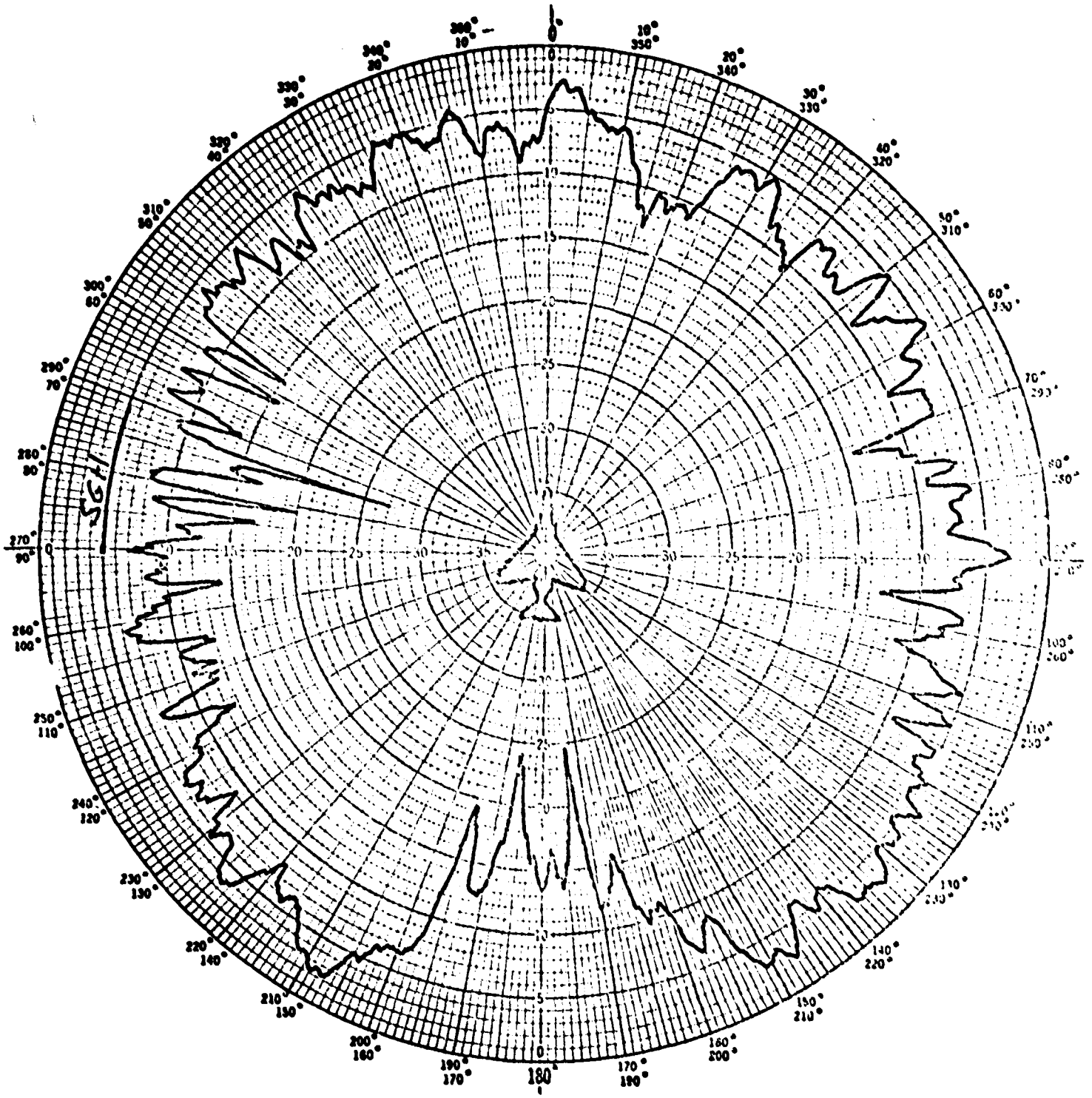

Figure 66. Data Plot: Antenna 3; elevation=-15°; frequency=385MHz.

VITA

Jeffrey L. Frack was born on 2 May 1956 in Allentown, Pennsylvania. He graduated from Absegami High School in Mays Landing, New Jersey in June 1974. He entered Lafayette College in September of that year and graduated in 1978 with a Bachelor of Science degree in Electrical Engineering. He married the former Linda L. George in October 1976 and now has two children; Jennifer, 2; and Michael, 7 months. In May 1978 he was commissioned a second lieutenant in the United States Air Force and since then has been enrolled in the School of Engineering, Air Force Institute of Technology.

Permanent Address: PO box 694
Leipzig Avenue
Cologne, New Jersey 08213

performance measures for the array: the probability that the array gain is above a threshold; probability level curves to show what threshold function the gain will be above a specified percentage of the time; and the probability that the array gain will be above some threshold on an entire interval. These performance measures are evaluated for a specific array configuration for a set of assumed statistics and then plotted versus arrival angle. The results for different array variance are compared and the result is that higher variance results in poorer average antenna performance. The same measures are then evaluated for an array whose statistics are determined from actual measured data.